A remote sensing change detection study in the arid Richtersveld region of South Africa

Russell Stuart Main

A thesis submitted in fulfilment of the requirements for the degree of Magister Scientiae in the Biodiversity and Conservation Biology Department, Faculty of Natural Sciences, University of the Western Cape

November 2007

A remote sensing change detection study in the arid Richtersveld region of South Africa

Russell Stuart Main

Keywords

- Remote sensing
- Change detection
- Arid / semi-arid
- Richtersveld
- Landsat
- MODIS
- Variable precipitation

ABSTRACT

A remote sensing change detection study in the arid Richtersveld region of South Africa

R.S. Main

MSc Thesis, Biodiversity and Conservation Biology Department

University of the Western Cape

The Richtersveld falls within the Succulent Karoo and Desert biomes. It forms part of a biodiversity hotspot with a high diversity of succulent plant species, many of which are endemic to the area. The area is also characterised by varied geological, socio-economic and climatic conditions, which are further complicated and accentuated by impacts such as open-cast mining, livestock grazing and the illegal harvesting of sensitive species. Existing research has pointed towards to the loss of keystone species, changes in vegetation cover and losses in overall biodiversity as a result of a combination of the above conditions and impacts. Remote sensing is increasingly being used to detect or monitor change, because of its ability to capture information on a large scale in a repeatable and digital manner. Remote sensing of vegetation cover changes in arid regions is, however, particularly challenging due to low vegetation cover, bright soil background, as well as morphological and physiological desert plant adaptations. This study made use of remote sensing technologies in order to investigate possible vegetation cover changes that have taken place over time, and which may have manifested through a combination of threats to the region. The aims of the study were addressed using three key questions that sought to a) gain an understanding of the relationship between vegetation response and moisture, in order to interpret b) temporal and c) spatial vegetation cover changes. A spatially and temporally representative remotely sensed dataset was used together with techniques that are repeatable and able to quantify change with limited human bias. The dataset consisted of periodic (1991, 1997 and 2004) 30 meter Landsat images as well as continuous (2000 to 2005) 16-day 250 meter MODIS NDVI imagery. The data were analysed using a combination of techniques that included pixel- and object-based classifications, vegetation index differencing, principle component analysis, and others. The results give an objective reflection of a region that, from a rather course remote sensing perspective, appears to have a temporally predictable yet spatially complex vegetation relationship with available moisture. However, the region appears to be without significant temporal or spatial vegetation cover changes. Despite the stable results, it is argued that remote sensing research in the Richtersveld, using updated technologies and techniques, should continue into the future as it still holds great potential as a decision support tool in sensitive environments with high propensities for change.

Declaration

I declare that “A remote sensing change detection study in the arid Richtersveld region of South Africa” is my own work, that it has not been submitted for any degree or examination in any other university, and that all the sources I have used or quoted have been indicated and acknowledged by complete references.

Russell Stuart Main

Signed …….

November 2007

Acknowledgements

Thanks be to God: “And whatever you do in word or deed, do all in the name of the Lord Jesus, giving thanks to God the Father through Him.” Colossians 3:17

Many, many thanks to Linda Van Heerden for all her administrative help through out the project.

Thank you to BIOTA-South, funded by The German Federal Ministry of Education and Research (BMBF), for my bursary and project finances. Thank you also to the German Remote Sensing Data Center (DFD) of the German Aerospace Centre (DLR) at the University of Wuertzburg, who made my two month stay possible. Thanks also to the Earth Observation group in the CSIR’s Natural Resources and Environment department for funding.

Thank you to my supervisor, Dr. Richard Knight, for his guidance and help.

Thank you to all those who offered up advice and information along the way: Dr. Micheal Schmidt, Prof. Dr. Norbert Jürgens, Dr. Melanie Vogel, Manfred Keil, Dr. Howard Hendricks, Prof. Madsen and Dr. Jan van Aardt. A special THANK YOU to Dr. René Colditz for all your advice and help.

Thank you to South African National Parks for permission to access the Richtersveld National Park.

To my friends and family, THANK YOU so much for all your support, encouragement and prayers over the years. To my loving wife, Gené, I will never truly be able to thank you enough for all your help and “look on the bright side” mentality during the tough times. To my parents, and especially my Dad who passed away during the writing of this thesis, THANK YOU for being all of the above to me though out my university career. You have been my funders, my supervisors, my advisors and my biggest friends and supporters, and I will never know how to repay the sacrifices you made for me. You inspire me and I love you.

Table of Contents

List of Tables

List of Figures

List of Equations

List of Acronyms

Advanced Spaceborne Thermal Emission and Reflection Radiometer (ASTER)

Advanced Very High Resolution Radiometer (AVHRR)

Airborne Visible and Infrared Imaging Spectrometer (AVIRIS)

American Society for Photogrammetry and Remote Sensing (ASPRS)

IPCC Assessment Report #4 (AR4)

Artificial Neural Networks (ANN)

Digital Elevation Model (DEM)

Digital Numbers (DNs)

Earth Observing System (EOS)

Electromagnetic radiation (EMR)

Enhanced Thematic Mapper (ETM+)

European Remote Sensing (ERS)

European Remote Sensing Satellite (ERS)

File Transfer Protocol (FTP)

German Aerospace Centre (DLR)

German Remote Sensing Data Center (DFD)

Gramm-Schmidt (GS)

Ground control points (GCPs)

Interface Description Language (IDL)

Intergovernmental Panel on Climate Change (IPCC)

Iterative Self Organising Data Analysis (ISODATA)

Moderate Resolution Imaging Spectroradiometer (MODIS)

Modified Soil Adjusted Vegetation Index (MSAVI)

Multispectral Scanner (MSS)

Near Infra-Red (NIR)

Non-Photosynthetic Vegetation (NPV)

Normalised Difference Vegetation Index (NDVI)

Perpendicular Vegetation Index (PVI)

Photosynthetically Active Radiation (PAR)

Principle Component Analysis (PCA)

Richtersveld National Park (RNP)

Root Mean Square (RMS)

Satellite Applications Centre (SAC)

Shuttle Radar Topography Mission (SRTM)

Soil Adjusted Vegetation Index (SAVI)

System Pour L'Observation de la Terre (SPOT)

System Pour L'Observation de la Terre Vegetation (SPOT VGT)

Thematic Mapper (TM)

Top of Atmosphere (TOA)

Transformed Soil Adjusted Vegetation Index (TSAVI)

Vegetation Index (VI)

Weighted Difference Vegetation Index (WDVI)

Chapter 1

Introduction

1.1 Habitat

The Richtersveld region is a biodiversity hotspot and forms part of the Succulent Karoo and Desert biomes. The Succulent Karoo biome forms part of the Namaqualand physio-geographical and bio-geographical domain, which stretches from the southwest to the north-western parts of Southern Africa (Cowling *et al*., 1999). Namaqualand is recognized as the Namaqualand-Namib Domain of the Succulent Karoo floristic region (Jürgens, 1991; Cowling *et al*., 1999). The Desert biome borders the Nama-Karoo biome in the east and then runs along the Orange River, not deeper than between 20 or 30 km, towards the mouth of the river at Alexander Bay (Mucina *et al*., 2006).

The Richtersveld region is regarded as a biological hotspot as it is one of the world's most diverse arid regions, with more than 5 000 plant species, many of which are endemic (Hilton-Taylor, 1996; Cowling & Hilton-Taylor, 1999). The Succulent Karoo is characterized by dwarf leaf-succulent shrubs that make the Succulent Karoo biome unique among the world's winter rainfall deserts, which include Western USA and Baja California, Central Chile, the Mediterranean Basin and Western Australia (Mucina *et al*., 2006). Esler & Rundel (1999) suggest that the Succulent Karoo is set apart from other Mediterranean type deserts due to its unique seasonal and inter-annual rainfall reliability (Mucina *et al*., 2006). Within the Richtersveld, there is very little difference between the Succulent Karoo and Desert biomes in terms of species richness and diversity (Mucina *et al*., 2006).

The presence of the cold Benguela Current significantly contributes to the aridity, and seasonality, of both biomes by causing an offshore local high pressure cell during summer, and by contributing to the formation of fogs that move inland during the winter months (Mucina *et al*., 2006). The mean annual precipitation for the Succulent Karoo biome is approximately 170 mm, with rainfall occurring almost exclusively during the winter months (Mucina *et al*., 2006). Despite the low rainfall, there is a degree of predictability and low inter-annual variability about the region's rainfall, which is seen to contribute towards the development and preservation of high species diversity in the biome (Hoffman & Cowling, 1987; Cowling *et al*., 1999). The biome's low rainfall is also supplemented by frequent coastal fogs, which create widespread dewfalls that can occur in both winter and summer months (Von Willert *et al*., 1990; Desmet & Cowling, 1999). The Desert biome has a spatially variable mean annual precipitation

of below 70 mm, which is influenced by both seasonal climatic oscillations and topographic variations (Mucina *et al*., 2006). These influences on precipitation cause there to be intense summer thundershowers in the eastern interior of the biome, while softer drizzle and advection fogs occur in the western parts of the biome (Mucina *et al*., 2006).

The Succulent Karoo biome is described as having a warm-temperate climate regime with mean annual temperatures of 16.8^0 C, while absolute temperatures can reach 44^0 C (Mucina *et al*., 2006). High temperatures such as this can also occur in winter and autumn months when berg wind conditions are prevalent (Desmet & Cowling, 1999; Mucina *et al*., 2006). Despite a lack of evidence, there is a perception that these berg winds have the potential to significantly affect vegetation population dynamics (Mucina *et al*., 2006). The Desert biome has a higher variability about its climate, with differences of about 15^0C in summer temperature maxima between the interior eastern region and the coastal western region (Mucina *et al*., 2006).

The geology of the Namaqualand domain, which includes the Succulent Karoo and Desert biomes that make up the Richtersveld region, is complex and has a history of intensive metamorphism, intrusion and marine transgressions (Cowling *et al*., 1999). The Richtersveld mountain deserts consist of pre-Gondwana granite and gneiss rocks of the Namaqua Metamorphic Province (Cowling *et al*., 1999). These mountains run in a north to south / south west direction, almost parallel to the coast. Sedimentary rocks of the Gariep, Numees and Nama Formations are also prominent in the region and were extensively folded and sheared during the formation of Gondwanaland (Cowling *et al*., 1999). A sandy coastal plain (the Sandveld) is also characteristic of the Richtersveld and consists of both marine and wind-blown, tertiary age, sands (Cowling *et al*., 1999). The geology and soils of the Succulent Karoo are thought to be a significant determinant of biome boundaries, together with length and temperatures of growing season, as the soils are more fine-grained, less leached and have higher pH values than adjacent biomes (Mucina *et al*., 2006).

1.2 Land Use

The biodiversity of the Succulent Karoo and Desert biomes is under pressure from land use such as mining, tourism and the expansion of agriculture, especially livestock grazing (Succulent Karoo Ecosystem Programme, 2006; Conservation International, 2006). Each of these land uses has the potential to increase in intensity or severity in the near future as anthropogenic variables and their influence on the biophysical environment is relatively erratic and can change rapidly with varying economic, social or cultural conditions (Succulent Karoo Ecosystem Programme, 2006; Conservation

International, 2006). Only 5.8 % of 111 000 km that make up the Succulent Karoo is formally protected, while 20 % of the Desert biomes surface area is formally protected, however, low levels of population have kept much of the sensitive biodiversity out of harms way, for now (Conservation International, 2006; Mucina *et al*., 2006). Livestock grazing is the dominant land use in 90 % of the region (Driver *et al*., 2003), and has been found to be responsible for degradation, through overgrazing, in a number of places (Hoffman *et al*., 1999). However, the relationship between grazing and biodiversity loss, especially in arid and/or semi-arid areas, has proven to be a complex one with an array of consequences (Todd & Hoffman, 1999). Todd & Hoffman (1999) mention various studies conducted on the consequences of grazing: light grazing resulting in increased species richness (Naveh & Whittaker, 1979; Waser & Price, 1981; Noy-Meir *et al*., 1989), heavier grazing resulting in reduced species richness (Waser & Price, 1981; Noy-Meir *et al*., 1989; Olsvig-Whittaker *et al*., 1993), and selective grazing of palatable species resulting in a shift towards unpalatable species composition (Westoby *et al*., 1989; Milton & Hoffman, 1994). West (1993) states that grazing can be an important part of rangeland ecosystems, and that if grazing practices were halted there could be a short term increase in biodiversity, but a potential for long term decline due to a decrease in the system's resilience to future disturbances. Current rangeland conditions tend to be the result of many years of interaction between biophysical and anthropogenic variables, and attempts at removing a particular variable may not produce a more desirable, or stable, situation (Hendricks, 2004).

Mining is also prevalent in the region, but despite its heavy impact in specific areas, it is also thought to have contributed to the protection of parts of the Succulent Karoo biome through large exclusion zones set up around the principle mining operations (Mucina *et al*., 2006). However, mining has tended to impact key habitats of importance, due to their ecological processes, such as riverine flood plains and coastal terraces of the Desert biome(Driver *et al*., 2003; Mucina *et al*., 2006). Milton (2001) points to new and emerging markets in titanium, zinc and copper, as well as increased demand for gypsum and quartz as future threats to limited habitat types.

Increasing tourism to the area has also brought about potential threats to sensitive species, through the impacts of off-road vehicles and increased access to sensitive fauna and flora that are collected and sold as novelties or for their medicinal value (Conservation International, 2006; Mucina *et al*., 2006). The construction and expansion of tourism facilities also pose a threat through increased availability, access and use.

1.2.1 The Richtersveld National Park

The Richtersveld National Park (RNP) (28° 15' S; 17° 10' E) is situated in the north-western corner of the Northern Cape Province and Succulent Karoo biome, and has an area of approximately 1 625 km^2 (Figure 1). The RNP is one of South Africa's contractual parks, which means the park is leased from the local people who continue to reside in the area and have representation in the administration of the park (Reid *et al*., 2004). The local inhabitants, the Nama, are traditionally livestock farmers and in agreement with park management are permitted to keep approximately 6 600 small stock units of livestock. The National Park can be described as a topographically, and geologically, complex mountain desert region that is characterised by temperature extremes and an annual average rainfall of below 80 millimetres (South African National Parks, 2005). The region that lies to the east of the Richtersveld highlands, which form the eastern border of the park, has a predominantly winter rainfall occurring between May and September, while the interior region to the west, which forms the leeward side of the highlands, has periodic summer thundershowers between February and April (Desmet, 2007). These variations in topography create a range of environmental conditions that support different ecological communities and ecosystem processes, such as vegetation adapted to making use of high altitude cloud or fog, especially on the south western slopes (Dorner *et al*., 2002; Mucina *et al*., 2006). North western slopes have higher temperatures, due to greater incoming solar radiation, and are therefore drier and less vegetated than the south western slopes (Mucina *et al*., 2006). Changing topographies can also influence vegetation boundaries and landscape pattern through variations in geomorphic and altitudinal gradients (Dorner *et al*., 2002).

This variability in available moisture and forage pose a challenge to the sustainable management of the Park (Hendricks, 2004). Tracking this moisture and the resultant forage, are the Nama pastoralists and their herds. These pastoralists temporarily make use of semi-permanent stock posts as places of residence, and places they return to after each day's herding in order to enclose the livestock in a 'kraal' (Hendricks *et al*., 2005a; b). There are approximately 298 (cumulative total) stock posts inside the park, many of which are only active for approximately 60 days per annum (Hendricks *et al*., 2004). The relatively short duration of the pastoralists' stay at one stockpost may present a problem for the continued and accurate measurement of grazing effects on vegetation communities, but Riginos & Hoffman (2003) suggest that herders be encouraged to relocate stockposts at frequent intervals so as not to suppress recruitment or cause adult shrub mortality. Keeping between 230 and 700 units of livestock in an area for 60 days tends to result in a gradient of grazing impact away from the stock post, which closely resembles the piosphere effects seen at watering points (Thrash, 1998; Hendricks *et al*., 2005a). Hendricks *et al*. (2005a) investigated vegetation dynamics along these grazing gradients, and showed

that species richness, community patchiness, and total plant cover all increased with increasing distance away from the stock post. This concurs with other literature (Cowling & Pierce, 1999), that suggest that continued grazing in the RNP poses a serious and ongoing threat to plant diversity in the area, but that it may be too early, or too late, for the detection of the real effects of the grazing.

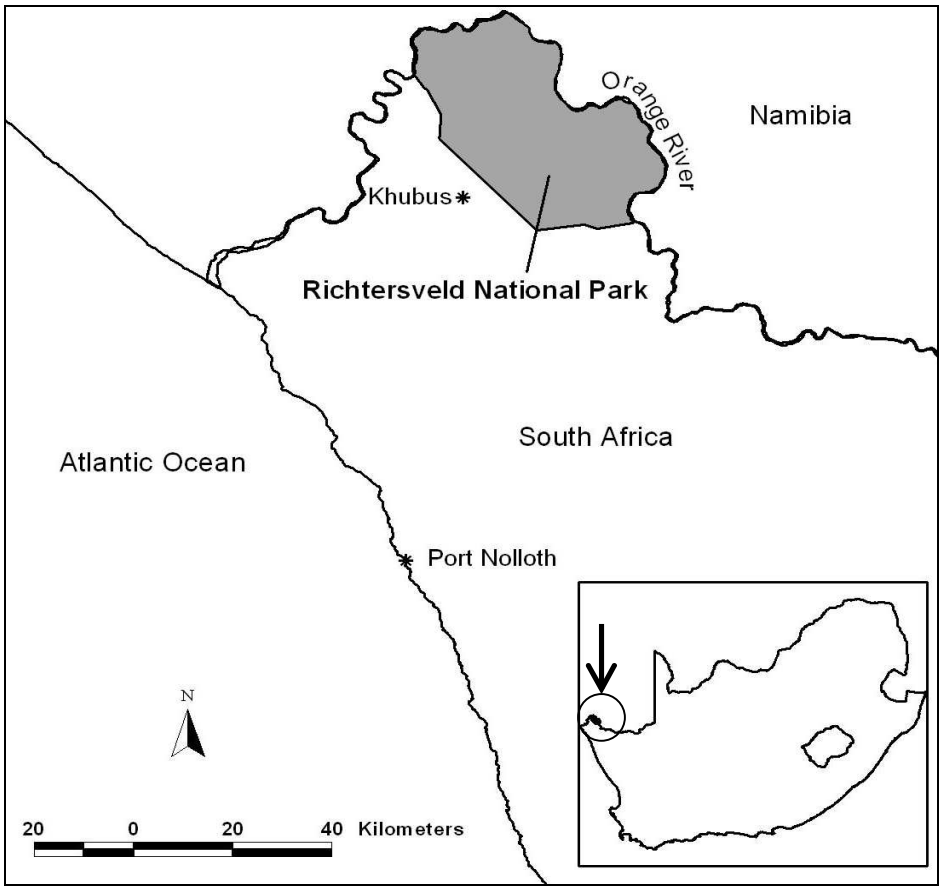

Figure 1: The Richtersveld National Park, with the Orange River as a border between South Africa and Namibia.

1.2 Climate Change Threats

In low nutrient, semi-arid environments that often have slow population dynamics it is common for the true effects of vegetation change to appear after 18 to 30 years (De Haan *et al*., 1997; Jürgens *et al*., 1999). This then leads to overlap and uncertainty between the anthropogenic and climatic effects on vegetation, which is a topic of great debate (West, 1993; Doughill & Cox, 1995; Adams, 1996; Friedel *et al*., 2000). Arid and semi-arid rangelands are often characterised by variable climates, which can cause extensive cyclical vegetation responses that mask, at least for short periods, the effects of grazing (Blench & Sommer, 1999).

Much like the uncertainty surrounding future anthropogenic impacts, the impact of changing climate scenarios as a result of global warming, is also an uncertain but widely debated research topic. The Fourth Assessment Report (AR4) of the United Nations Intergovernmental Panel on Climate Change (IPCC) states that the warming of the planet is unmistakably taking place, most likely due to human activity (IPCC, 2007a). The AR4 report makes a number of observations concerning the warming of the planet; rising sea levels and increases in hurricane intensities. The AR4 report provides some model based projections of temperature and sea levels for a number of scenarios. Even the most optimistic of scenarios predicts temperature increases of 1.8 °C and sea level rises of between 18 and 38 cm (IPCC, 2007a). The AR4 report also projects, with very high confidence, that climate change will affect ecosystems by making spring events occur earlier, causing species ranges to shift, and combined with other stress factors it will affect the resilience of ecosystems (IPCC, 2007b). Scenarios for Southern Africa suggest an increase in temperature, and therefore evapo-transpiration, as well as increased rainfall variability (Rutherford *et al*., 1999b; Dudley, 2003; Mukheibir & Sparks, 2005). The combination of these effects is predicted to have significant impacts on plant diversity, plant composition, and resultant changes in vegetation structure (Midgley & O'Callaghan, 1993; Rutherford *et al*., 1999b). Precipitation in the Richtersveld region has a high inter-annual variability, with extreme events skewing the analysis of trends (Midgley *et al.*, 2005). Mukheibir & Sparks (2005) point out that while there is uncertainty as to the general response to climate change in South Africa, it is likely that rainfall patterns will change and that climate change planning should in the very least account for an increase in climate variability.

Rutherford *et al*. (1999b) used complex climate models, which made use of climate parameters perceived to be key to plant physiological function and survival, in order to predict the spatial distribution of the five dominant South African biomes under three different climate scenarios. The results showed increases in mean minimum temperatures, summed annual daily temperatures, and a decrease in winter soil moisture days, which when combined, predicted that the Succulent Karoo biome "…disappears almost completely from its current range…" (Rutherford *et al*., 1999b, p.12). Furthermore, they predict dire consequences for the sensitive species that have narrow tolerance limits, i.e. endemic species (Rutherford *et al*., 1999b). From this research, Rutherford *et al*. (1999a) predict a 19.7 % extinction of 608 species analysed in the Richtersveld National Park. This then has serious implications for the reserve's management strategies, and the very concept of species conservation (Rutherford *et al*., 1999a). Rutherford *et al*. (1999b) does, however, warn that these predictions are complicated by interactions between biophysical and anthropogenic variables, and should therefore be viewed with caution and a degree of uncertainty. If these scenarios prove to have any truth to them, the

resulting biodiversity loss could be severe. Consequently, serious attempts should be made by conservation planners, and policy makers, to understand and monitor the spatio-temporal variability of anthropogenic and climatic influences on biodiversity (Behnke & Scoones, 1993; Scoones, 1995). This should be undertaken by initiating studies across a range of differing landscapes and land uses (Miller & Hobbs, 2002).

1.4 Remote Sensing

The advent of remote sensing and its ability to quantitatively monitor large expanses of the earth's surface, means that it is increasingly being used to aid labour intensive ground-based monitoring techniques (Blench & Sommer, 1999). Remote sensing involves the measurement of variations in the reflected electromagnetic radiation (EMR) of an object or phenomenon, without being in contact with the object or phenomenon (Lillisand & Kiefer, 1979; Jensen, 1996). It is able to provide cost effective information on the state of landscapes on a regular, continuous and near real-time basis, at various spatial and temporal scales (Zhou *et al*., 1998). Remotely sensed data has proven to be useful in the quantification, and monitoring, of variable vegetation responses to semi-arid ecosystem driving forces, such as rainfall, fire and grazing (Pickup *et al*., 1994; Hudak & Brockett, 2004). Satellites, such as Landsat, and its associated sensors the Multispectral Scanner (MSS), Thematic Mapper (TM), or Enhanced Thematic Mapper (ETM+), have been successfully employed in studies that aim to highlight variations in vegetation community characteristics, usually by measuring the relationship between observed reflectance and total plant cover (Pech *et al*., 1986; Milton *et al*., 1990; Pickup *et al*., 1993; Pickup, 1995). This relationship between reflectance and plant cover is normally portrayed in the form of a vegetation index image that models the relationship between red and near-infrared wavelengths in order to exploit spectral properties of healthy vegetation (Nordberg & Evertson, 2003). The Normalised Difference Vegetation Index (NDVI) is regarded as the most recognised and widely used vegetation index (Jensen, 1996). Tucker & Sellers (1986) demonstrated that NDVI was an effective measure of photosynthetically active biomass. Semi-arid rangelands have benefited from the integration of remotely sensed data into ecological investigations (Trodd & Dougill, 1998). These investigations include Tucker *et al*. (1991) who showed that certain ecosystems have a resilience to change due to rapid vegetation recovery after rainfall events. O'Neill *et al*. (1993) investigated the impacts on, and subsequent recovery of, vegetation after fire. Remote sensing has been used to investigate differences in vegetation structure, cover, and species composition as a result of varying land uses (communal, commercial and conservation) and management strategies (Palmer & van Rooyen, 1998; Dube & Pickup, 2001). But perhaps the most popular use of remotely sensed data, in rangeland management, is

in measuring the grazing impacts of livestock. Grazing impacts surrounding watering points and villages have been investigated using remotely sensed data by Hanan *et al*. (1991); Fusco *et al*., (1995); and Ringrose *et al*., (1996)

Remotely sensed data is predominantly used in change detection studies. Change detection involves the application of various image analysis techniques to multi-temporal images, in order that variations in the state and spatial distribution of objects and phenomena can be quantified (Lu *et al*., 2003). This information should then provide land managers with improved understanding of relationships and interactions between the anthropogenic and natural phenomena, allowing for the efficient distribution and management of available resources (Lu *et al*., 2003). Successful change detection studies require careful consideration of all external influences on the reflected EMR signal, within and between multi-temporal images. Differences within and between particular remote sensor systems being used, as well as differences in the environmental characteristics of the study area and resultant image, are examples of external influences on the EMR signal. Remote sensor systems differ in their temporal, spatial, spectral, radiometric and economic resolutions, and care must be taken to either minimise these differences when using different systems, or to simply make use of only one system (Lu *et al*., 2003). Environmental considerations include the atmospheric conditions, soil types and soil moistures, as well as the phenological characteristics of the region under investigation (Jensen, 1996). Environmental factors are dealt with by utilizing anniversary date imagery, in order to minimise differences in phenologies and soil moistures, and through various image pre-processing steps aimed at reducing, or eliminating, atmospheric influences on the EMR signal. Common pre-processing steps include the accurate pixel-to-pixel registration of multi-temporal images, the conversion of digital numbers to radiance or reflectance values, as well as topographic correction for study areas characterised by rugged terrain. Substrate brightness, or ‘soil noise’, makes up a significant portion of the total signal noise in semi-arid and arid environments, where vegetation cover is sparse. The correction of ‘soil noise’ is particularly important when making use of vegetation indices, as it can cause significant errors in the measurement of healthy vegetation (Richardson & Wiegand, 1977; Huete, 1988; Schmidt & Karnieli, 2000).

Despite the provision of regular, continuous, and near-real time images, remote sensing usually requires ground truthing in order to properly identify objects, precise image registration, and the verification of results. Ground truthing is often cumbersome and slow, especially in rugged terrain. However, it is a necessary part of most remote sensing projects, and is as important for accurate analysis as is the pre-processing of images. Remote sensing projects are expensive and should not be oversold as an

alternative to ground-based monitoring. A balance needs to be found between the questions that need answering, the imagery available, the pre-processing and techniques required, and appropriate levels of ground-based measurements. Once this balance is achieved then remote sensing becomes cost effective and useful to land managers needing to better manage, and monitor, their resources.

Chapter 2

Remote Sensing Background

2.1 Remote Sensing and Remote Sensing Products

Remote sensing is a means of obtaining information about an object without physical contact between the device collecting the data and the object being studied (Campbell, 1996; Jensen, 2000). The American Society for Photogrammetry and Remote Sensing (ASPRS) formally defines remote sensing as "the art, science, and technology of obtaining reliable information about physical objects and the environment through the process of recording, measuring, and interpreting imagery and digital representations of energy patterns derived from non-contact sensor systems" (Colwell, 1997, p. 3).

The electromagnetic energy emitted by the sun will be reflected, absorbed, scattered or transmitted by different materials on the earth's surface (Elachi, 1987). The majority of sensors record the reflected or re-radiated EMR of objects on the earth's surface (Jenson, 2000). Objects on the earth's surface have a characteristic reflectance, texture and shape, which can combine to influence the remotely sensed variations in the amount and properties of the EMR. These variations then play an important role in the interpretation of the data (Campbell, 2002; Lillisand & Kiefer, 1979; Jensen, 2000). The sensors collect and record these variations of reflectance within the EMR as analogue and/or digital matrices (raster) of digital numbers, or brightness values, which make up remotely sensed images (Jensen, 2000; ERDAS, 1997).

In order to make meaningful and appropriate use of remotely sensed images, the user must understand and evaluate the four resolutions associated with different remote sensing systems. **Spectral resolution** relates to the sensor's ability to detect different widths, or portions, of the electromagnetic spectrum. The number and width of portions, or bands, collected by the sensor, influence the ability of the user to detect unique differences in spectral signatures of various objects (Turner *et al*., 2003). For example, a common hand-held camera would record three bands of information, namely the visible blue, red and green bands, ranging from 0.4 to 0.7 μm; while a satellite sensor such as the Landsat 5 TM, records seven bands of information (Table 1), spanning the visible blue, green and red bands (0.4 - 0.7 μm) to the invisible infra-red bands (0.7 – 14 μm) (Jensen, 2000; Mather, 2003).

Sensors that record radiant energy in multiple, spectrally-*broad*, bands of the EMR are called multispectral scanners (Jensen, 2000; USGS, 2006). The Moderate Resolution Imaging

Spectroradiometer (MODIS), onboard the Earth Observing System (EOS) satellite, Terra, also records wavelengths spanning from the visible blue to the invisible infra-red. But the MODIS sensor records these wavelengths at much narrower spectral widths, and therefore has 36 spectral bands between 0.405 μm and 14.385 μm (Maccherone, date unknown). Sensors, such as MODIS and the Airborne Visible and Infrared Imaging Spectrometer (AVIRIS), that record radiant energy in a multitude of spectrally-*narrow* bands are called hyperspectral scanners (Jensen, 2000; Mather, 2003).

Table 1: Spectral and spatial resolution of the common Landsat TM sensor (USGS, 2006)

Landsat 5 TM	Resolution (micrometers)	Meters
Band 1	0.45 – 0.52	30
Band 2	0.52 – 0.60	30
Band 3	0.63 – 0.69	30
Band 4	0.76 – 0.90	30
Band 5	1.55 – 1.75	30
Band 6	10.40 – 12.50	120
Band 7	2.08 – 2.35	30

The previously mentioned sensors are referred to as passive sensors, as they only record the EMR that is naturally reflected from the earth's surface (Jensen, 2000). Active sensors, such as the European Remote Sensing Satellite (ERS) and the Canadian RADARSAT emit their own EMR, usually microwaves (1 mm – 1 m), and then record the amount of radiance scattered back to the sensor (ERDAS, 1997; Jensen, 2000; Mather, 2003). Table 2 provides other examples of common remote sensors.

Spatial Resolution refers to the size of the picture elements (or pixels) that make up an image and therefore equates to a measure of the smallest object detectable by a sensor and the area on the ground represented by each pixel (ERDAS, 1997). Sensors that have broad spectral resolutions are often limited in their spatial resolutions, and visa versa. Hyperspectral sensors, such as MODIS, System Pour L'Observation de la Terre (SPOT), or Advanced Very High Resolution Radiometer (AVHRR) have spatial resolutions of between two hundred and fifty meters (250 m) and one kilometer (1 km). Multispectral scanners, such as Space Imaging IKONOS, Advanced Spaceborne Thermal Emission and Reflection Radiometer (ASTER), or Landsat (TM), can have spatial resolutions of between four, fifteen and thirty meters respectively. The total size of the resultant image (or scene) is also influenced by the sensors spatial resolution.

Radiometric resolution is a measure of how sensitive the sensor is at detecting variations in the intensity of the reflected EMR. The higher the radiometric resolution the better the sensor is able to distinguish between objects of similar reflection, which in turn aids the interpretation of remotely

sensed imagery. The different intensities are recorded in the image as different shades of colour and, depending on whether the remote sensing system records data at 8, 12 or 14 bits; it can be expressed through between 256 and 16 384 different shades (Jensen, 2000).

According to Lu *et al*. (2003), acquiring anniversary date imagery in order to eliminate any seasonal influences is one of the most important considerations in change detection studies. Being able to acquire these anniversary dates is influenced by the **temporal resolution** of a remote system, i.e. how often the satellite passes over, and records, a particular area. Systems with high temporal resolution (1 – 2 days) often have low spatial resolutions, due to data capacity constraints. Temporal resolution is an important factor in obtaining scenes that are least affected by atmospheric phenomena, such as cloud or haze (Turner *et al*., 2003). Sensors that capture data repetitively are favored for change detection studies (ERDAS, 1997). Systems such as Landsat have temporal resolutions of sixteen days; MODIS has a revisit time of one to two days; while systems like IKONOS have variable temporal resolutions because they can be pointed according to user requirements.

Table 2: Common sensor characteristics from various satellite platforms (sourced and adapted from Terhorst, 2004).

Sensor	Resolution	Swath	Website
IKONOS	4m Multispectral 1m Panchromatic	11 x 11 km	http://www.geoeye.com/
Landsat 5	120m Thermal 30m Multispectral	180 x 180 km	http://landsat7.usgs.gov/
Landsat 7	60m Thermal 30m Multispectral 15m Panchromatic	180 x 180 km	http://landsat7.usgs.gov/
MODIS	250m (Band 1 – 2) 500m (Band 3 – 7) 1km (Band 8 – 36)	2330 km	http://modis.gsfc.nasa.gov/
NOAA series	1.1 km AVHRR	2000 km	http://noaasis.noaa.gov/
Quickbird	2.4m Multispectral 0.6m Panchromatic	16 x 16 km	http://www.digitalglobe.com/
SPOT 2 & 4	20m Multispectral 10m Panchromatic	60 x 60 km	http://www.spot.com/
SPOT 5	10m Multispectral 5m Panchromatic HRG instrument: 5m Multispectral 2.5m Panchromatic	60 x 60 km	http://www.spot.com/

The final and sometimes most important, or limiting, factor is the **economic resolution**. This resolution can be defined as the amount of imagery or data you are able to obtain, or process, per unit money (Wikipedia, 2006). Each of the previously mentioned resolutions often influences the cost of the imagery. For instance the medium to high spectral resolution (0.45 – 0.9 μm) and high spatial resolution (1 – 4 m) of the pointable IKONOS system will cost the user between US$ 7 and US$ 15 per square kilometer, with a minimum of between forty nine and one hundred square kilometers that have to be ordered (Leroux, 2004). Programs such as Landsat will cost about US $ 600 per scene (185 x 172 km) and, depending on the area of interest; there is also a large amount of archived data that is freely available (Leroux, 2004). Course spatial resolution imagery, such as the SPOT satellite's VEGETATION product, NOAA AVHRR imagery, and MODIS imagery are freely available for download over the internet.

2.2 Change detection using remote sensing technology

With an increased emphasis on sustainability in resource and ecosystem management principles, there is an important need for timely, continuous, and accurate monitoring of natural resources in order that they be effectively and efficiently managed (Lu *et al*., 2003; Coppin *et al*., 2004). Remote sensing data has proved to be a powerful tool in providing information on natural resources at various spatial and temporal scales, largely due to its repetitive coverage, 'birds eye' view, and digital format (Brogaard & Ólafsdóttir, 1997). For remote sensing data to be truly useful, it has to be analysed for spatial or spectral differences in the state of objects or phenomena over time (Lu *et al*., 2003). Change detection, using remote sensing, is based on the premise that a change in land cover will result in a large enough change in the reflected EMR for the sensor to detect it, over and above other superfluous changes in the EMR (Nordberg & Evertson, 2003). There have been a variety of non-military satellite sensors used over the decades in order to monitor the Earth's surface, with the most common being Landsat MSS, Landsat TM, SPOT, AVHRR, and aerial photography (Lu *et al*., 2003). As a result there are a variety of change detection techniques that have been and are being developed. These techniques use multi-date imagery from multi- and hyper-spectral sensors, in order that differences, in object or phenomena, be properly identified, quantified and if necessary monitored (Jensen, 1996; Civico *et al*., 2002; Coppin *et al*., 2004). Making use of remote sensing technology in the detection and monitoring of changes on the earth's surface is fraught with challenges. Some of which include: (a) detecting modifications as well as conversions of land cover, (b) separating intra- from inter-annual vegetation changes, (c) monitoring rapid as well as progressive changes, (d) appropriate scaling of the results, and (e) matching temporal rates of observations with the scale of the processes (Coppin *et al*., 2004).

Not all change detection methods are appropriate to all areas, or all types of imagery (Nordberg & Evertson, 2003). Before implementing a change detection study, or choosing a change detection method, careful consideration must be given to the characteristics of the area of interest, the remote sensor system being used, its image pre-processing requirements, the processing/computing abilities of available systems, as well as time and finances (Jensen, 1996; Coppin & Bauer, 1996).

2.3 Pre-processing of satellite imagery for change detection

"Given this catalogue of problems one might be tempted to conclude that quantitative remote sensing is the art of the impossible" (Mather, 2003, p. 108)

A single satellite image does not hold much value when viewed or analysed on its own (Jensen, 1996). The strength and usefulness of remote sensing technology lies in its ability to detect temporal changes occurring over vast tracks of land (Lillisand & Kiefer, 1979; Jensen, 1996). This often has to be done by combining imagery from different sensors. Being able to accurately detect changes in the properties and/or extent of an object or phenomenon requires that all the imagery be pre-processed and effectively standardized. Common pre-processing steps include (1) geometric and ortho-correction, (2) atmospheric or radiometric correction, and occasionally (3) topographic correction, which is necessary in mountainous terrain (Lu *et al*., 2003; Coppin *et al*., 2004; Bruce & Hilbert, 2004). These steps should then correct the imagery for radiometric and geometric defects, atmospheric interferences, variations in illumination geometry, as well as calibrating images for sensor degradation and the effects of topography (Mather, 2003). There is an extensive body of research regarding appropriate pre-processing methods for change detection (Lillisand & Kiefer, 1979; Jensen, 1996, 2000; Mather, 2003; Coppin *et al*, 2004). Choosing the appropriate pre-processing methods often depends on factors such as the research question being investigated, environmental characteristics of the study area, the remote sensors being used to capture these, the processing/computing capabilities, as well as the amount of time and finances available (Jensen, 1996).

2.3.1 Geometric correction

Multi-temporal change detection techniques often involve overlaying numerous images, collecting ground-based measurements to relate back to the image information, and combining the imagery with ancillary datasets in order to refine results (Bruce & Hilbert, 2004). Hence, the importance of image-to-image registration and geometric correction in change detection studies. The thematic accuracy of any potential results is directly dependant on the positional accuracy of the imagery (Townshend *et al*.,

1992; Stow, 1999; Bruce & Hilbert, 2004). A raw remotely sensed image is given a spatial location through the process of image-to-map rectification, by modelling the relationship between the image and known map coordinates, or ground control points (GCPs) that are derived using global positioning systems (GPS) (Armston *et al*., 2002). This rectification to known map coordinates, or GCPs, gives the raw image a spatial location by conforming it to a particular map projection system; this is often called 'rubber sheeting' (ERDAS, 1997). Once an image has been geo-rectified, image-to-image registration is undertaken on subsequent images, ensuring accurate pixel-to-pixel co-registration between multi-date imagery. Accuracy of image geo-rectification is based on the root mean square (RMS) error. The amount of acceptable RMS error is largely a matter of opinion and dependant on the aim of the change detection study. Townshend *et al*. (1992) states that an RMS error of less than 0.2 pixels for densely vegetated areas, and between 0.5 and 1 pixels for sparsely vegetated areas, should be achieved. Any geometric distortions within the imagery are multiplied when there is variable topography within the area of interest. This requires the imagery to be orthorectified using a digital elevation model (DEM) of the area, which has the same or similar spatial resolution.

2.3.2 Radiometric correction

When dealing with multi-image change detection studies, consideration must also be given to variations that exist between images, which are caused by changes in sensor characteristics, atmospheric conditions, solar angle, and sensor view angle (Chen *et al*., 2005). The radiated portions of the EMR, which the passive satellite records, are modified through scattering and absorption by gasses and aerosols as they travel through the atmosphere towards the satellite sensor (Figure 2) (Song *et al*., 2001; Mather, 2003). The ability to accurately retrieve landscape information from remotely sensed imagery is hampered by the fact that atmospheric scattering adds brightness, while atmospheric absorption subtracts brightness, from ground target reflectance's (Jensen, 1996). Radiometric corrections are applied to remotely sensed images in order to reduce the influence of these factors and thereby strive for radiometric uniformity between multiple images. If radiometric corrections are not carried out, the accurate interpretation of imagery is at risk, especially when dealing with ratio or transformed data such as NDVI (Goyot & Gu, 1994; Verstraete, 1994; Vogelmann *et al*., 2001). There are two types of radiometric corrections, namely absolute and relative (Mather, 2003). Absolute radiometric correction methods attempt to remove all radiometric errors from the image and produce an output image of absolute surface reflectance for each pixel (Chavez, 1996; Song *et al*., 2001; Bruce & Hilbert, 2004; Chen *et al*., 2005). Absolute radiometric correction makes use of the satellite calibration parameters as well as atmospheric properties to correct the errors (Chen *et al*., 2005). Relative radiometric correction, also known as relative radiometric normalisation, attempts to reduce radiometric error within and

between multiple images by empirically normalising the radiometry of all the images to the radiometry of a single reference image (Song *et al*., 2001; Bruce & Hilbert, 2004; Chen *et al*., 2005). Relative radiometric normalisation does not make use of external measurements, but rather uses information from sensor calibration metadata and from within the images themselves, so that they appear to have been acquired by identical sensors, with the same calibration and under identical atmospheric conditions (Song *et al*., 2001; Chen *et al*., 2005). As long as the measurement of surface reflectance between multitemporal images is kept consistent, there should be no need to favour absolute correction over relative normalisation according to Song *et al*. (2001).

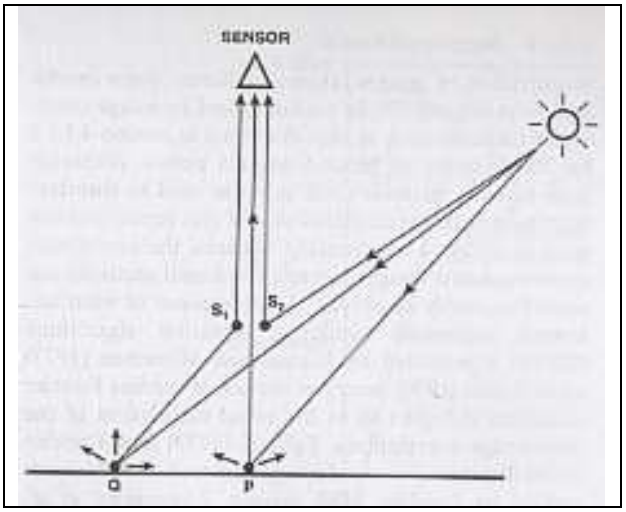

Figure 2: Components of the EMR spectrum being scattered in the atmosphere. Where Q and P are independent ground objects, and S1 and S2 are points where scattering occurs in the atmosphere (from Mather, 2003).

The relative radiometric correction process often includes the conversion of measured brightness values into top of atmosphere (TOA), or apparent, reflectance units (Mather, 2003; Bruce & Hilbert, 2004). Since this step does not result in ground level reflectance, which is a more accurate reflection of ground targets, Chander & Markham (2003) believe this step to be particularly appropriate for scenes with little or no noticeable atmospheric influence. Relative radiometric correction is used to normalise for variations between multitemporal scene's solar irradiances, sensor differences, earth-sun distances and solar zenith angles, by converting spectral radiances to top of atmosphere reflectance (Chander & Markham, 2003; Bruce & Hilbert, 2004).

Converting brightness values, or digital numbers (DNs), into TOA consists of two principle steps. The first step involves using in-flight sensor calibration parameters, usually provided as metadata by the vendors, to convert the DNs into radiance units that are measured in milliwatts per square centimetre per steradian per micrometer [mW/ ($cm^2 \cdot sr \cdot \mu m$)] (Chander & Markham, 2003; Mather, 2003; Bruce &

Hilbert, 2004; Smith, 2005). The sensor calibration parameters, for Landsat data, come in the form of gain and bias measurements for each spectral band, which represent the original rescaling factors used to convert spectral radiances into DNs. Radiance is therefore calculated using the following equation:

Equation 1:

$$\mathbf{L} = \mathbf{Gain \times DN + Bias}$$

Where:

L = the measured spectral radiance
Gain = $(L_{max} - L_{min})/255$
Bias = L_{min}
L_{max} = radiance measured at sensor saturation in mW/ ($cm^2 \cdot sr \cdot \mu m$)
L_{min} = lowest radiance measured by sensor in mW/ ($cm^2 \cdot sr \cdot \mu m$)

The next step would be to convert the calculated spectral radiance (L) into TOA reflectance, using the following equation:

Equation 2:

$$\mathbf{P_\lambda} = \frac{\boldsymbol{\pi} \cdot \mathbf{d^2} \cdot \mathbf{L_\lambda}}{\mathbf{E_\lambda} \cdot \mathbf{\cos \theta_s}}$$

Where:

$\mathbf{P_\lambda}$ = Reflectance per band
$\mathbf{d^2}$ = Earth-sun distance in astronomical units
$\mathbf{L_\lambda}$ = Radiance per band
$\mathbf{E_\lambda}$ = Exoatmospheric irradiance
$\mathbf{\theta_s}$ = Solar zenith angle in degrees

2.3.3 Topographic Correction

Each pixel's spectral character is also influenced by the terrain in which it is situated. Influences such as slope, aspect and angle of the sun all play a role in determining how a particular pixel is illuminated, and therefore combine to form dark slopes facing away from the sun, and bright slopes facing the sun (Figure 3). Topographic correction, or topographic normalisation, is used to compensate for these variations in the illumination of pixels (Colby, 1991; Conese *et al*., 1993; Mather, 2003; Riaño *et al*., 2003; Bruce & Hilbert, 2004). Topographic correction is regarded as an important step in achieving increased multispectral, and multitemporal, image classification accuracies (Jensen, 1996; Riaño *et al*., 2003). Topographic correction methods can be divided into two groups. The first makes use of band ratios and does not require any external data. This is a simple method to carry out, but it results in a loss of spectral resolution and is therefore not desirable for multispectral classifications. The second group

of topographic corrections makes use of external data in the form of DEMs. The DEMs are used in combination with a variety of algorithms to model the correct amount of illumination a pixel should exhibit (Bruce & Hilbert, 2004). For this reason it is important that the DEM be of the same geometric precision and spatial resolution as the accompanying imagery (Pons & Sole-Sugranes, 1994; Jensen, 1996).

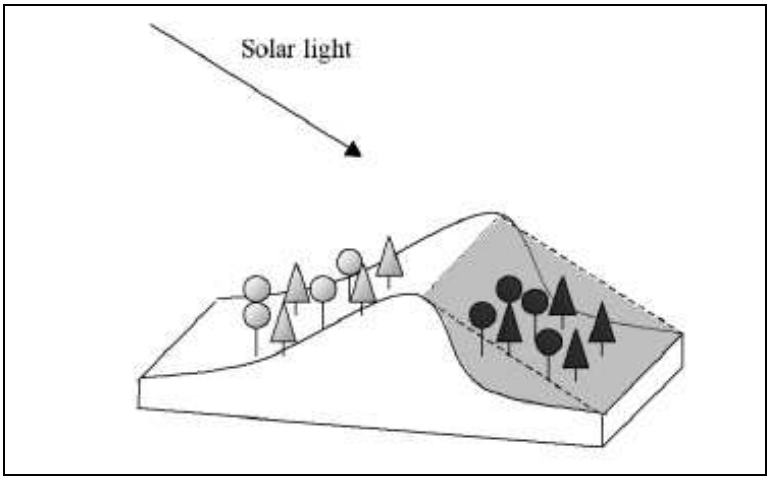

Figure 3: Topographic effects on reflectance (from Riaño et al. 2003).

The DEM-based topographic correction methods generally use two types of models for the topographic correction, namely the lambertian and non-lambertian models (Colby, 1991; Conese *et al*., 1993; Mather, 2003). The difference between the two models depends on whether or not they assume reflectance to be independent of observation and incident angles (Riaño *et al*., 2003). The lambertian model is computationally simpler but has been described as unrealistic, and has been shown to produce overcorrection and/or inaccurate results (Colby, 1991; Jensen, 1996; Colby & Keating, 1998; Riaño *et al*., 2003). The non-lambertian model has been shown to better reflect the true nature of surfaces and is therefore regarded as being more accurate, especially when using the Minnaert constant/correction in the model (Smith *et al*., 1980; Colby & Keating, 1998). The Minnaert correction method involves a constant (K) that models the non-lambertian behaviour of the surface, and appears in the non-lambertian model in the following equation:

Equation 3:

$$\mathbf{L_N} = \frac{\mathrm{L}\cos(e)}{\cos^k(f)\cos^k(e)}$$

Where:
$\mathbf{L_N}$ = Normalised brightness values
$\mathbf{L}$ = Observed brightness values
$\mathbf{\cos(e)}$ = Cosine of the existence angle, or DEM slope
$\mathbf{\cos(f)}$ = Cosine of the sun incidence angle of radiation
$\boldsymbol{k}$ = The Minnaert constant
= slope of the least squares line that relates log[L cos(*e*)] and log[$\cos^k(f)$ $\cos^k(e)$]

It is often necessary to separate the images into different samples representing similar ground covers, since the value *k* is dependant on the nature of the ground cover (Mather, 2003). This, however, causes a circular problem in that topographic correction is applied in order to better determine land cover types (Mather, 2003). Topographic correction procedures are often unable to properly correct areas of shadow that are caused by deep valleys, and therefore Meyer *et al*. (1993) suggest that these areas be masked out.

2.3.4 Filtering of Time Series Data

The temporal and spatial resolution of satellite sensors such as MODIS and the AVHRR, provide the scientific community with long term information on the changing nature of the earth's surface. More specifically, Vegetation Index (VI) products derived from these satellite programs, such as 16-day (MODIS), or 10-day (AVHRR) NDVI or SPOT VGT composite images, provide valuable information on the state of vegetation. Products such as the 16-day or 10-day NDVI images are the result of filtering and compositing algorithms applied to 16-days, or 10-days, of individual images by the data suppliers. The VI products are produced using daily surface reflectance images, which are corrected for atmospheric influences (Vermote *et al*., 2002), and then subjected to the compositing algorithms. The images are filtered, on a per pixel basis, according to the quality of the data, the presence of cloud, and the viewing geometry of the sensor (Didan, 2005). Pixels that contain cloud, or have oblique geometries (off-Nadir) because of the angle of the sensor, are flagged as lower quality pixels and often fall away during the filtering process (van Leeuwen *et al*., 1999). This filtering process often then cuts the available pixels from 16 to between five or ten (Didan, 2005). Compositing methodologies are then applied to the remaining images, also on a per pixel basis, in order to find the remaining pixels that will best represent that particular period. These methodologies select pixels based on either their maximum value, or the combination of a pixel's maximum value and its viewing angle (Didan, 2005). Despite each composite being subjected to the above methods in order to 'clean' it, it is still possible that many

of the pixels in the resultant composite are of a low quality because of the consistent presence of clouds. It is then up to the researcher to evaluate the presence of these pixels and, if necessary, make use of statistical techniques, such as interpolation and harmonic analysis, to correct for these data. In so doing, they create a 'smooth', uninterrupted time series of good quality data.

2.4 Change detection techniques

As mentioned before, there are a multitude of digital image change detection techniques, each of which could be spatially, spectrally or temporally constrained (Lu *et al*., 2003). This makes choosing the right one particularly difficult. The change detection techniques discussed below will be grouped into four categories, namely (1) visual analysis, (2) algebra, (3) transformation, and (4) classification.

2.4.1 Visual Analysis

This is the simplest, and probably oldest, of the change detection techniques. Visual analysis was often used to interpret aerial photography in the days prior to digital satellite imagery (Lu *et al.*, 2003). Visual analysis makes use of an analyst's knowledge of the area, and their ability to interpret changes in texture, shape, size and patterns of elements in the image (Lillisand & Kiefer, 1994). It also includes the analysis of multi-date image composites, which involve assigning images of different dates to either a red, green or blue colour palette in the imaging software. This means that changes are easily identifiable, because, depending on the date when they occur, they will appear as different colours in the composite. This category of methods is seldom used due to the difficulty in extracting quantitative data, except through the arduous task of manual digitising (Lu *et al*., 2003).

2.4.2 Algebra

This category includes popular methods such as image differencing, image regression, image ratioing, and vegetation index differencing (Singh, 1988). The basic premise behind these methods is to use basic algebra, such as subtraction or division, to extract the change between two images of different dates. The change is then identified and quantified using different thresholds. The most common method of thresholding is the standard deviation method, which only identifies change that occurs within a certain number of standard deviations away from the mean. The only major considerations that need to be taken into account when using methods in this category are which bands, vegetation indices, and thresholding techniques are to be used. The initial ratioing of bands, often before performing vegetation index differencing, has the advantage of reducing topographic effects and normalising radiometric errors between multi-date images (Singh, 1988). The one recognised disadvantage of this category is the lack of any change matrices that indicate directions of change; instead it merely provides an indication of

change, and no change data. There are numerous examples of researchers using this method, often in combination with other methods, in order to detect change (Lu *et al*., 2003).

2.4.3 Transformation

The transformation category includes the common methods of Principle Component Analysis (PCA) and the Kauth-Thomas (KT), or tasselled cap, transformation. It also includes the more complex, and less frequently used Gramm-Schmidt (GS) and chi-square transformations. The PCA removes redundant data by combining bands that are highly correlated to form new images, or principal components (ERDAS, 1997). Most of a scene's information will appear in the first few principal components, and will continue to decrease with increasing principle components. A PCA is commonly used in time series analysis, where there is a high data redundancy among hundreds of images. The tasselled cap transformation is similar to the PCA, except that the tasselled cap has predetermined coefficients applied to it, and it is therefore scene independent (Kauth & Thomas, 1976; Jensen, 1996). The coefficients used can depend on the sensor (e.g. TM or ETM+), as well as the characteristics of the scene (e.g. arid or humid environment) (Huang *et al*., 2002). As with the algebra category, change matrices are not provided and thresholding must be used to identify change. The advantage of this category lies in its ability to use information from each of the bands of an image, and then highlight different aspects of this information in the resultant components.

Vegetation indices can be seen as a form of image transformation, as they use information from certain bands, namely the red and near infra-red (NIR), in order to produce an image that closely represents leaf area index, or vegetative cover in an area. Healthy vegetation absorbs red wavelengths (600 - 700 nm), while reflecting NIR wavelengths (700 – 1 000 nm), which also correspond to the spectral ranges of the red and NIR bands found on most remote sensors. Using the ratio between the red and NIR bands, the analyst is able to exploit these distinctive spectral properties of green vegetation, and create vegetation index images (Nordberg & Evertson, 2003). These vegetation index images are commonly used in differencing techniques, in order to analyse spatio-temporal vegetation patterns (Schmidt & Karnieli, 2000).

2.4.4 Classification

Included in the classification category, are the common post-classification comparisons and unsupervised change detection. It also includes more complicated methods, such as Artificial Neural Networks (ANN) and hybrid change detection methods. This category involves the spectral classification of images, usually of different dates, followed by spatial comparisons of the different

classes. This spatial comparison results in the all important change matrix that refers to the amount, and direction, of change taking place. One advantage of the post-classification comparisons is that images are usually classified independently of each other, hence minimising any environmental, or atmospheric, differences between the images (Lu *et al*., 2003). This, however, does not apply when making use of combined bi-seasonal (winter / summer or autumn / spring) imagery in order to improve classification results. Fuller *et al*. (1994) improved their classification accuracies by combining winter and summer scenes (i.e. classification is carried out on a 12 band image made up of 2 different scenes), but they also warn of the potential error that image-to-image mis-registration can have on the end results. The difficulty in using post classification comparisons lies in the amount and quality of training data needed for an accurate classification result, especially when historical data is involved (Lu *et al*., 2003). Errors in image mis-registration and/or classification are often exaggerated in the thematic results, as well as the change matrix results. It has also been noted that the post-classification comparison method tends to underestimate areas of change, while overestimating degrees of change (Foody, 2001).

There are two main classification methods, namely the supervised and the unsupervised. The supervised approach is more popular but requires more detailed *a priori* knowledge of the area, as well as analyst skill, in order that appropriate training sites, and resultant spectra, are identified for classification (ERDAS, 1997). One of the most common and robust supervised classification algorithms is the maximum likelihood algorithm (Jensen, 1996). The probability that a pixel belongs to a particular class is what defines the maximum likelihood decision rule (ERDAS, 1997). Unsupervised classification algorithms, such as the Iterative Self Organising Data Analysis (ISODATA) algorithm, use differences in spectral distances in order to automatically cluster pixels into classes (ERDAS, 1997). Unsupervised classifications do not require the analyst to designate training sites at the beginning of the classification procedure, but rather requires that the analyst label the automatically determined classes that result from the unsupervised classification.

The above mentioned classifiers are often undertaken on a pixel-by-pixel basis and make use of different statistical distances between the pixels and the training site signatures (Lillisand & Kiefer, 1994). Recently another type of classifier, an object-based one, has emerged, and has generally had better success with the narrow band, high spatial resolution data, such as IKONOS, SPOT 5 or Quickbird (Willhauck, 2000). The object-based method not only makes use of the available spectral information, but also of texture, shape, area and scale information (Laliberte *et al*., 2004). The classification process, in this case, begins with a segmentation of neighbouring pixels into homogenous

units or objects (Baatz *et al*., 2004). Multiple segmentations can be run, each with different scale, form or textual information, and in so doing create a hierarchical network of image objects (Baatz *et al*., 2004). Due to the hierarchical nature of the image segmentation, relationship-based classification is possible because each pixel is aware of its neighbour on the same, lower, or higher level as itself (Laliberte *et al*., 2004). Classification is performed using fuzzy logic. Fuzzy logic uses logical operators in order to define a class, and then uses degrees of assignment in order to allocate classes to objects (Brandtberg, 2002). The fuzzy logic is either applied via the rather simple supervised nearest neighbour approach or through the combination of rather complex fuzzy rule sets or decision trees (Baatz *et al*., 2004).

2.5 Change detection in semi-arid and arid environments

Almost 50 % of the world's total surface area consists of semi-arid and arid lands (Meadows & Hoffman, 2002). Despite their remoteness and small numbers of human inhabitants, these areas often support a variety of economic activities, such as communal and commercial grazing, mining operations and tourism. The sensitive nature of these lands means that it only requires a small number of disturbances to cause major changes within the landscape (Okin *et al*., 2001a). Mismanaged anthropogenic activities can therefore cause, or exacerbate, desertification and degradation processes in these areas. It is usually difficult and expensive to map or monitor these landscapes due to their size, remoteness, rugged terrain, and climatic extremes (Okin & Roberts, 2004). As a result, remote sensing is fast becoming an important tool to use in the study of these areas, as it can provide cost-effective information on the state of the land on a regular, continuous and near real-time basis (Zhou *et al*., 1998).

Analysis of available literature reveals that when compared to change detection studies involving forests or temperate environments, the study of vegetative change detection in arid environments is in the minority. A number of change detection studies, such as Ram & Kolarkar (1993), Ray (1995), and Kwarteng & Chavez (1998), rely on the good contrast between agricultural lands or urban settlements, and the surrounding arid landscape, in order to detect land use or land cover change. However, the remote detection of vegetative change within arid areas is significantly more difficult, with the selection of appropriate methods being heavily scene dependant. Image differencing, and more specifically vegetation index differencing, is one of the most common vegetation change detection methods, mostly due to its simplicity (Singh, 1988; Lu *et al*, 2003). Lyon *et al*. (1998) concluded that the NDVI vegetation index differencing method performed the best when comparing several vegetation indices for change detection. However, Chavez & Mackinnon (1994) found that the red band differencing method provided better vegetation change information than NDVI could provide in an arid environment. Further

to this Pilon *et al*. (1988) preferred to use the visible red band data to detect changes in spectra for their semi-arid study site.

Using course resolution imagery, such as MODIS or AVHRR, for vegetation change detection, offers various advantages in that it covers larger areas on an almost daily basis, and costs far less than high resolution imagery. Tucker *et al*. (1986, 1991, 1994) have shown the usefulness of course resolution imagery in detecting inter-annual variations of vegetation, over long time periods, in the arid regions of Africa. In addition, desert vegetation phenology and its response to available moisture were successfully analysed, using course resolution data (Peters & Eve) 1995.

Change detection studies conducted on arid landscapes should, in addition to previously mentioned considerations, take cognisance of a range of other issues that complicate the detection of variations in the reflected EMR. Some of these issues include the following:

1) Low erratic rainfall and high potential evapo-transpiration characterise the arid and semi-arid regions of the world. The resultant low vegetation cover is therefore spatially limited by available moisture. This low vegetation cover means that the majority of the area-averaged reflectance of a pixel is of the soil substrate (Smith *et al*., 1990). Soils in these regions are also low in organic matter, and therefore tend to be bright. All these factors combine to effectively cancel out, or minimise, the vegetation signal present within a particular pixel (Huete *et al*., 1985; Huete & Jackson, 1987; Qi *et al*., 1994).

2) The variability of soils, and their spectral characteristics, throughout the landscape and resultant image also poses problems to the detection of vegetation. Huete & Jackson (1987) found that NDVI values were underestimated in areas of light soils and overestimated for areas with dark soils. This proposed weakness in one of the most common and widely used vegetation indices prompted an enormous amount of research into vegetation indices that accounted for or corrected soil noise (Bannari *et al*., 1995; Baret & Guyot, 1991). The research can be divided into two categories of vegetation indices, namely those that make use of the slope of the regression between red and NIR bands (slope-based), and those that made use of the perpendicular distance from a pixel to the bare soil line (distance-based) (Schmidt & Karnieli, 2000). Some of these indices will briefly be discussed:

a. Slope-based methods

The most common of the slope based methods, NDVI, was proposed by Rouse *et al*. (1974) and is expressed as the difference between the near infra-red (**NIR**) and red (**red**) bands normalized by the sum of those bands:

Equation 4:

$$\mathbf{NDVI} = \frac{\mathbf{NIR - red}}{\mathbf{NIR + red}}$$

Huete (1988) introduced a constant soil adjustment factor, *L*, into the NDVI equation in order to minimize the influence of soil background. Huete's (1988) Soil Adjusted Vegetation Index (SAVI), is represented by the following equation:

Equation 5:

$$\mathbf{SAVI} = \frac{\mathbf{NIR - red}}{(\mathbf{NIR + red + L}) \cdot \mathbf{(1+L)}}$$

The soil adjustment factor is represented here by ***L,*** and can vary between a value of 1.0 for low vegetation densities, 0.5 for intermediate densities, and 0.25 for high densities.

Qi *et al*. (1994) then proposed using a variable soil adjustment factor, as opposed to the constant one used in SAVI. The Modified Soil Adjusted Vegetation Index ($MSAVI_1$) requires a value for the slope of the soil line and the calculation of the Weighted Difference Vegetation Index (WDVI) of Richardson & Wiegand (1977):

Equation 6:

$$\mathbf{MSAVI_1} = \frac{\mathbf{NIR - red}}{(\mathbf{NIR + red + \mathit{L}}) \cdot \mathbf{(1+\mathit{L})}}$$

Where:
L = **1 - 2*s*NDVI*WDVI**
s = slope of the soil line

NDVI = as described above
WDVI = **NIR - (slope*red)**

The second Modified Soil Adjusted Vegetation Index ($MSAVI_2$), also by Qi *et al*. (1994), does away with having to calculate the slope of the soil line and the WDVI:

Equation 7:

$$\mathbf{MSAVI_2} = \frac{\mathbf{2NIR + 1 - \sqrt{(2NIR + 1)^2 - [8(NIR - red)]}}}{\mathbf{2}}$$

b. Distance-based methods

Richardson & Wiegand (1977) developed the Perpendicular Vegetation Index (PVI), after observing that bare soil pixels formed a straight line when scatter plots of red versus NIR were created. This straight line has a slope (**a**) and an intercept (**b**) value, and was called the 'soil line' (Richardson & Wiegand, 1977). The PVI therefore assumes that vegetation cover is linearly related to the distance of a pixel from a soil line, and can be calculated as follows:

Equation 8:

$$\mathbf{PVI_2} = \frac{\mathbf{(NIR - a(red) - b)}}{\mathbf{\sqrt{a^2 + 1}}}$$

Baret *et al*. (1989) altered the SAVI concept, by removing the soil adjustment factor and adding the soil parameters concept of the PVI. This resulted in the Transformed Soil Adjusted Vegetation Index (TSAVI), which can be calculated as follows:

Equation 9:

$$\mathbf{TSAVI_1} = \frac{\mathbf{[\,a(NIR - a(red) - b)]}}{\mathbf{(red + a(NIR) - a(b))}}$$

These are just a few of the multitude of available vegetation indices, and have been the subjects of soil background experiments that have ranged from using narrow band field-based reflectance in agricultural settings (Huete *et al*., 1985; Huete & Jackson, 1987; Qi *et al*., 1994), to using broad-band satellite-based measurements (Schmidt & Karnieli, 2000). All of these studies acknowledge the amount of noise and error that soil background contributes to the measurement of a vegetation signal, and therefore state that the removal of soil background effects should be a primary goal in any vegetation applications (Schmidt & Karnieli, 2000). NDVI is widely regarded as having the highest level of soil

noise, while soil noise specific vegetation indices tend to remove the noise in part and to various degrees (Schmidt & Karnieli, 2000).

3) Many remote sensing techniques, including VIs, are insensitive to non-photosynthetic vegetation (NPV), which can make up a significant, and biologically important, portion of the total ground cover in an arid region (Okin & Roberts, 2004). Therefore, vegetation indices, or any other NPV insensitive techniques, may not be used as surrogates for vegetation cover, if the area in question is characterised by a significant NPV component (Okin & Roberts, 2004).

4) Roberts *et al*. (1990) suggest that a plant's linear reflectance, especially in the NIR, is affected by canopy structure. In arid regions where open canopies and underlying bright soils are common place, there is enormous potential for multiple scattering and non-linear mixing of the reflected EMR (Okin & Roberts, 2004).

5) Vegetation in arid regions has adapted to its harsh environment by limiting the use of photosynthetically active radiation (PAR), as excessive PAR can lead to overheating and moisture loss for the plant (Okin & Roberts, 2004). Limiting the use of PAR means that plants reduce their surface areas through which they would lose moisture, hence leaves are significantly reduced in size or are even replaced by spines or fine hairs (Okin & Roberts, 2004). Plants in these areas also reduce the amount of chlorophyll present, in order to further reduce overheating, which when combined with reduced surface areas, results in this vegetation being spectrally difficult to detect (Okin & Roberts, 2004).

6) Arid land vegetation has adapted its phenological cycles to coincide with available moisture, which can show enormous spatial and temporal variability in an arid landscape (Okin & Roberts, 2004). In this vein, a number of studies have shown that perceived human-induced degradation and/or desertification often turned out to be variations in rainfall instead (Tucker *et al*., 1991; Anyamba & Tucker, 2005; Nicholson, 2005). These phenological changes result in varying inter-species, and intra-species, spectral characteristics that make the accurate discernment of vegetation types extremely difficult (Okin & Roberts, 2004). Intra-species spectral variability can often be greater than the inter-species variability according to Franklin *et al*. (1993).

This chapter has outlined what remote sensing is, how it works, some examples of remote sensing data products and systems, as well as why and how remotely sensed data is increasingly being used for change detection studies. The important tasks that prelude a change detection study and ensure precise

image pre-processing where explained, as where the positives and negatives of various change detection techniques. Finally the chapter touched on more specific challenges facing remotely sensed change detection methods in semi-arid and arid environments.

Chapter 3

Rationale and Research Questions

3.1 Rationale

The Richtersveld is under direct pressure from anthropogenic activities such as mining, semi-commercial / subsistence livestock rearing and illegal harvesting of sensitive species. Combined with these anthropogenic threats are the possible indirect effects of global warming and climate change. The Richtersveld is also a biologically intricate, event driven, hyper-arid ecosystem with complex topographies that, together with its proximity to the cold Benguela ocean current, contribute toward there being two rainfall seasons, namely the low but predictable winter rainfall season and the low but more unpredictable summer rainfall season. Research such as Foden *et al*. (2007), and Midgley & Thuiller (2007) suggest that the Richtersveld and its sensitive species are potentially at greater risk to climate change than previously believed. Therefore the complexity of this biologically valuable region and its present and future threats need to be understood in order that informed management decisions can be made about the co-existence of biodiversity conservation and semi-commercial livestock activities. Remote sensing provides a synoptic, and objective, tool with which landscape change can be detected and/or monitored over time. Before a remote sensing change detection study takes place, it is crucial that the relationship between available moisture and vegetation response be understood. This relationship should then aid in the interpretation of results from spatial and temporal change detection techniques. The following research questions address the need for an understanding of relationships between available moisture and vegetation response, as well as the detection of vegetation cover change that may have occurred over time and space.

3.2 Research Questions

1) Given the need to understand the vegetation response within the Richtersveld to available moisture the following question was posed: Using measured rainfall data, and synoptic course scale imagery, Is it possible to determine the relationship between available moisture and vegetation response, in order to aid in the interpretation of vegetation cover change results.

2) Course spatial and fine temporal resolution MODIS imagery of 250m is available, but it is relatively recent imagery (i.e. since early 2000). Imagery such as SPOT VGT and NOAA AVHRR can provide a longer time series of data than MODIS can, but they were deemed to have too course a spatial resolution (1 km) to capture some of the complexity of Richtersveld. Therefore, using six years (2000 to 2005) of

available MODIS imagery: Can this course scale imagery discern cycles of vegetation response to available moisture? Does this response suggest any inter- or intra-annual climate variations in the region?

3) Finally, with an understanding of how the region's vegetation responds to available moisture rainfall: Is it possible to detect specific areas of vegetation cover change using medium spatial and temporal resolution imagery over a 14-year period?

Figure 4 presents a flow diagram that illustrates the flow of the thesis from here on. Each question is addressed in a different chapter, and makes use of different data sets, but it is the interpretation of all three sets of results that allows for synthesis and conclusions to be made.

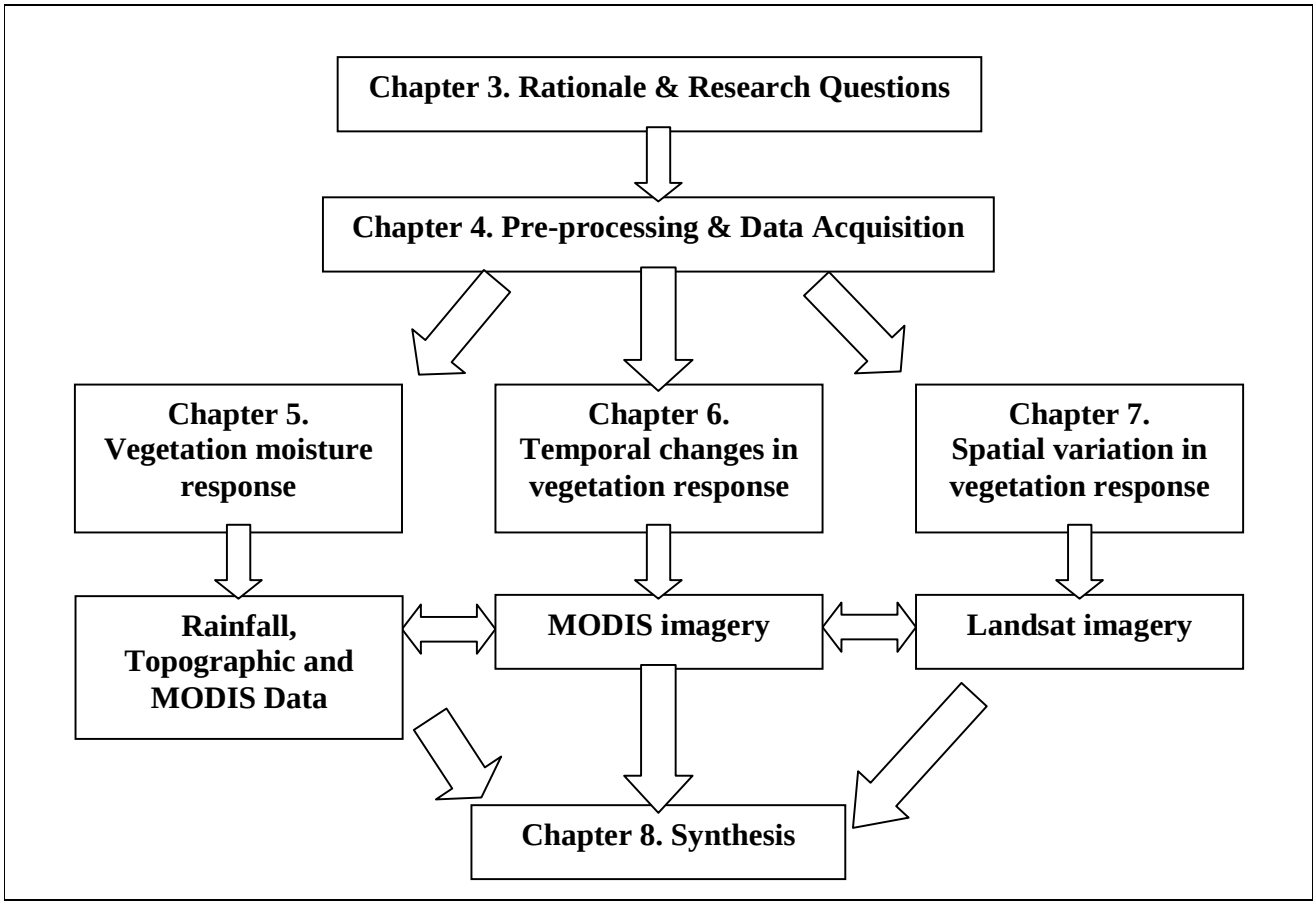

Figure 4: Flow diagram illustrating layout of thesis

Chapter 4

Acquisition and Pre-processing of Data

4.1 Acquisition

The acquisition of available and affordable imagery was procured through the Satellite Applications Centre's (SAC) online data catalogue. All available Landsat images for acquisition Path 177, Row 80 were viewed and qualitatively assessed according to atmospheric interferences (cloud, haze, dust) and for matched anniversary dates (Table 3). Acquiring anniversary wet and dry imagery for the Richtersveld region posed some problems due to the fact that the region exhibits, albeit very sparse, winter and summer rainfall characteristics. Nevertheless, ten anniversary date Landsat TM, and two Landsat ETM+, level 1G corrected images were acquired. This broadly equated to a wet and dry image for each of the following years: 1989, 1991, 1994, 1997, 2001 and 2004.

Table 3: Purchased image characteristics for Landsat scene, path 177, row 80.

Date	Sensor	Resolution
02/04/1989	Landsat 5 TM	30m
25/09/1989	Landsat 5 TM	30m
23/03/1991	Landsat 5 TM	30m
17/10/1991	Landsat 5 TM	30m
31/03/1994	Landsat 5 TM	30m
25/10/1994	Landsat 5 TM	30m
23/03/1997	Landsat 5 TM	30m
17/10/1997	Landsat 5 TM	30m
11/04/2001	Landsat 7 ETM+	30m
20/10/2001	Landsat 7 ETM+	30m
11/04/2004	Landsat 5 TM	30m
02/09/2004	Landsat 5 TM	30m

4.2 Pre-processing

Despite the images being level 1G corrected[1], they did not have sufficiently accurate pixel-to-pixel registration and were not atmospherically corrected. For the sake of continuity and data sharing within the BIOTA project, the images were therefore manually geo-corrected, to a previously corrected BIOTA 2001 Landsat 7 ETM+ panchromatic band. The geo-correction was carried out using approximately 80 Ground Control Points (GCP's), evenly distributed across the image, and made use of a nearest neighbour 2nd order

[1] Level 1G correction includes some basic radiometric and geometric corrections that may require additional correction by the user.

polynomial correction within the ERDAS 8.6 software range. The nearest neighbourhood resampling procedure was preferred to others such as bilinear or cubic convolution, because it is superior in retaining the spectral information of the image (Colby, 1991). As per the remote sensing literature, the root mean square (RMS) error per image was kept below half the spatial resolution of the image pixels, i.e. < 15 meters (Townshend *et al*., 1992; Jensen, 1996; Mather, 2003).

In order to get the images topographically and atmospherically corrected, they needed to be subset according to available digital elevation models (DEMs), which are integral to the topographic correction as explained above in section 2.3.3. There were three available DEMs, namely a European Remote Sensing (ERS) 90 meter DEM, which was resampled to 30 meters; a 90 meter Shuttle Radar Topography Mission (SRTM) derived DEM that was also resampled to 30m, and a DEM constructed from 20 meter contour data, and then resampled to a resolution of 30 meters. The software programme ATCOR 3 (Richter, 2001 & 2003) was then used in an attempt to atmospherically and topographically correct the images, using whichever DEM gave the best results. Unfortunately the ATCOR results, using all three DEMs, yielded unsatisfactory corrections, potentially due to SAC pre-processing procedures that were applied to the images (Richter, 2005, pers.com), or a software glitch (Vogel, 2005, pers.com). The alternative is that ATCOR has not been applied to such hyper-arid and topographically extreme environments. Due to time and cost constraints, and based on the reasoning that the study area was a desert environment with a relatively clear atmosphere, it was deemed reasonable that the images be radiometrically corrected to top of atmosphere reflectance using interface description language (IDL) algorithms (see equations 1 and 2)[2]. The gain and bias information necessary for the calculations are usually retrieved from the header files of each image, however it is suspected that these were also incorrect values as the results of the TOA conversion produced negative reflectances. New gain and bias values, derived from invariant features in the imagery, were calculated and used for the conversion (Richter, 2005, pers. com.). Each pair of images, from each year, were then normalised using the dark object subtraction method (DOS). The DOS method normalises images according to a base image, in this case the dry season image of each year, so that they appear to have been taken under the same atmospheric conditions (Chavez, 1996). This was required as the classification was to be conducted on an image stack of both wet and dry images. IDL was also used to create a model, based on the Minneart constant correction method that would attempt to topographically correct the images. Unfortunately neither of the DEMs could accurately capture the complexity of the Richtersveld topography, which resulted in poor topographic correction of the images. In the absence of topographically corrected images, all the images had to be masked for shadows.

[2] IDL is a programming language that enables communication between software components that do not share a common language (Wikipedia, 11 November 2007).

Low spatial but high temporal resolution MODIS data also became available for the study area. Due to bandwidth and FTP access constraints at the University of the Western Cape, the data was downloaded, via the MODIS website, by colleagues at the German Remote Sensing Data Center (DFD) of the German Aerospace Centre (DLR) at the University of Wuertzburg, Germany. The data consisted of 250 meter, 16-day NDVI composites for years 2000 through to the end of 2005 (product code MOD13Q1). As described previously (section 2.3.4), the 16-day NDVI products are produced by filtering and compositing daily reflectance images, some of which can be of poor quality due to the presence of clouds or other atmospheric anomalies. An IDL code-based programme called TiSeg, which was written by members of the DFD/DLR group in Wuertzburg, was used to subset the images, as well as identify and then interpolate for these poor quality pixels in order to get more continuous temporal NDVI signatures for all pixels. TiSeg, using a pixel-based iterative approach, evaluates the pixels using MODIS metadata, such as quality, cloud index, and sun and sensor geometry (Colditz *et al*., 2006; Colditz, 2006, pers.com). Any data gaps, usually smaller than or equal to five days, that existed due to invalid/poor pixels were identified and linearly interpolated (Colditz *et al*., 2006; Colditz, 2006, pers.com). All remaining data gaps were filled by a final interpolation followed by the removal of unnatural short term variations, using harmonic analysis (Colditz *et al*., 2006; Colditz, 2006, pers.com).

Daily rainfall figures, dating back to 1995, for stations within the study area were also acquired from the South African Weather Bureau. The stations were spatially disparate and the data was interspersed with too many zero rainfall days for there to be any possibility to interpolate rainfall maps, or conduct any detrending analysis such as Archer (2004). Only five of the available rainfall stations were used together with an appropriate subset of the NDVI images, due to the spatial disparity of the rainfall stations. In order to analyse the data in combination with the NDVI image data, the sum of 16-days of rainfall, from January 2000 to December 2005, were created for each of the five selected rainfall stations. A ‘regional average’ was then taken by averaging the summed rainfall for the five stations, which was then analysed against the appropriate MODIS NDVI subset.

4.3 Validation

An attempt was made to collect validation data during the study, to perform accuracy assessments on the classification and image differencing results. Unfortunately, field sampling was curtailed by two unplanned events, which resulted in budgetary constraints for further field validation[3]. Some field validation data (33 points) was collected during field campaigns in March of 2005 and 2006, as well as September of 2005. Alternative validation procedures were also sought. Given that no independent data existed at the time, the

following technique was used: five hundred stratified random reference pixels, which were geographically representative, were generated using the appropriate software methods (Figure 5). Then, based on field validation exercises that had taken place, as well as the local knowledge of various people, these pixels were subjectively allocated to what was considered to be the correct class and used in an accuracy assessment. Theoretically, vegetation cover data should also have been collected in order to validate the vegetation index images. However, even if this data had been collected, the ability to distinguish between 0 % and 20 % sparse vegetation cover using 30m multispectral imagery would have been very limited (Okin *et al*., 2001a). Okin *et al*. (2001a) points out that although some authors have managed to measure extremely sparse vegetation covers (Elmore *et al*., 2000; McGwire *et al*., 2000; Okin *et al*., 2001b), it was done using high precision in situ data, advanced spectral unmixing techniques and/or low signal to noise hyperspectral sensors.

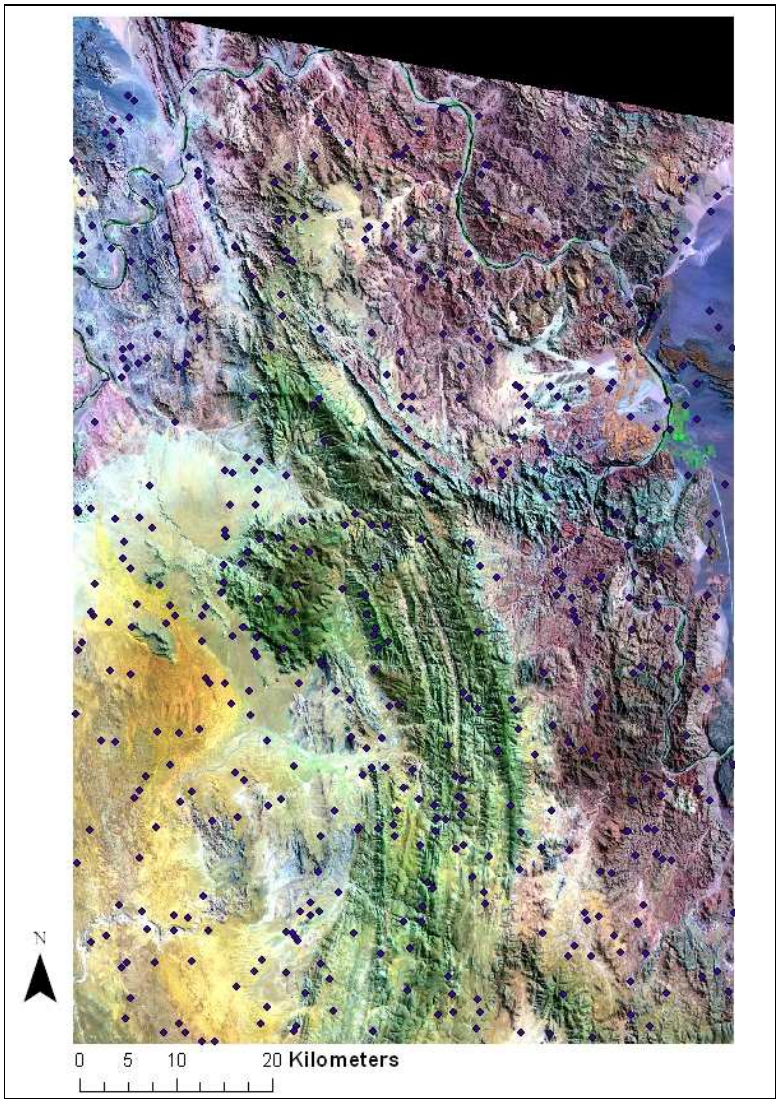

Figure 5: A 30m Landsat image (band combinations: R:3,G:4,B:1) showing the study area, as well as the random validation points used in the accuracy assessment.

[3] One field validation exercise was cut short due to unexpected flooding that resulted in the RNP being evacuated and closed, while another was cut short due to a medical situation that required urgent attention.

Chapter 5

Vegetation Moisture Response

5.1 Methods

To answer question 1, the relationship between moisture and vegetation response was investigated. Nicholson *et al*. (1990) and Schmidt & Karnieli (2000) investigated the possible correlations between the NDVI signal and the rainfall records. Nicholson *et al*. (1990), in their study on NDVI's dependency on precipitation variability, determined that NDVI was best correlated to the concurrent plus two previous months of rainfall. The analysis made use of 16-day averaged rainfall values calculated from daily rainfall figures, of five different stations (see Figure 11). An appropriately positioned subset of NDVI values were retrieved and correlated to the 16-day averaged rainfall, as well as the sum of the current rainfall value plus the rainfall for *n* prior time periods, so as to account for the lag time between rainfall and vegetation green-up. Given the nature of the rainfall data (i.e. many zero days with erratic rainfall events) and the number of rainfall stations to work with, it was unlikely that a detrending of the NDVI signal would work (Archer, 2004).

Together with rainfall, vegetation also responds to other sources of moisture, such as fog, dew or cloud. The availability of these alternative sources of moisture to vegetation is influenced by topography. Therefore, trends of vegetation response (i.e. NDVI) in relation to topography were investigated, in order to further aid in the interpretation of vegetation responses to available moisture. This was carried out by resampling, using Nearest Neighbour techniques, the 90 m SRTM DEM to a 250 m DEM. Altitude, slope and aspect images were then created. These images were then made into class images, with each class having an equal amount of pixels. The class images were then used to extract NDVI statistics from the MODIS imagery. Mean MODIS NDVI values were also extracted for each of the vegetation classes (from Mucina & Rutherford, 2006) that make up the Richtersveld study area. This would provide an idea on the spatial variation of vegetation cover, and implied available moisture, and would hopefully comply with appropriate literature with regards to climatic conditions that determine available moisture and therefore vegetation cover.

5.2 Results and Discussion

The results from the rainfall/NDVI correlation analysis appear to agree with literature in that the NDVI signal has a small, but significant ($p < 0.005$), relationship with the cumulative rainfall of *n* time periods (Table 4, Figures 6 and 7). The small correlations could be seen as disappointing given the usually rapid

vegetation response to rainfall in arid areas, and the quality of the rainfall data should possibly be questioned. However, the small correlations could be indicative of the fact that rainfall is not the only major driver of vegetation response in this region, and therefore points towards the vegetation response being reliant on other sources of moisture such as fog and dew (Desmet, 2007). The mean NDVI response curves (Figure 6) show the major green-up in the year to be during the autumn and winter months (June to August), which corresponds with the documented winter fog and dew that take place in the region (Desmet, 2007).

Table 4: Pearson correlation coefficients for the relationships between MODIS mean NDVI values and rainfall, as well as the cumulative rainfall for n number of periods.

Pearson Correlation Coefficients	Rain	Rain-4-Period	Rain-5-Period	Rain-6-Period	Rain-7-Period
Correlation	0.088	0.315	0.398	0.450	0.488
P-value	0.306	0.000	<.0001	<.0001	<.0001
n	138	135	134	133	132

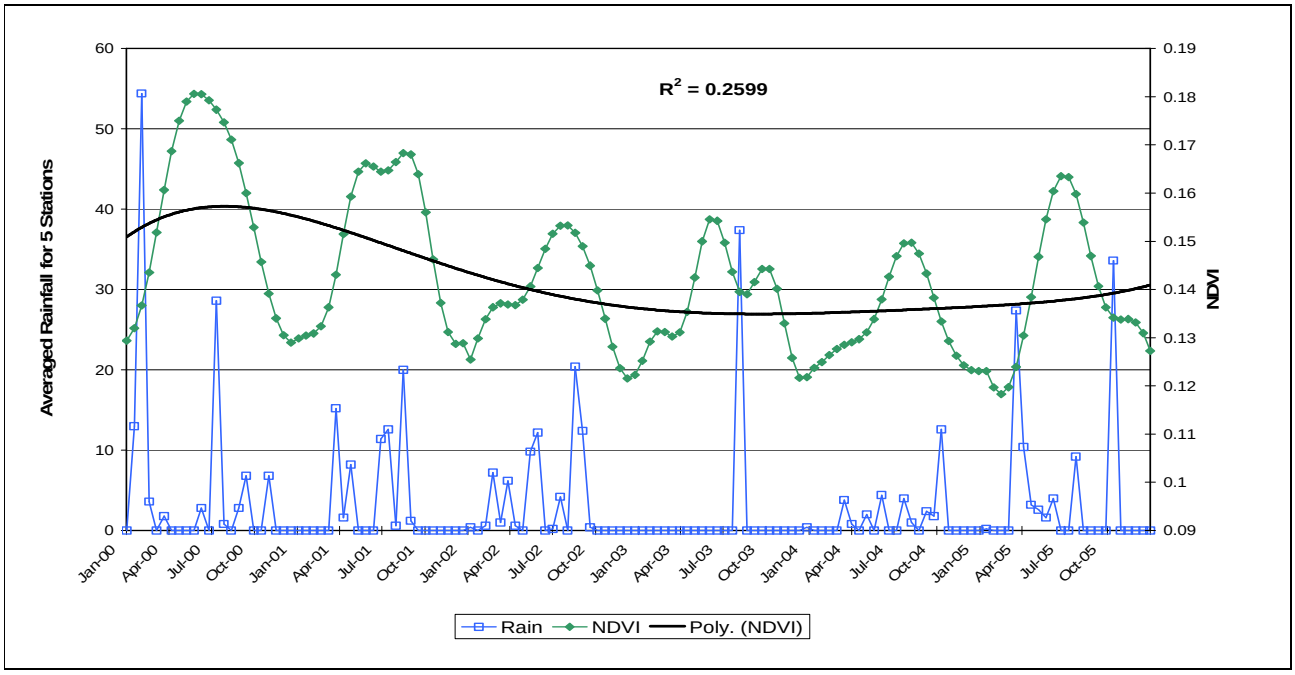

Figure 6: The 16-day averaged rainfall, for five rainfall stations (Claims Peak, Helskloof, Koeroegab, Kuboes and Tatasberg), with the MODIS 250m mean NDVI signal for same area, and its corresponding 5th order polynomial trend line

Box and whisker plots are presented (Figures 8, 9, 10) in order to show MODIS NDVI trends that exist as evidence of vegetation response to variations in topography, which indirectly affects the availability of moisture. Figure 8 shows the mean NDVI per altitude class where vegetation biomass appears to correlate to increases in altitude. Increases in altitude, in this particular case to a maximum of 1 365 meters, would be

associated with cooler temperatures and an increase in available moisture due to fog and cloud having to rise up over the uplands as they push in from the coast towards the interior.

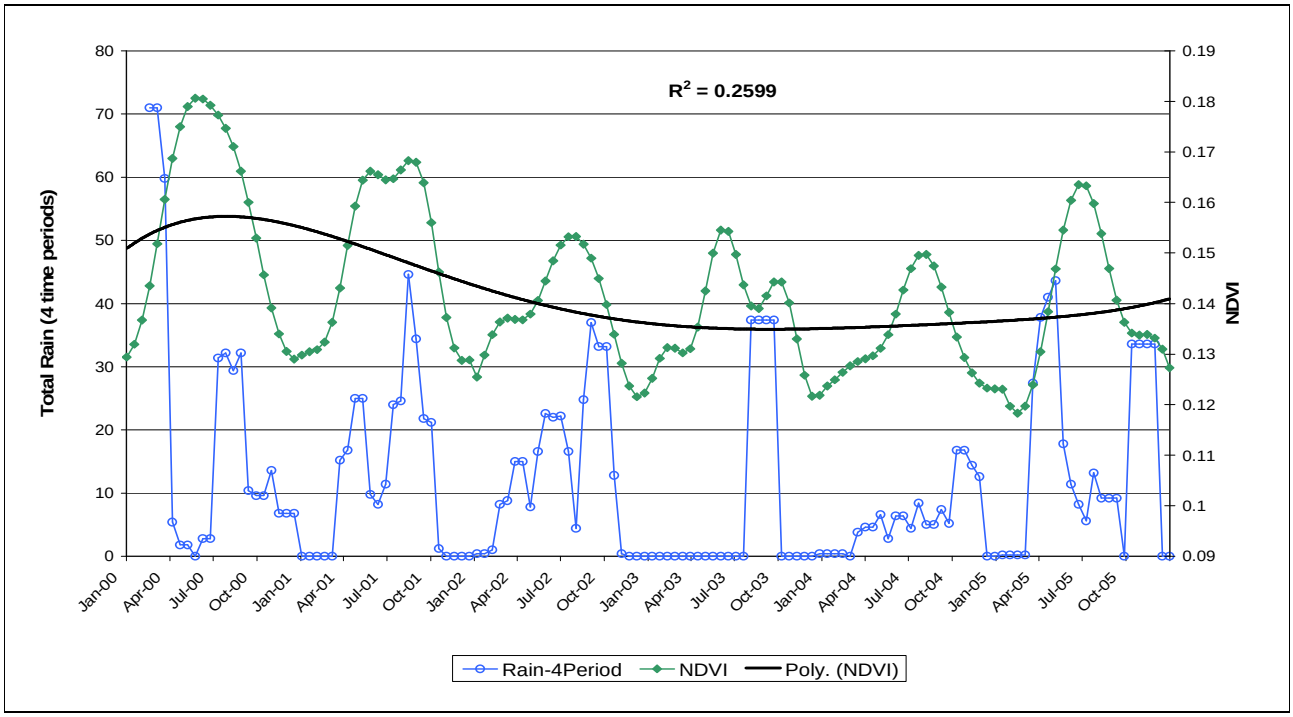

Figure 7: The concurrent plus four previous time periods of rainfall, with the mean MODIS 250m NDVI signal, and its corresponding 5th order polynomial trend line

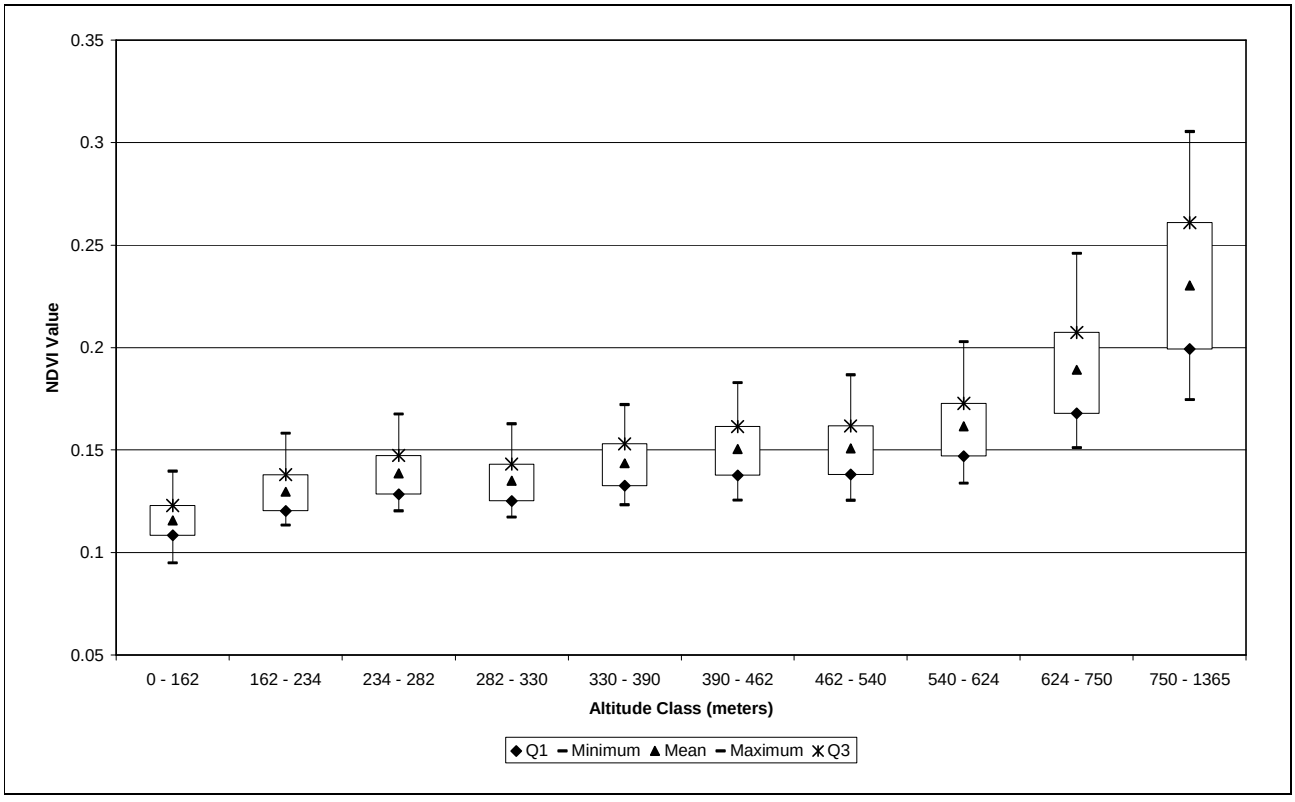

Figure 8: Mean MODIS NDVI per altitude class

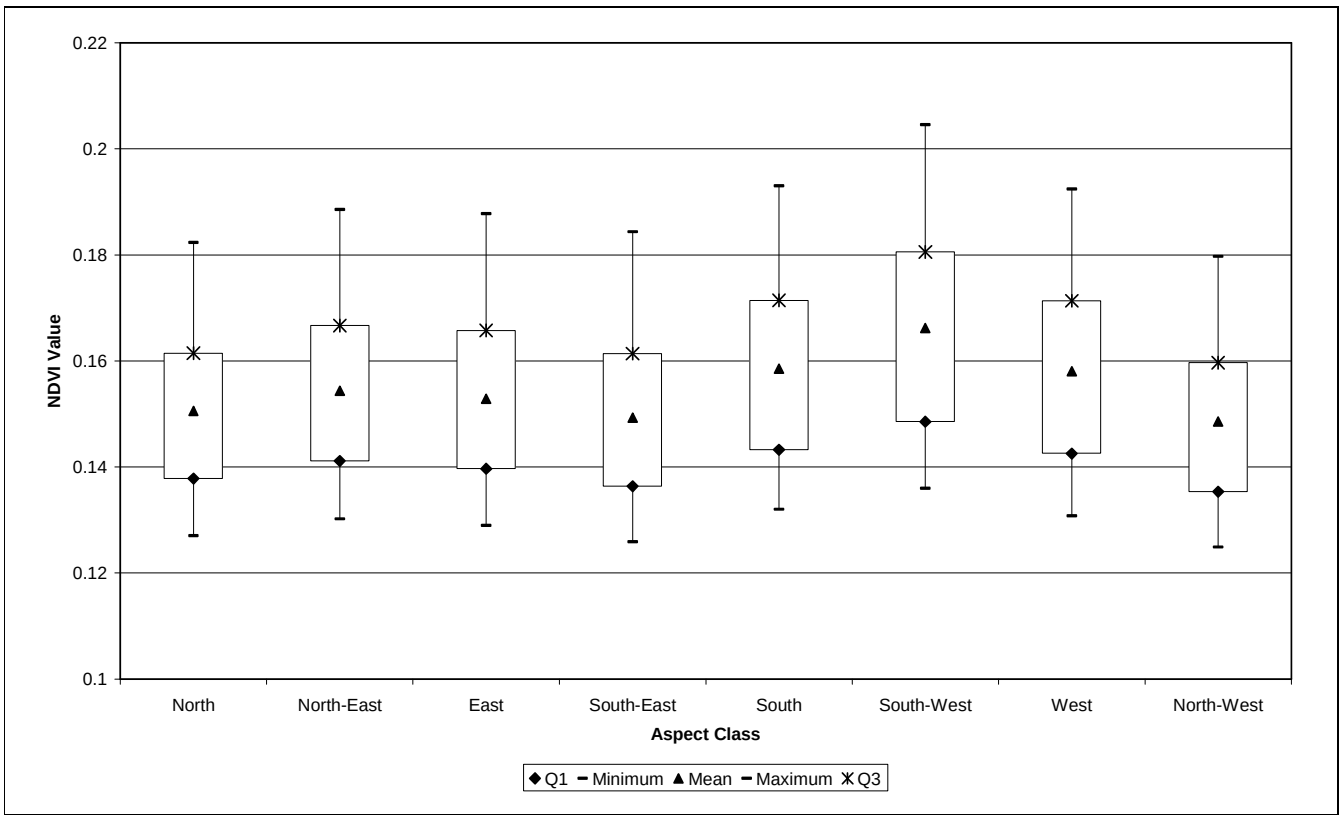

Figure 9: Mean MODIS NDVI per aspect class

Figure 9 shows the mean MODIS NDVI response to different topographic aspects, the results of which corroborate Mucina et al. (2006) who point out that the south western slopes have increased vegetation covers compared to the north western slopes. North western slopes, because of their orientation to the sun for much of the day, would have higher temperatures than south western slopes and therefore a greater potential for moisture loss. Together with having cooler temperatures, because of their orientation away from the sun, the south and south western slopes of the Richtersveld uplands also face the west coast and therefore are in line to intercept the incoming fogs and cloud. The mean MODIS NDVI response to slope is presented in Figure 10, which shows a dip in the vegetation response between very flat areas and areas that are very steep. This graph, when viewed as if it were a cross section through a landscape, could be interpreted as showing that flat areas have slightly more vegetation biomass than footslopes or gullies, but obviously less vegetation biomass than the steeper slopes associated with higher altitudes. Footslopes and/or gullies would have less vegetation biomass than flat areas because their relief would inherently deprive them of the water due to runoff, and they could be areas of high energy prone to erosion and destructive flooding. Areas with steeper slopes, up to a point where it becomes impossible for vegetation to grow, would be associated with higher vegetation biomass as they would occur at higher altitudes and the discussion around Figure 8 would then apply.

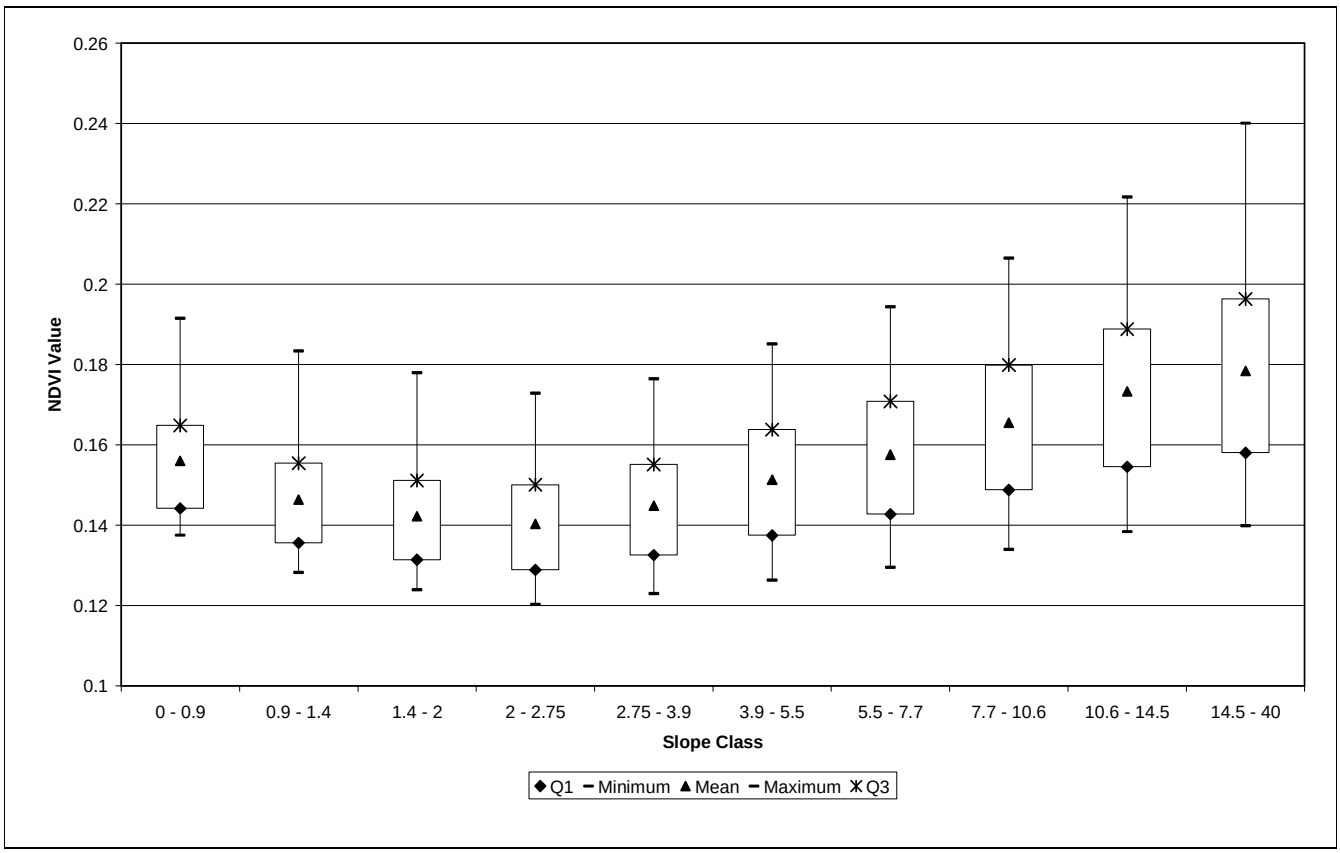

Figure 10: Mean MODIS NDVI per slope class

Figure 11 shows evidence of the spatial expression of vegetation response to factors such as altitude, slope, aspect, which combine with seasonal climatic oscillations to create spatially variable and unpredictable precipitation in some areas, while in other areas they combine to create more predictable and spatially invariable precipitation. The vegetation classes of the Richtersveld study area, derived from the 2006 vegetation map of Mucina & Rutherford (2006) are overlaid on a Landsat image in Figure 11 (a), along with the mean MODIS NDVI values for each class. The mean MODIS NDVI values (Figure 11 b) show evidence of differences between the Succulent Karoo biome and the Desert biome, with the later having vegetation classes that run along the river and show less of an NDVI vegetation signal than those classes that make up the Succulent Karoo. Obviously the south west facing upland areas, which intercept most of the winter precipitation, as well as some of the winter rainfall lowland areas, have the highest NDVI values.

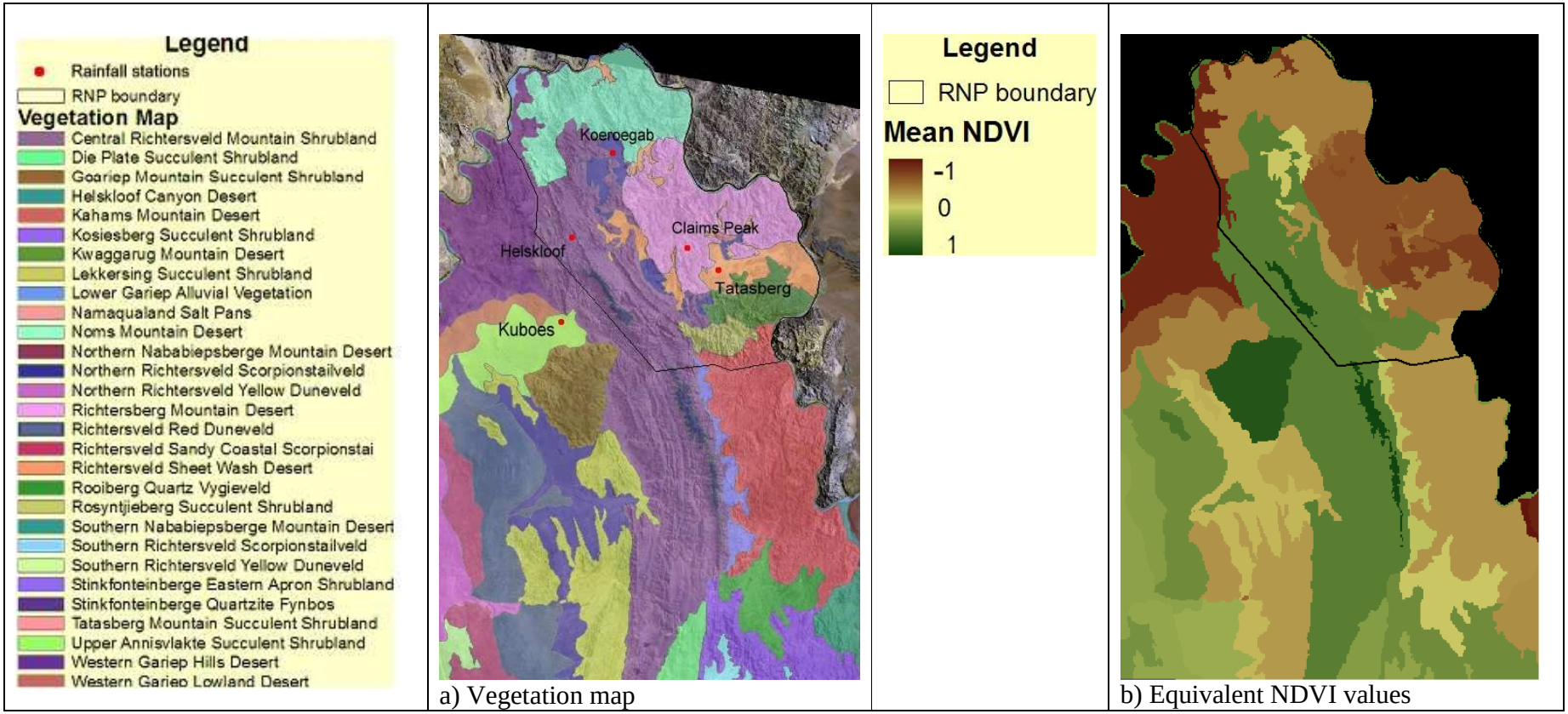

a) Vegetation map

b) Equivalent NDVI values

Figure 11 (a & b): The vegetation map (of Mucina and Rutherford, 2006) for the Richtersveld study area, as well as the mean MODIS NDVI value for each of these classes. The positions of the rainfall stations used for analysis are also shown

Chapter 6

Temporal Changes in the Cycles of Vegetation Response

6.1 Methods

For question 2, relating to the natural cycle of events in the region, all six years (2000 – 2005) of the MODIS data were analysed using a standardised principle component analysis (PCA). By removing redundant data and combining bands that are highly correlated, the PCA forms new images, or principal components, that often reflect the major components of variation over time (ERDAS, 1997). The PCA produces two outputs, namely the component images, which give an idea of the spatial variation taking place, as well as the component loadings that can be viewed in a graph and used for the interpretation of temporal variation taking place. In order to focus only on natural cycles of events, the agricultural area on the Namibian side of the river was masked out for all MODIS level data analysis.

A seasonality shift analysis was performed in order to determine if any temporal shifts in the seasonality of the region were occurring. For each year, a modality mask was created, making use only of pixels that exhibited a significant modal signature (i.e. unimodal or bimodal). The non-modal pixels of the mask were identified using either a difference between minimum and maximum threshold, or a standard deviation thresholding technique, while unimodal or bimodal pixels were identified using the explained variances from the harmonic analysis results. All non-modal pixels were then excluded. In order to investigate the temporal variability between years with similar modalities (i.e. the temporal shift caused by earlier or later seasons) each annual time series of significantly modal pixels (i.e. 2000, 2001, 2002, 2003, 2004 and 2005) was cross correlated with the six year mean NDVI signal for the whole region. Shifts of between one and four composites (i.e. between 16 and 64 days) were tested (both forwards and backwards) in order to produce lag images showing which pixels had or hadn't shifted in seasonality.

6.2 Results and Discussion

6.2.1. Principal Component's Analysis

Having investigated the role of rainfall as a vegetation driver, the time series of MODIS NDVI data provided an opportunity to look at the natural cycle of events taking place in the Richtersveld region. One of the first aspects noticed, concerning the natural cycle of events, was a small decrease in the mean NDVI signal between 2000 and 2005 (Figure 6). With only six years of data, it is difficult to interpret the significance of this trend to the region as a whole, especially considering the absolute value by which the NDVI decreased.

Table 5: The percentage variance explained by each of the resultant PCA components

	CMP 1	CMP 2	CMP 3	CMP 4	CMP 5	CMP 6
% Variance	89.23	3.91	1.21	1.04	0.61	0.44

The results of the PCA should do well to explain some of the variation, in terms of vegetation cover, taking place in the landscape between 2000 and 2005. As Table 5 shows, component 1 accounts for 89.23 % of all the variance in the images. This is typically described as showing the most common vegetation / NDVI distribution over time, while all subsequent components illustrate, in order, those change events that took place (Eastman, 2006). Since the components are not correlated to each other, every one of the components contains new information and explains different variations in the data time series. It is important when attempting to interpret component loadings and images that all available data is viewed in context and in relation to the component data. The loadings of component 1 (Figure 12) show a relatively straight line, except for three noteworthy dips or events in the data. These dips / events appear to also correspond to peaks / events in the component 2 loadings, as well as peaks in the NDVI maximum signal. These dips / events occur during the autumn and winter months of years 2000, 2001 and 2003. The NDVI images (Figure 14) that correspond to the dates of these dips / events show a possible explanation, in that these dates appear to show drier autumns, with less overall vegetation cover, than the remaining years 2002, 2004 and 2005. The fact that the NDVI maximum peaks during these same periods is difficult to interpret, but could point to a very strong vegetation response, in the uplands, to an alternative source of moisture, such as low level clouds, fog or dew.

Component 2 is meant to represent the biggest source of variation in the images over time, which usually equates to changes in seasonality over time. It seems as though component 2, which explains 3.91 % of the variation, is the opposite of component 1 and shows characteristic sinusoidal seasonality peaks, which highlight the differences in NDVI / vegetation cover between the winter and summer images. Due to the fact that this region exhibits both winter and summer rainfall regimes, it is assumed that the seasonality curves would be less pronounced in component 2. But because of the unusually low winter vegetation cover during years 2000, 2001 and 2003, component 2 highlights this difference between the seasons by exhibiting sinusoidal seasonality peaks during the years that exhibit the dips / events of component 1 (Figure 12).

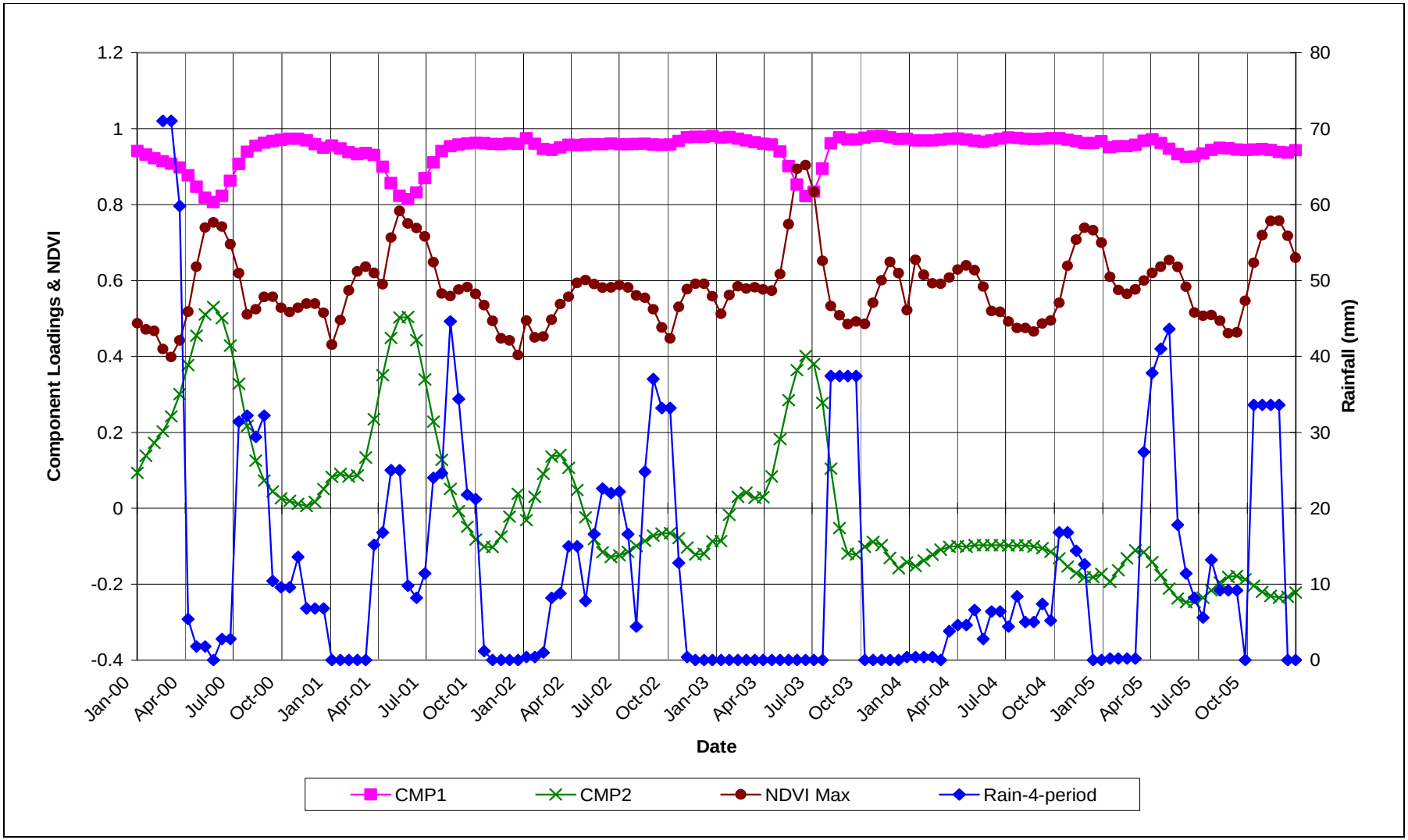

Figure 12: The MODIS imagery component one and two loadings, MODIS NDVI maximum and cumulative rainfall plotted over time.

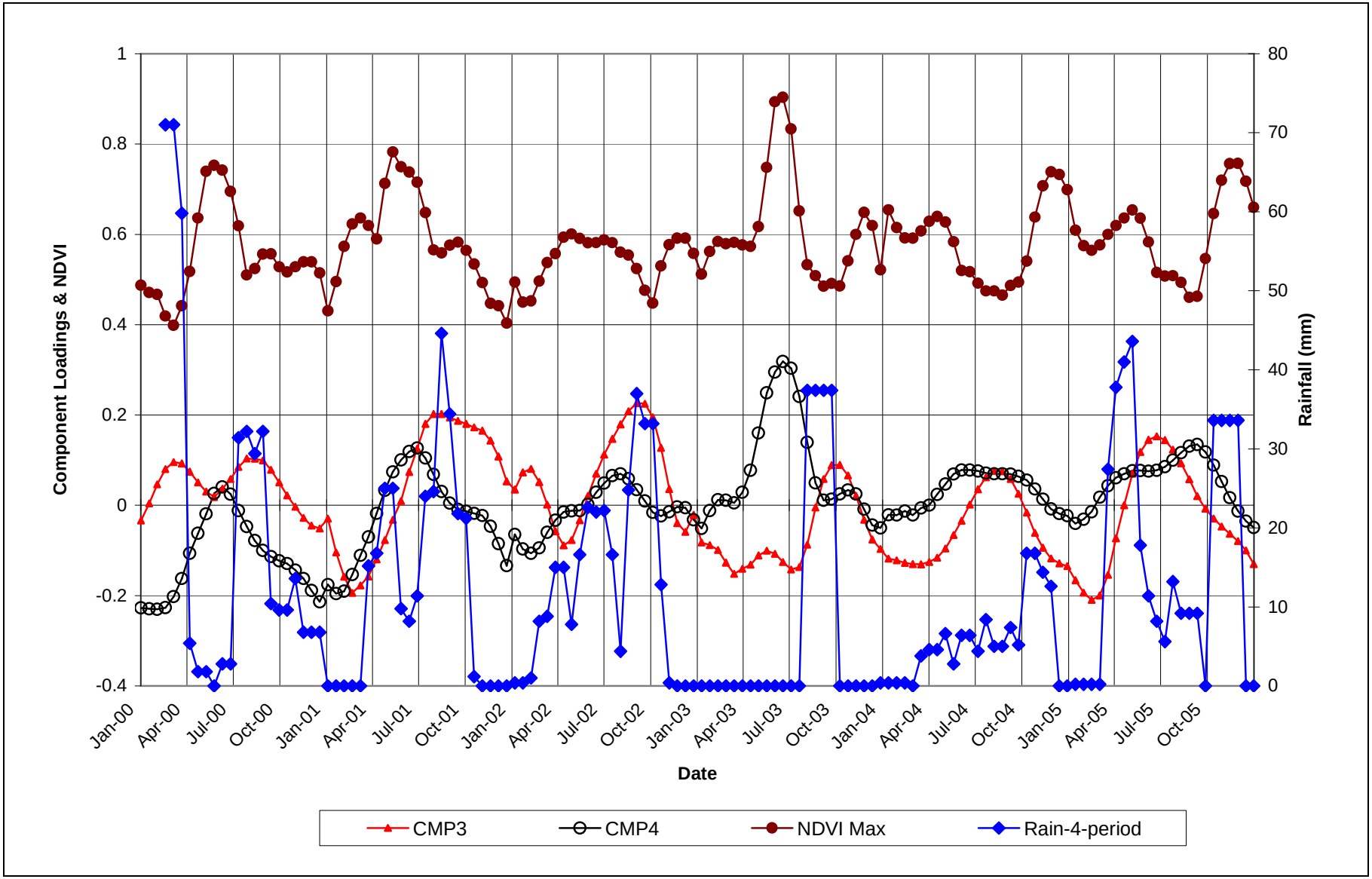

Figure 13: The MODIS imagery component three and four loadings, MODIS NDVI maximum and cumulative rainfall plotted over time

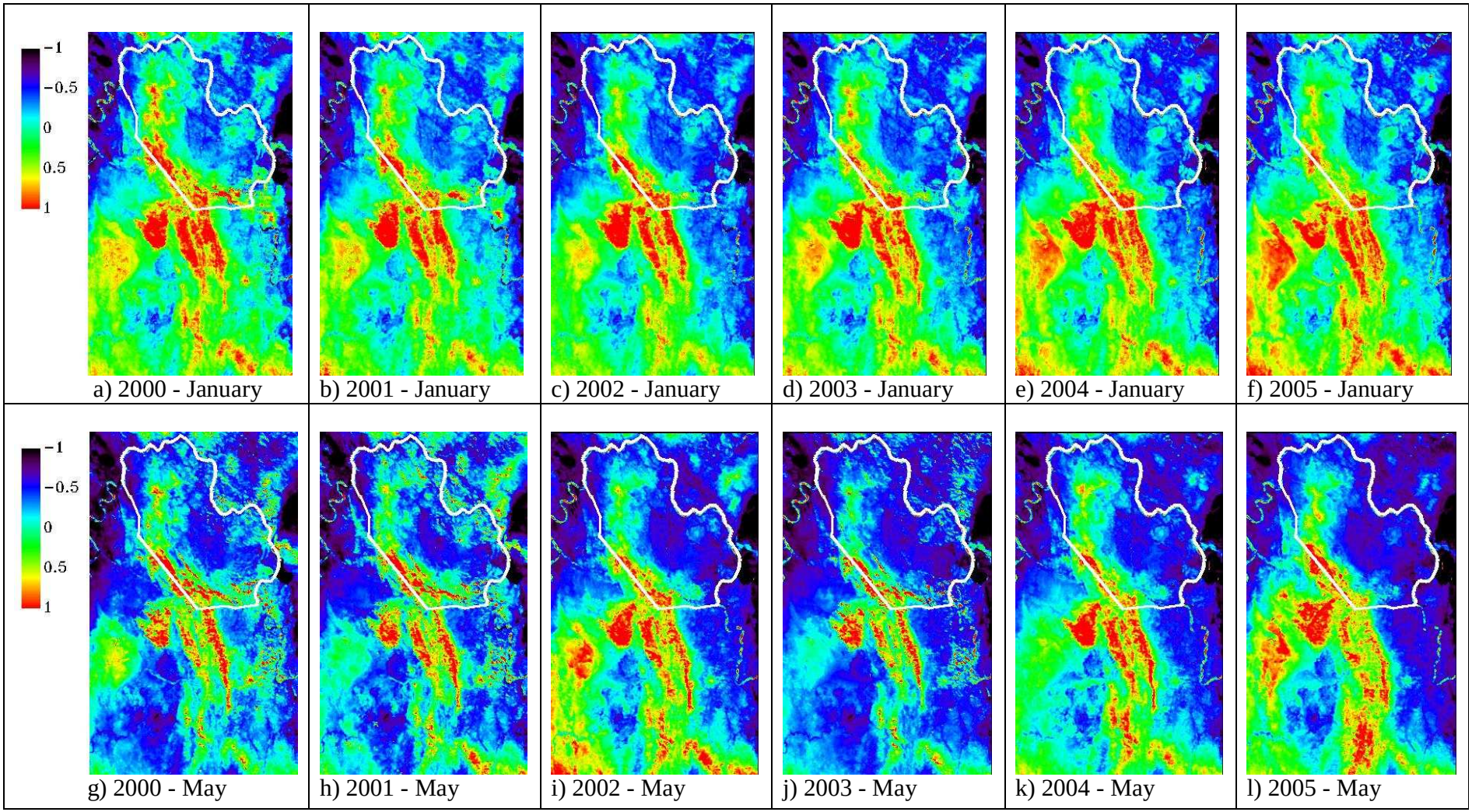

Figure 14 (a – l): NDVI images showing the difference in vegetation cover between a summer (January) and an autumn (May) image. The autumn images for years 2000, 2001, and 2003 appear to exhibit comparatively low NDVI values. The NDVI images are scaled between -1 (low vegetation) and 1 (high vegetation).

Components 3 and 4 in Figure 13, which explain 1.21 % and 1.04 % variance respectively, are particularly difficult to interpret. However, it appears as though component 3 corresponds well with the cumulative four-period rainfall, and is also opposite to component 2 to some extent. Since component 2 has explained seasonality and component 3 is expected to explain the next greatest source of variation, the argument could be made that based on its apparent correspondence with rainfall, component 3 explains those episodic green-up events that follow rainfall.

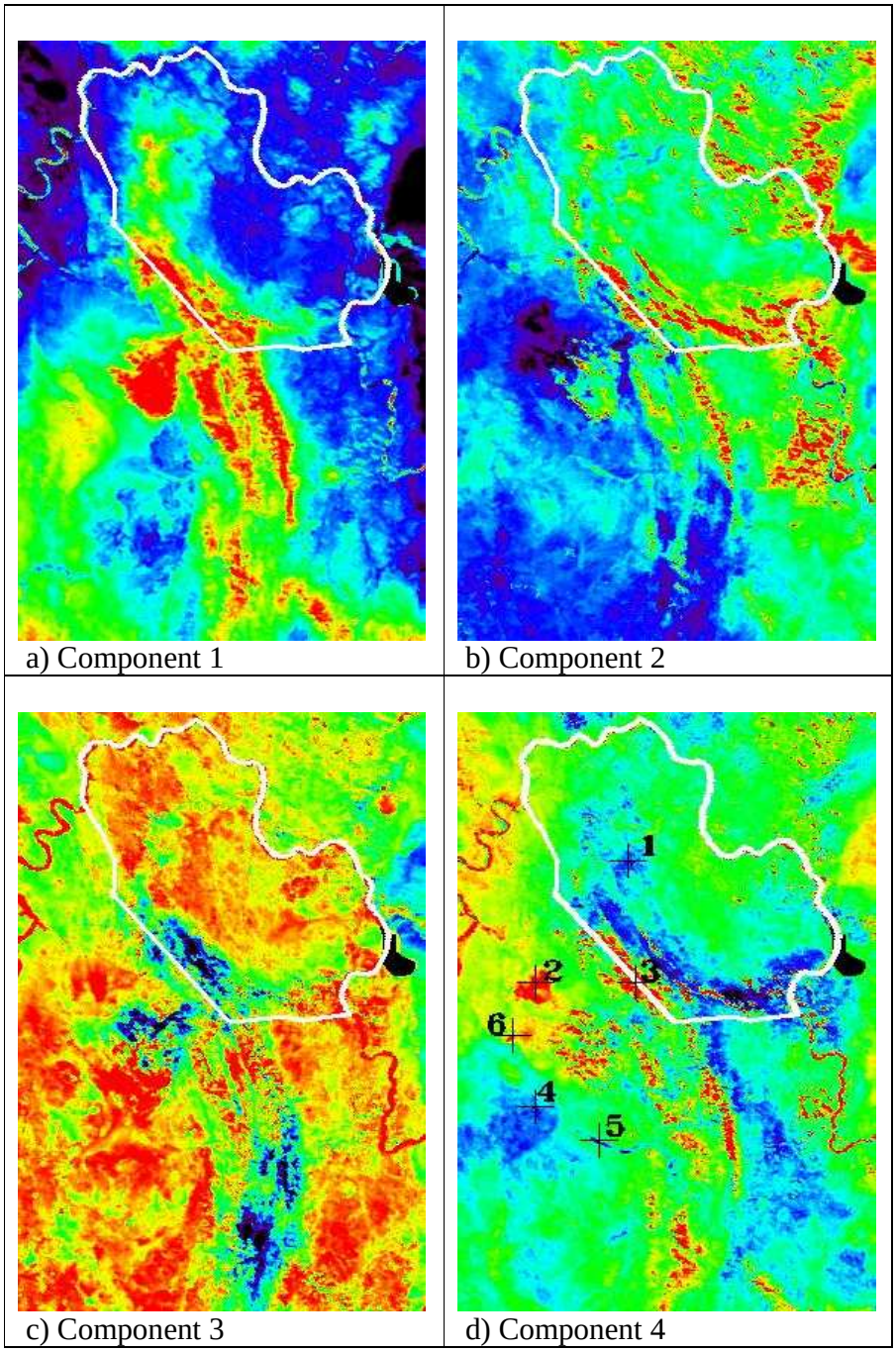

a) Component 1 b) Component 2

c) Component 3 d) Component 4

Figure 15 (a – d): Component image results explaining 95.39 % of all variation in the NDVI time series. Six time series profiles (each 3x3 pixels) were taken and illustrated in image (d)

From Figure 15, we can see the spatial explanation of the loadings that appear in Figures 12 and 13. The image of component 1 shows the typical spatial and temporal distribution of NDVI, with the highland areas dominating the NDVI signal. Based on the interpretation of the component 2 loadings (Figure 12), the component 2 image could also be interpreted as showing the winter / summer rainfall divide, which has formed between the winter precipitation-fed (rain, fog and dew) western lowlands, and the eastern, summer rainfall interior that forms the leeward side of the Richtersveld highlands. As with the loadings of component 3, the respective images are not easy to interpret and could point towards the episodic green-up events that follow rainfall. Component 4 is also difficult to interpret using the loadings, but looking at its respective image it appears to show areas of noteworthy vegetation cover change. In order to further investigate this, six (3 x 3 pixel) sample points were plotted in some of the areas of interest. From these plots, it was possible to generate NDVI profiles that showed how the vegetation cover for those pixels had changed over the years. Figure 16 presents the NDVI time series signature and its 5^{th} order polynomial trend line that shows sample points one, four and five (blue colour in Figure 15) to have decreasing trends in vegetation cover between years 2000 and 2005, while points two, three and six (red colour in Figure 15) show varying degrees of increasing trends in vegetation cover over the same period. The rest of the components were unable to be interpreted and were therefore assumed to be the left over noise in the images.

6.2.2 Seasonality Shift Analysis

The results of the seasonality shift analysis indicate the percentage of pixels, with either uni- or bi-modal signatures, that show seasonal shifts in either the positive or negative direction. Positive shifts indicate that the season was comparatively later in the year, than the six-year mean, and visa versa for negative shifts. As can be expected, and is shown in Figure 17 (a – f), the majority of pixels that exhibited modal signatures appear in the mountainous areas of the scene. In the year 2000, there appears to be a stable to negative shift in the seasonality of the region, while almost the complete opposite is true for year 2001, see Table 6 and Figure 17. The years 2002, 2003, and 2004 are seen as being very similar to the six year mean, with the majority of modal pixels being labelled as stable, while year 2005 tends towards a slightly negative shift in the seasons. The results do not show any clear trends in terms of shifting seasons, and given that a shift of "1" only equates to one NDVI image in the time series (i.e. 16-days) it is therefore highly unlikely that this result is of much significance.

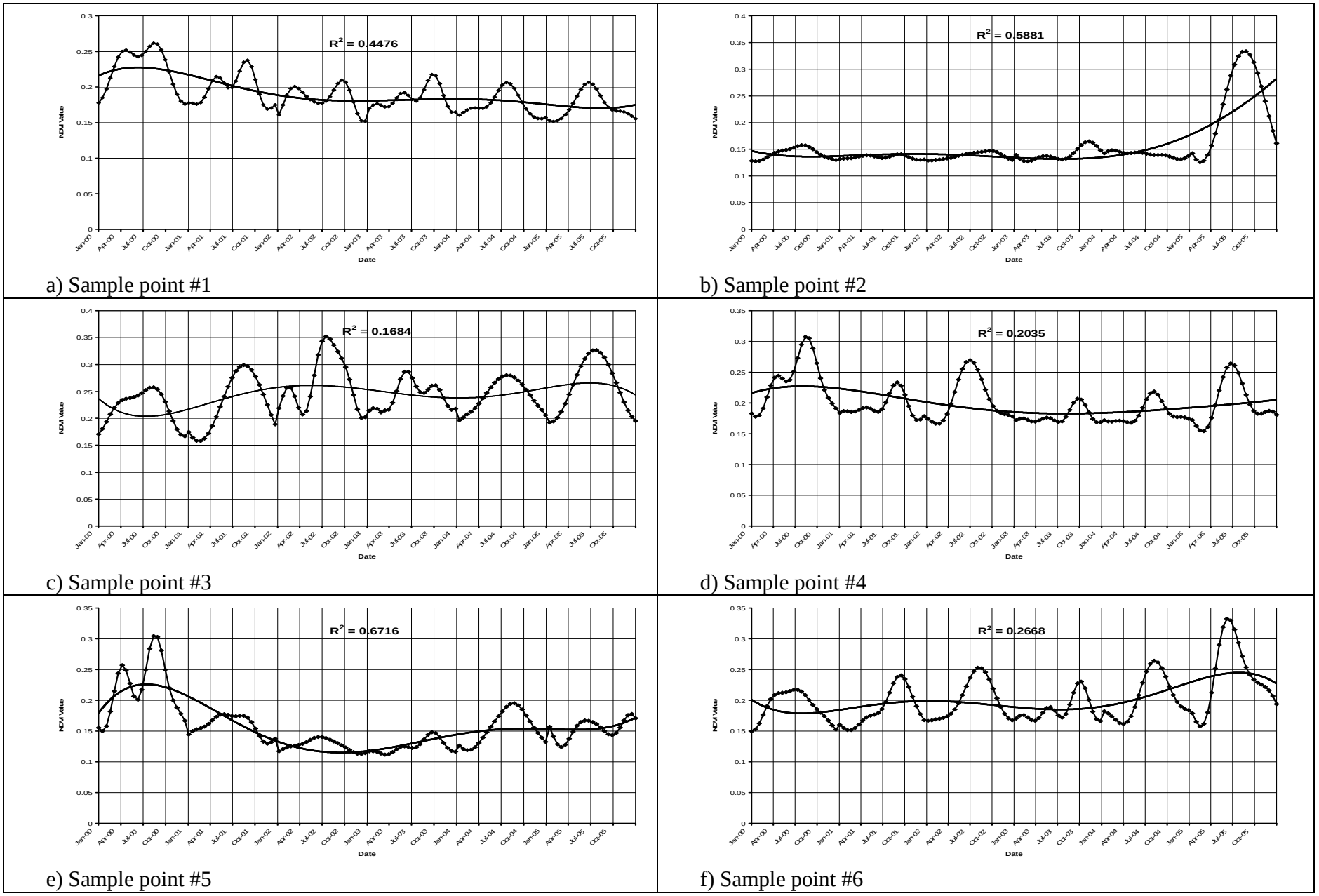

Figure 16 (a – f): NDVI time series profiles of selected 3x3 pixel plots explaining observed anomalies in PCA component 4.

Table 6: The percentage of pixels per seasonality shift class

Class	2000	2001	2002	2003	2004	2005
-4	0.0	0.0	0.2	0.0	0.0	0.3
-3	0.0	0.0	0.0	0.1	0.1	7.5
-2	12.1	0.4	0.0	0.9	0.4	17.7
-1	**55.4**	3.5	6.5	34.3	11.0	**45.6**
Stable	26.5	17.0	**56.6**	**57.8**	**51.7**	26.4
1	4.6	**48.7**	31.4	5.1	32.3	2.2
2	0.7	28.2	4.4	1.1	4.1	0.2
3	0.3	1.8	0.6	0.6	0.4	0.0
4	0.3	0.3	0.3	0.1	0.0	0.0

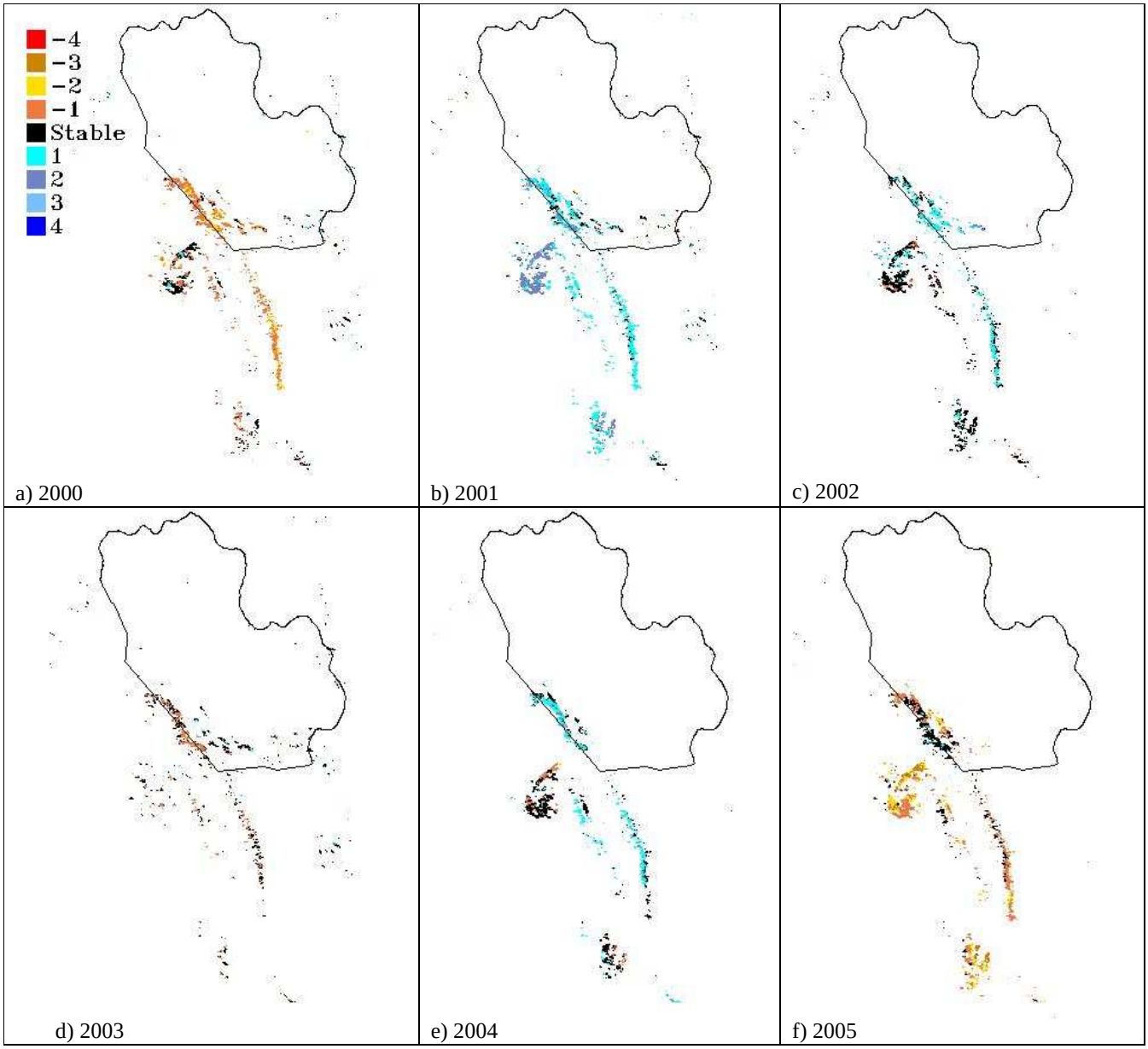

Figure 17: Spatial results of the MODIS NDVI seasonality shift analysis. Only unimodal pixels contributed to the analysis

Chapter 7

Spatial Variation in Vegetation Response

7.1 Methods

7.1.1 Vegetation Index Differencing

Due, in part, to the difficulties experienced in the pre-processing of the 12 images, and in order to cut down on computer processing workloads, two images (wet and dry season images) from each of the years 1991, 1997 and 2004 were eventually used for analysis.

Depending on how the index is calculated, vegetation indices can be grouped into those that are slope-based (e.g. NDVI and SAVI), distance-based (e.g. TSAVI and PVI), and those based on orthogonal transformations (e.g. Tasseled Cap). After qualitatively testing vegetation indices from each of these groups, it was decided to use the common slope-based Normalised Difference Vegetation Index (NDVI), the distance-based Modified Soil Adjusted Vegetation Index ($MSAVI_1$), which makes use of constant soil adjustment factor (L), and the distance-based Perpendicular Vegetation Index (PVI_2) that uses the slope and intercept of the 'soil line'. An L factor of 1.0 was used for the $MSAVI_1$ equation, after Huete *et al*. (1988) suggested that an L factor of 1.0 be used for areas of sparse vegetation. The slope and intercept of the soil line (Table 7) were calculated by regressing bare soil reflectance values for the dependant red band against the independent infrared band (Richardson & Wiegand, 1977).

Table 7: The slope and intercept values for the regression line between soil pixels of the Red and NIR bands respectively.

Landsat Scene	Slope	Intercept
23/03/1991	1.23	-0.03
17/10/1991	1.22	-0.02
23/03/1997	1.20	-0.02
17/10/1997	1.19	-0.01
11/04/2004	1.20	-0.02
02/09/2004	1.20	-0.02

Vegetation indices were calculated for: a) each of the individual scenes/seasons, b) the dry season scene for each of the years (in order to eliminate the seasonal component and presence of annuals in the wet season image), and c) an averaged wet and dry season image (which would hopefully also reduce the strong seasonal difference in the images and emulate the theory behind classifying the images with 12 band image stacks of both seasons). The resulting vegetation index images were then normalised, so as to reduce errors when thresholding, and then differenced, by subtracting an earlier image from a later one. Areas of change

were identified using a standard deviation thresholding technique. The standard deviation thresholding technique identifies change as those pixels with values that fall outside of a certain number of standard deviations, in this case two standard deviations, away from the mean. All values not outside of two standard deviations from the mean are then considered to show no significant change.

7.1.2 Post-classification Change Detection

Post classification change detection was conducted on all of the scenes for years 1991, 1997 and 2004. Based on guidelines from the standard land-cover classification scheme for remote sensing applications in South Africa (Thompson, 1996), the analysis of different and available spectral signatures, unsupervised classification results, ancillary data, as well as field visits, a classification scheme with 10 classes was decided upon, for which training areas were delineated (Table 8). These classification training areas were then used to train both the maximum-likelihood pixel and nearest-neighbour object-based classification algorithms. The classifications were run on yearly image stacks, which consisted of the two wet and dry images per year and stacked into a twelve band image (Landsat bands 1, 2, 3, 4, 5, and 7).

Table 8: Classification scheme for Landsat analysis

Class code	Class Name
1	Shadow
2	Barren Land – Rocky Substrate
3	Barren Land – Sandy Substrate
4	Upland Succulent Shrubland
5	Plains - Succulent Shrubland
6	Strandveld Shrubland – Sand/Dune veld
7	Cultivated land
8	Riverine Vegetation
9	Unimproved Desert Grassland
10	Waterbodies

The classification results were filtered using a majority filter, in order to eliminate ‘salt and pepper’ effects in the thematic results (Jensen, 1996). Majority filters operate using a moving window that is passed over the classification result, and the majority class within the window is determined and applied to center pixels that are not the majority class. The filtering was performed using a 5-by-5 pixel window. An accuracy assessment, using randomly generated digital points as well as ground truth validation points, was conducted on the filtered classification results. The images were then subjected to a post-classification change detection analysis within the ENVI software, which produces a classification change matrix, and change matrix images that show were the classes have differed between years. A class stability analysis was also conducted on the classification results. This entailed removing or buffering the edges of each class, so as to test the core stability of the class.

7.2 Results and Discussion

7.2.1 Vegetation Index Differencing

The results of the vegetation index differencing using a second standard deviation thresholding technique can be seen in Table 9. As with the post-classification change detection results, the vegetation index differencing results appear to be very stable, with the majority of tests (i.e. between seasons/years/dry seasons) for each of the vegetation indices resulting in greater than 95 % of pixels being stable, or without significant change. 'Positive changes' mean that there has been an increase in vegetation between the earlier image and the later image and visa versa for 'negative changes'. The total number of 30m x 30m pixels included in this analysis was 7 083 058, which equates to an area of 6374.75 km^2. This excludes those pixels that were masked out, but does however include the pixels representing the cultivated lands as these provided a source of reference for qualitative testing of the vegetation indices and they were deemed not to have a significant impact on the regions change statistics, other than to possibly inflate the 'positive change' class. When viewing these statistical results together with the image results (Figure 18), one gets an idea of the spatial distribution of the supposed change. Much of the 'positive change' in the 'between seasons' test can observably be explained by the differences in rainfall seasons, with the September / October scene being the wet season image with more vegetation present, and visa versa for the April / March images. Figure 19 shows an example of some seasonal differences that were detected, in this case it appears as though an erosion gully has been populated by annuals in the wet season, hence the appearance of positive change when differenced with the dry season image. The slightly positive trend, between 1991 and 1997, and then negative trend, between 1997 and 2004, in the 'between years' test could also be explained by the fact that 1997 was a particularly wet year (Figures 18 and 20), while 1991 and 2004 were comparatively drier. The October image of 2004 was also a particularly wet image, which explains why when it is combined with the dry image, to form a yearly vegetation index image, and then differenced against, especially, the 1991 image there is so much 'positive' change. There is also some evidence of 'negative' change in the region surrounding the town of Kuboes. Without appropriate ground truthing through time, this could be assumed to be vegetation cover change as a result of grazing animals on the slopes of the upland areas. Again, much of the change being detected appears to be as a result of differences in seasonality. No where in the image results could any of the change be linked specifically to anthropogenic activities.

In order to get a further idea of where most of the change was taking place, a cross tabulation was carried out between the vegetation index difference images and the equivalent classification images (Table 10). The classification images, excluding the cultivated land class that is not situated in the RNP itself, were subtracted from each other, in order to compare the same time instance as the vegetation index difference images, i.e. 1991 classification subtracted from 1997 classification and then compared to the 1997 minus 1991 vegetation index difference image. These results of Table 10 show where the change was taking place.

Despite the Upland succulent shrubland and Plains - succulent shrubland only being third or fourth biggest classes respectively, they often accounted for the most positive, and/or negative, change out of all the classes. This can be explained firstly by the fact that the Plains - succulent shrublands are of the more dynamic and active classes when compared to the rest, and therefore show up the seasonal changes more often. Secondly, the Upland succulent shrubland class shows up the majority of the negative change occurring in the topographically complex highlands, where a lack of topographic correction and resultant differences in shadow effects between dates can cause unsubstantiated change.

Table 9: Class statistics for the differencing of the vegetation index images

Between Seasons			
Change between 1991/03 and 1991/10	**NDVI**	**MSAVI**	**PVI**
Negative (%)	0.66	0.92	0.30
Stable (%)	95.20	94.50	95.44
Positive (%)	4.14	4.58	4.26
Change between 1997/03 and 1997/10	**NDVI**	**MSAVI**	**PVI**
Negative (%)	1.16	1.43	1.09
Stable (%)	95.93	95.04	95.44
Positive (%)	2.91	3.53	3.47
Change between 2004/04 and 2004/09	**NDVI**	**MSAVI**	**PVI**
Negative (%)	0.50	0.42	0.38
Stable (%)	95.67	96.73	96.11
Positive (%)	3.83	2.85	3.51
Between Years			
Change between 1991 and 1997	**NDVI**	**MSAVI**	**PVI**
Negative (%)	0.74	0.63	0.92
Stable (%)	97.65	98.32	97.30
Positive (%)	1.61	1.05	1.78
Change between 1997 and 2004	**NDVI**	**MSAVI**	**PVI**
Negative (%)	1.53	0.91	1.36
Stable (%)	97.64	98.08	97.97
Positive (%)	0.83	1.01	0.67
Change between 1991 and 2004	**NDVI**	**MSAVI**	**PVI**
Negative (%)	0.99	0.66	1.02
Stable (%)	98.03	98.18	97.89
Positive (%)	0.98	1.16	1.09
Between Dry Seasons			
Change between 1991/03 and 1997/03	**NDVI**	**MSAVI**	**PVI**
Negative (%)	1.02	0.58	0.59
Stable (%)	96.76	98.14	97.34
Positive (%)	2.22	1.28	2.05
Change between 1997/03 and 2004/04	**NDVI**	**MSAVI**	**PVI**
Negative (%)	0.98	0.50	0.78
Stable (%)	98.46	99.02	98.75
Positive (%)	0.56	0.48	0.47
Change between 1991/03 and 2004/04	**NDVI**	**MSAVI**	**PVI**
Negative (%)	0.70	0.28	0.31
Stable (%)	98.58	99.21	99.14
Positive (%)	0.72	0.51	0.55

Confusion matrix statistics were calculated using the vegetation index difference images, in order to determine the agreement between change images of different years and seasons. Table 12 shows that the change taking place between 1991 and 2004 is notably similar between years and seasons, with Kappa statistics in excess of 0.8 and 0.9 for the majority of tests. These results reaffirm previous results that indicate that the area is predominantly stable.

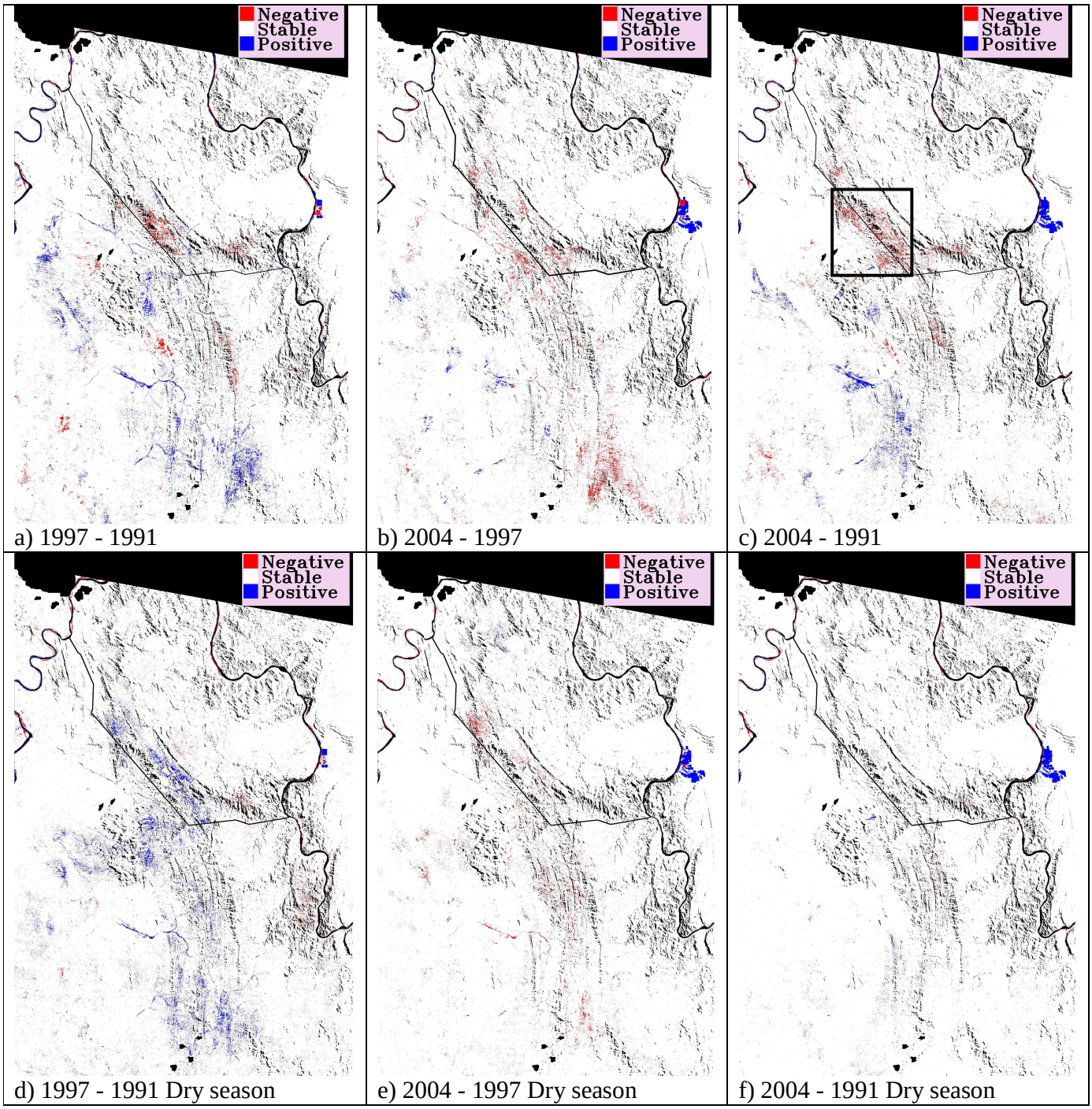

Figure 18 (a – f): Vegetation index differencing results for between year change (a-c) and change between the dry seasons of respective years (d-f). The region, showing 'negative' change,in the vicinity of Kuboes is demarcated by a square in image(c)

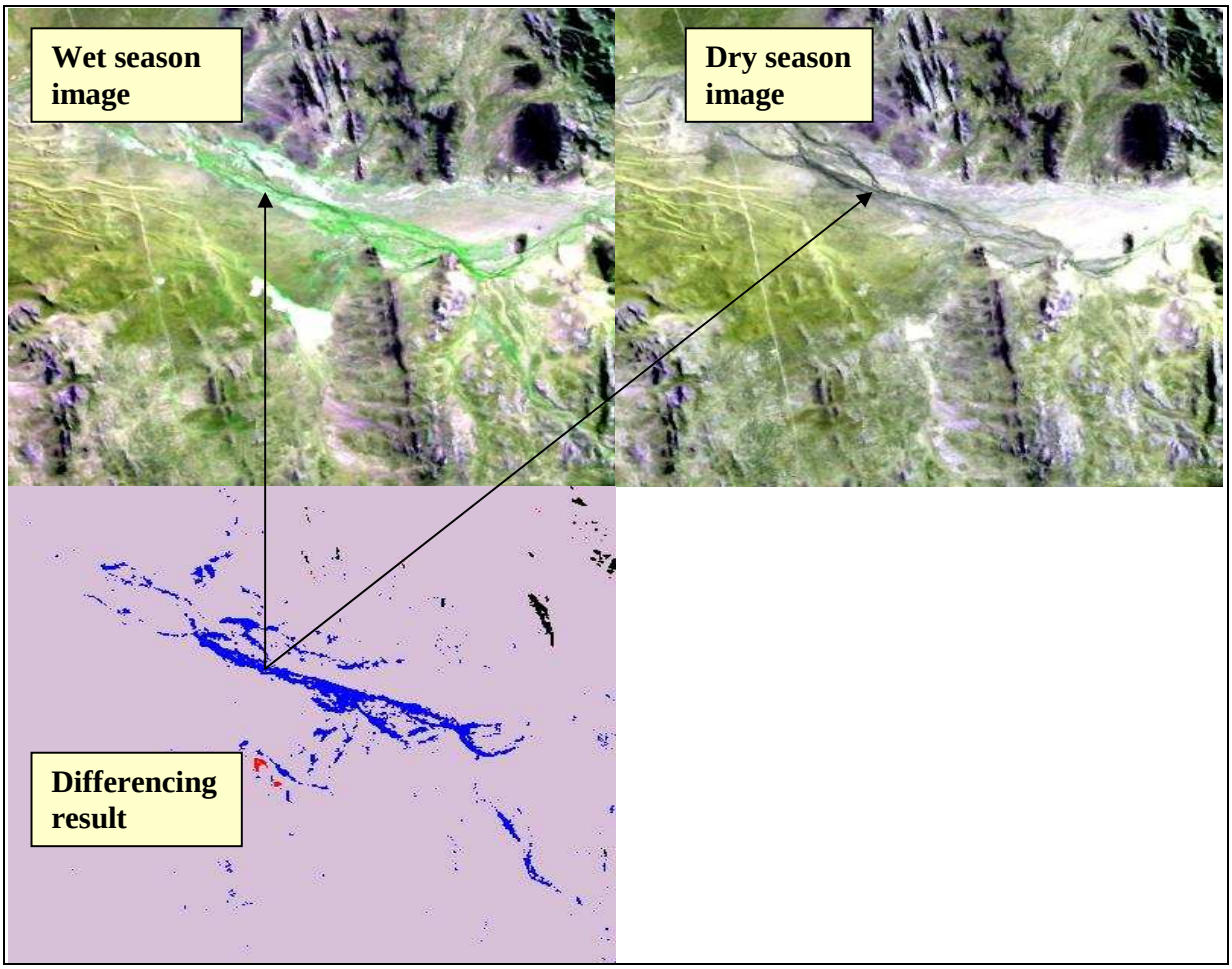

Figure 19: An illustration of seasonal 'positive' change detected in the vegetation index differencing method. Wet and dry season images are Landsat scenes (R:3,B:4,G:1) from October 2004 and April 2004 respectively.

A principle component analysis was conducted on the vegetation index images from each season, in order to determine which of the vegetation indices was performing better at detecting vegetation in an arid environment. When comparing 25 different vegetation indices for an arid scene, Thiam (1998) found that the first principle component described a general vegetation index that included elements of soil background, whereas the second component better described those vegetation indices that specifically corrected for soil background effects. This is apparent in Table 11, where all the MSAVI images that correct for soil background using the somewhat arbitrary L factor, have the highest component weightings for the first component, whereas the PVI images, which correct for soil background using the scene-dependant soil line, have the highest weightings for the second component. The NDVI vegetation index, whose limitations in arid environments spawned research into other indices such as MSAVI and PVI, had the highest weightings for the third component and therefore adhered to the assumption that it would perform worse than those vegetation indices that do correct for soil background noise.

Table 10: Cross tabulation between yearly vegetation index difference image, and the difference between the respective classification results.

1997-1991 vs Classification		Rocky substrate	Sandy substrate	Strandveld shrubland	Upland succulent shrubland	Plains - succulent shrubland	Riverine vegetation	Desert grassland	Total
	Negative (%)	0.07	0.08	0.13	0.39	0.16	0.00	0.06	0.89
	Stable (%)	35.55	15.84	9.54	16.36	20.08	0.12	0.19	97.68
	Positive (%)	0.02	0.02	0.17	0.48	0.56	0.00	0.18	1.43
	Total (%)	35.64	15.94	9.84	17.22	20.80	0.12	0.44	100.00
2004-1997 vs Classification		**Rocky substrate**	**Sandy substrate**	**Strandveld shrubland**	**Upland succulent shrubland**	**Plains - succulent shrubland**	**Riverine vegetation**	**Desert grassland**	**Total**
	Negative (%)	0.02	0.02	0.03	0.61	0.40	0.00	0.12	1.18
	Stable (%)	34.72	17.26	9.50	17.05	19.55	0.08	0.17	98.34
	Positive (%)	0.04	0.03	0.16	0.07	0.12	0.00	0.06	0.48
	Total (%)	34.77	17.30	9.69	17.73	20.07	0.08	0.34	100.00
2004-1991 vs Classification		**Rocky substrate**	**Sandy substrate**	**Strandveld shrubland**	**Upland succulent shrubland**	**Plains - succulent shrubland**	**Riverine vegetation**	**Desert grassland**	**Total**
	Negative (%)	0.02	0.04	0.02	0.62	0.17	0.00	0.07	0.95
	Stable (%)	36.10	17.51	9.62	17.30	17.57	0.09	0.15	98.35
	Positive (%)	0.02	0.02	0.18	0.16	0.21	0.00	0.12	0.71
	Total (%)	36.14	17.58	9.82	18.08	17.95	0.09	0.34	100.00

Table 11: Results of the principle components analysis between the vegetation index images. The table shows the principle component weightings as a percentage.

1991/03	NDVI	MSAVI	PVI		1997/03	NDVI	MSAVI	PVI		2004/04	NDVI	MSAVI	PVI
PC1 (%)	24.82	**69.55**	5.64			26.06	**67.53**	6.41			26.85	**65.94**	7.20
PC2 (%)	5.11	15.15	**79.73**			18.68	24.97	**56.35**			17.77	26.58	**55.65**
PC3 (%)	**70.07**	15.30	14.63			**55.26**	7.50	37.24			**55.38**	7.48	37.14
1991/10	**NDVI**	**MSAVI**	**PVI**		**1997/10**	**NDVI**	**MSAVI**	**PVI**		**2004/09**	**NDVI**	**MSAVI**	**PVI**
PC1 (%)	27.07	**64.54**	8.39			27.43	**64.67**	7.91			27.26	**65.30**	7.44
PC2 (%)	7.86	23.15	**68.99**			17.45	28.10	**54.45**			4.99	19.20	**75.81**
PC3 (%)	**65.06**	12.31	22.62			**55.13**	7.23	37.64			**67.75**	15.50	16.75

Table 12: Similarity of change between vegetation index difference images, calculated using accuracy assessment methods with one image regarded as a 'ground truth' image and the other regarded as the classification result.

Similarity of between season differences			
NDVI	**1991/03 – 1991/10 vs 1997/03 – 1997/10**	**1997/03 – 1997/10 vs 2004/04 – 2004/09**	**1991/03 – 1991/10 vs 2004/04 – 2004/09**
Accuracy (%)	94.49	94.65	95.10
Kappa	0.82	0.82	0.84
MSAVI			
Accuracy (%)	93.83	94.43	94.61
Kappa	0.80	0.81	0.82
PVI			
Accuracy (%)	94.19	94.40	95.14
Kappa	0.81	0.81	0.84
Similarity of between dry season differences			
NDVI	**1997/03 – 1991/03 vs 2004/04 – 1991/03**	**2004/04 – 1997/03 vs 2004/04 – 1991/03**	**1997/03 – 1991/03 vs 2004/04 – 1997/03**
Accuracy (%)	96.85	98.60	96.40
Kappa	0.88	0.95	0.86
MSAVI			
Accuracy (%)	98.25	99.21	97.87
Kappa	0.93	0.96	0.92
PVI			
Accuracy (%)	97.56	98.84	97.15
Kappa	0.9	0.95	0.89
Similarity of between year differences			
NDVI	**1997 – 1991 vs 2004 – 1991**	**2004 – 1997 vs 2004 – 1991**	**1997 – 1991 vs 2004 – 1997**
Accuracy (%)	97.12	98.22	96.45
Kappa	0.89	0.93	0.87
MSAVI			
Accuracy (%)	97.70	98.40	97.27
Kappa	0.91	0.93	0.89
PVI			
Accuracy (%)	96.89	97.58	96.55
Kappa	0.88	0.91	0.87

7.2.2 Pixel and object-based post classification change analysis

The maximum likelihood pixel-based, and nearest neighbour object-based classification results are presented in Figure 21 (a – f). The change matrix results are presented in Table 13, and show very few clear trends in the spatial extents of the different classes. The only major trend to appear is the significant increase in the spatial extent of the cultivated land class. Many of the remaining classes appear to increase between 1991 and 1997, and then decrease again between 1997 and 2004. An explanation of this, could be found in the fact that 1997 appeared to be a particularly wet year, and was also preceded by a very wet year, as shown in Figure 20, whereas 2004 appears to be a comparatively drier year.

The classification images, as seen in Figure 21 (a - f), are very similar to each other and without any major differences in the extents of each class. An indication of the similarity of the classes, within each method, is given in Table 14, with the results of the core class stability analysis. The results show very high core class stabilities (in excess of 90 %), once edge effects are removed using 60 or 90 meter buffers, and the class images are subtracted from each other. It is quite possible that any change being detected could have been revealed on the edges of the classes, and was subsequently eliminated by the buffers. This was taken into consideration, but having qualitatively studied the change matrix images it was deemed not to be a major issue and would only serve as an illustration of the stability, and lack of significant change, in the images.

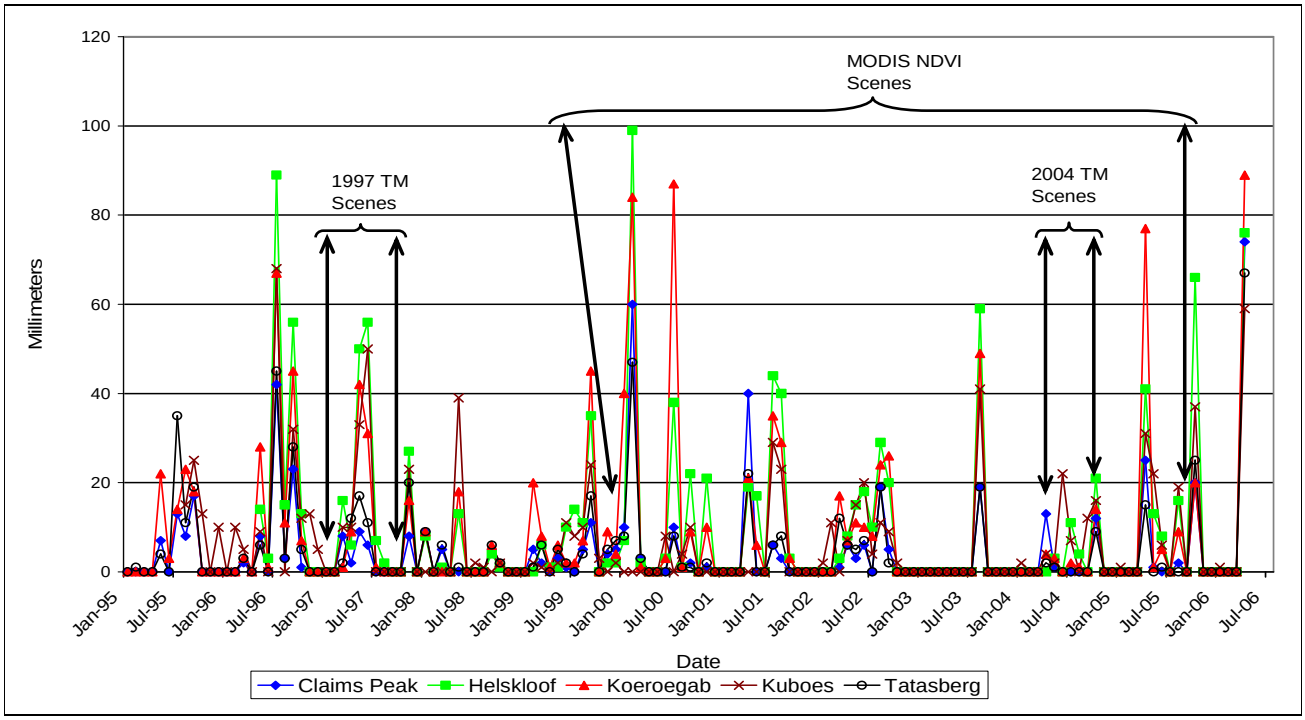

Figure 20: Richtersveld monthly rainfall and satellite imagery

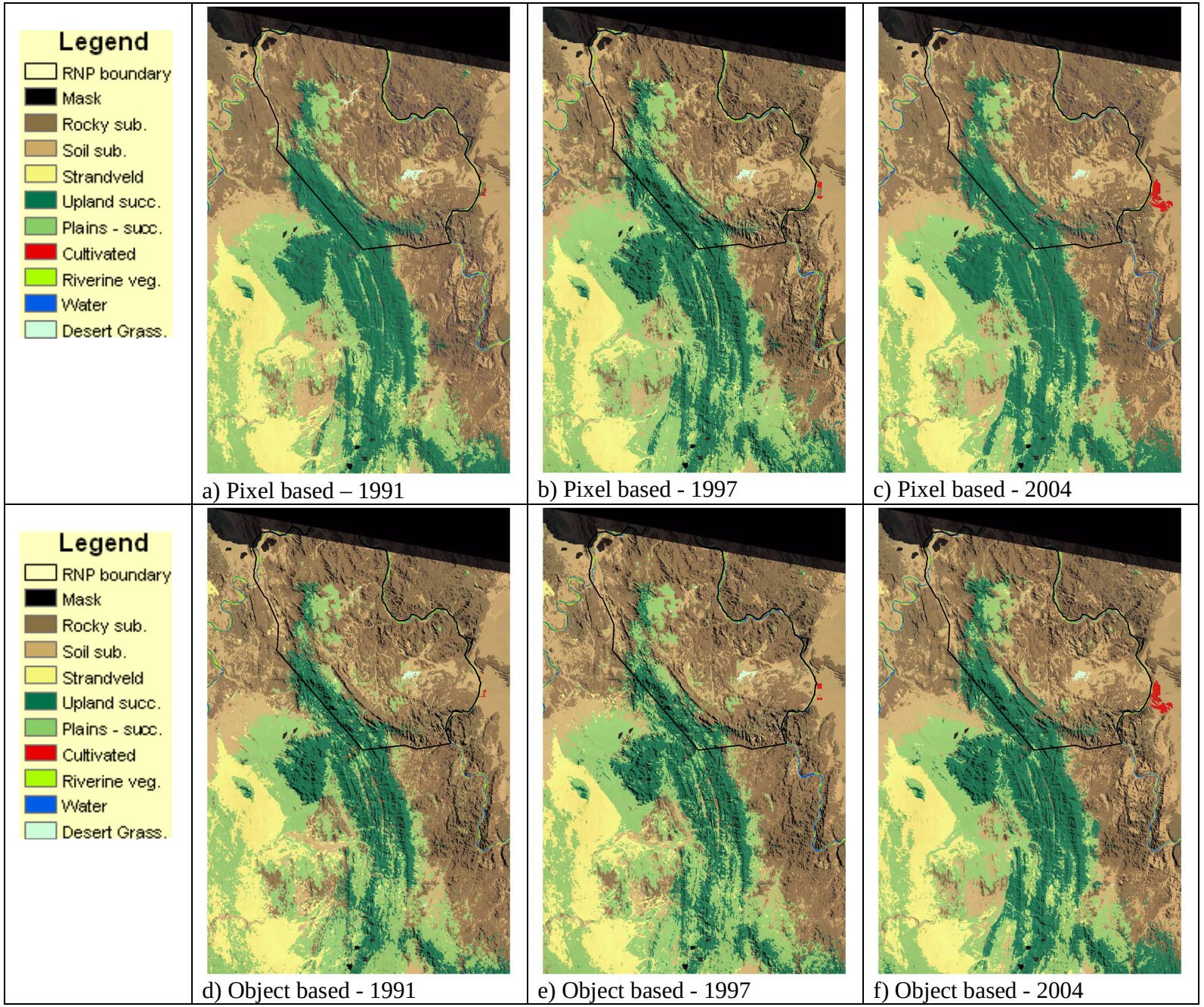

Figure 21 (a – f): The image results for both pixel and object based classifications. Class names are abbreviated; full names in Table 8.

Table 13: Change matrix results for the pixel and object based classifications, shown as percentage difference per class per image. Class names are abbreviated, refer to Table 8 for full class descriptions.

Object-based	Rocky substrate	Sandy substrate	Strandveld shrubland	Upland succulent shrubland	Plains - succulent shrubland	Cultivated land	Riverine vegetation	Desert grassland
1991-1997	-2.18	-2.13	-2.49	1.91	6.03	102.53	11.25	-18.87
1997-2004	2.17	6.14	6.25	10.54	-18.56	582.76	-25.52	-2.72
1991-2004	-0.06	3.88	3.61	12.65	-13.65	1282.82	-33.90	-21.07
Pixel-based	**Rocky substrate**	**Sandy substrate**	**Strandveld shrubland**	**Upland succulent shrubland**	**Plains - succulent shrubland**	**Cultivated land**	**Riverine vegetation**	**Desert grassland**
1991-1997	-7.99	0.91	-11.02	-0.51	25.55	76.63	11.62	-44.38
1997-2004	4.80	17.27	1.37	11.10	-23.77	549.75	-37.54	-2.07
1991-2004	-3.57	18.33	-9.80	10.54	-4.29	1047.63	-30.28	-45.54

Table 14: Core class stability (buffer sizes are in meters, i.e. 0, 60 and 90 meters).

Pixel-based	1991-1997	1997-2004	1991-2004
0m (%)	78.45	76.76	76.22
60m (%)	94.00	93.16	92.59
90m (%)	96.80	96.26	95.72
Object-based	**1991-1997**	**1997-2004**	**1991-2004**
0m (%)	83.96	83.29	84.03
60m (%)	96.44	96.61	97.07
90m (%)	97.95	98.03	98.43

The results of the two different types of classification, the object- and pixel-based approaches, were compared, using accuracy assessment methods, in order to get an idea of their similarity. Each pixel-based classification result was used as a 'ground truth' image against which the accuracy of the object-based classification result was tested (Table 15). Despite very similar results, the assumption behind using the pixel-based results as the 'ground truth' image was that they were deemed to be qualitatively more accurate than the object-based results.

Accuracy assessments were also conducted using both the collected field validation points, as well as the random reference pixels, which are presented in Table 16 and Table 17 respectively. The 33 field validation points were only used to validate the 2004 classification results, due to the time gap between the field validation points and the other two sets of imagery, namely 1991 and 1997. The classification error matrix, for both pixel and object-based approaches, using the field validation points is presented in Table 16.

Based on the assumption that the field validation points best represented the situation on the ground, Table 16 gives an account of the classification accuracy, by reporting on the errors of commission and omission as well as the producer's and user's accuracies. Producer's accuracies, a measure of omission, give an account of the accuracy of the validation point pixels per cover type classified, while the user's accuracy, or error of commission, is a measure of the probability that a pixel classified as a given class does actually represent that same class on the ground. Given the nature of some of the classes and the difficulty associated with training classifiers to recognise the respective pixels, due to spectral confusion, the errors of omission and commission appear to be within acceptable limits. Although limited, the results appear to be an accurate reflection of ground conditions, with final accuracies, for both the field validation points and random points, ranging between 75 and 95 percent, and Kappa statistics pointing towards the probability that the results are much more than just a random assortment of pixels. However, the results are to be viewed with caution due to the lack of independent imagery available for accuracy assessments, the subjective allocation of classes to the random reference pixels and the small number of field validation points collected. These shortcomings are indicative of the fact that the study area was remote and difficult to access.

Table 15: Similarity between object-based and pixel-based classifications.

	1991	**1997**	**2004**
Overall Accuracy (%)	75.92	77.19	76.92
Kappa Coefficient	0.68	0.70	0.70

Table 16: Classification error matrix, using the field validation points.

Pixel-based	Commission (%)	Omission (%)	Class	Producer's accuracy (%)	User's accuracy (%)	Final accuracy (%)	Kappa
Soil substrate	42.86	11.11	Sandy substrate	88.89	57.14	75.76	0.69
Rocky substrate	0	28.57	Rocky substrate	71.43	100		
Upland succulent shrubland	0	0	Upland succulent shrubland	100	100		
Plains – succulent shrubland	28.57	44.44	Plains – succulent shrubland	55.56	71.43		
Strandveld shrubland	0	0	Strandveld shrubland	100	100		
Riverine vegetation	0	33.33	Riverine vegetation	66.67	100		
Desert grassland	0	0	Desert grassland	100	100		
Object-based	**Commission (%)**	**Omission (%)**	**Class**	**Producer's accuracy (%)**	**User's accuracy (%)**	**Final accuracy (%)**	**Kappa**
Soil substrate	0	33.33	Soil substrate	66.67	100	75.76	0.69
Rocky substrate	0	66.67	Rocky substrate	33.33	100		
Upland succulent shrubland	14.29	14.29	Upland succulent shrubland	85.71	85.71		
Plains - succulent shrubland	43.75	0	Plains - succulent shrubland	100	56.25		
Strandveld shrubland	0	0	Strandveld shrubland	100	100		
Riverine vegetation	0	0	Riverine vegetation	100	100		
Desert grassland	0	0	Desert grassland	100	100		

Table 17: Final accuracies for both classification methods, using the stratified random samples.

Pixel-based	**1991**	**1997**	**2004**
Accuracy (%)	94.30	95.77	93.87
Kappa	0.94	0.95	0.93
Object-based	**1991**	**1997**	**2004**
Accuracy (%)	92.78	86.91	93.11
Kappa	0.92	0.85	0.92

In an attempt to further validate the classification images, a more qualitative and assumption based approach was tested. Using mean vegetation index image values, certain assumptions were tested, which if true would add some weight to the accuracy of the classification images. Using results from a PCA on the three different vegetation index images, presented earlier, it was decided to use the PVI vegetation index as it

appeared to be qualitatively and quantitatively better at detecting vegetation in this arid environment. For this analysis the two classes *Barren land – sandy substrate* and *Barren land – rocky substrate* were joined to form one class called *Bare*. The PVI image used was effectively a yearly mean, calculated by combining the two PVI images of each season and then dividing by two. As was referred to earlier, only the pixel-based classification results were used due to them being deemed qualitatively more accurate than the object-based results.

The assumptions were, a) that the *Cultivated land* class would have the highest mean PVI value for all the classes, b) that either the *Upland succulent shrubland* class or the *Riverine vegetation* class would have the second highest mean PVI value, c) the *Upland succulent shrubland* class would have the highest mean PVI between classes when the *Cultivated land* and *Riverine vegetation* classes were excluded, d) based on rainfall records and results that will be presented later on, the mean PVI values, excluding *Cultivated land* and possibly *Riverine vegetation*, would be higher for the 1997 year. From Figure 22 it becomes apparent that most of these assumptions are backed up by the mean PVI values. The *Cultivated land* class has the highest mean PVI value during 1997, which is a little surprising seeing as though this class more than doubled in expanse between 1997 and 2004 (Table 13). This could be attributed to the rotation of crops and the time of year at which the imagery was taken. The *Upland succulent shrubland* class has the third highest mean PVI value behind the *Cultivated* and *Riverine vegetation* classes, but more importantly it is higher than the rest of the classes, which are assumed to have less vegetation cover and which do not receive as much rainfall. The assumption that the wet year of 1997 would show up in the results also holds true, except for the *Riverine vegetation* class, which could be due to the fact that there was less riverine vegetation because the high waters of the year had washed it away, or covered it with silt. These results, although rather crude, show the classification results, and to some extent the PVI results, to be sufficiently accurate in order that some basic assumptions are met, regarding the regions characteristics and the performance of the classification methods on this type of imagery.

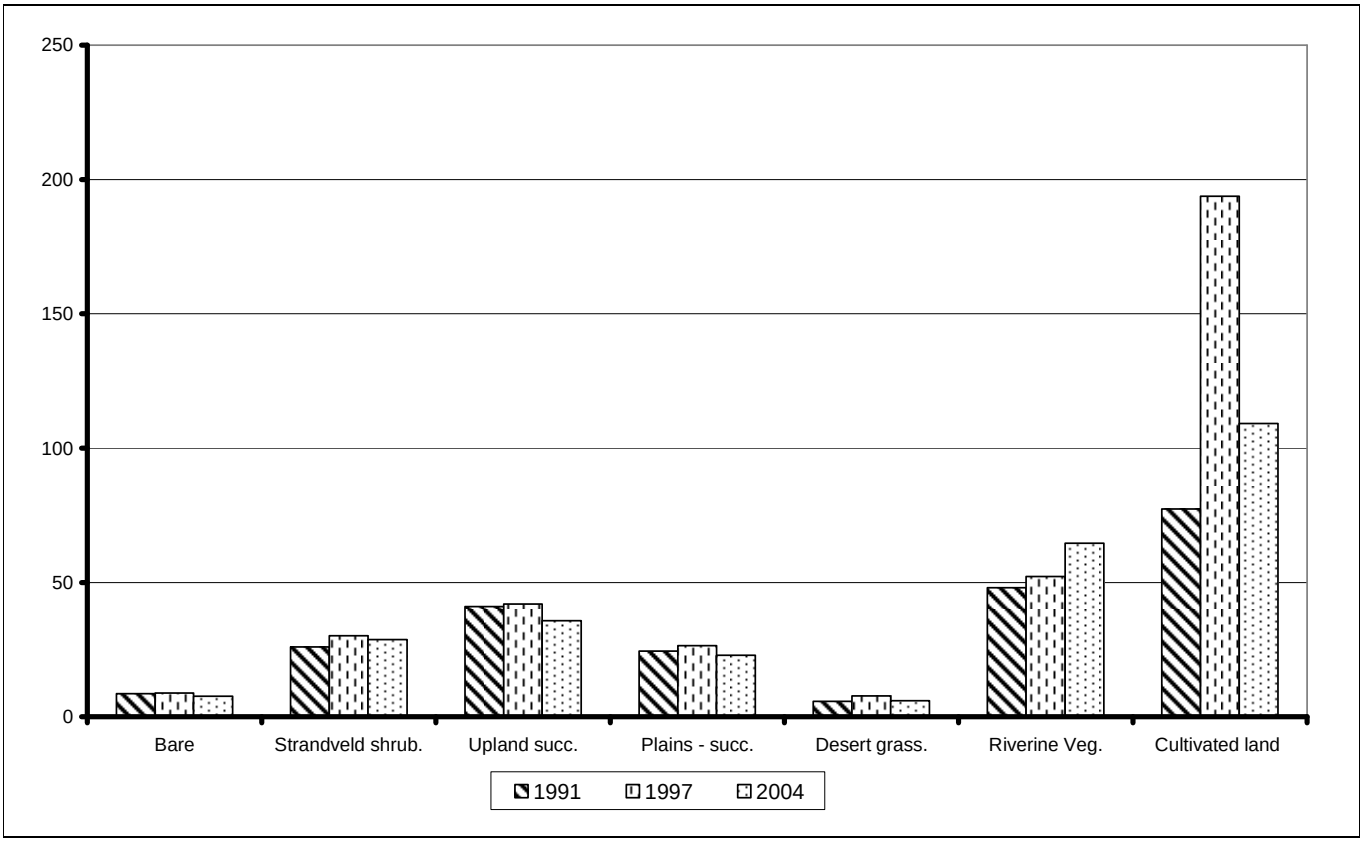

Figure 22: The mean PVI values per classification class. Class names have been abbreviated.

Chapter 8

Synthesis

8.1 Available moisture and vegetation dynamics

In order to detect vegetative change using remote sensing, particularly in semi-arid or arid environments, it is essential that regional patterns of precipitation, and their resultant natural cycles of vegetation change, are properly understood. The interpretation of the relationship between precipitation and resultant vegetation dynamics was undertaken using various sources of data. One of the principle data sources was MODIS NDVI data. Despite its relatively short existence, when compared to other continuous course scale sensors, MODIS data had the advantage of a 250 meter resolution, as well as a novel technique (TiSeg) of using data quality layers, interpolation and harmonic analysis to accurately pre-process the imagery.

The correlation that was detected between the available rainfall data and the NDVI of the region may be a very small correlation but it can be seen as being significant none the less. Firstly, it corresponds with common knowledge that vegetation response to rainfall is lagged, and it also corresponds to literature that has quantitatively proven this to be true (i.e. Nicholson *et al*., 1990; Schmidt & Karnieli, 2000). This could have implications for other researchers in this region, who may wish to use MODIS imagery for similar regional type research. Secondly, the fact that the correlation was so small could point towards the poor and sparse nature of the rainfall data, but it could also be indicative of the fact that rainfall is not the only form of precipitation that dictates vegetation response in the region. The importance and prominence of other sources of precipitation is alluded to extensively in literature such as Mucina *et al*. (2006) and Jürgens, (2006). Seely (1978) states that plants of the coastal Namib desert regions, some of which appear in the Richtersveld, are heavily dependant on fog as their additional source of water. The investigation into vegetation response to available moisture also revealed the influence of topography on the distribution of moisture, and therefore vegetation. The spatial variation of moisture and resultant vegetation, as defined by the vegetation classes of Mucina & Rutherford (2006), was also apparent. From the analysis conducted in order to understand vegetation response to moisture, it appears as though the results agree with literature on a number of aspects. Firstly, there is a small but significant lagged relationship between rainfall and vegetation response. Secondly, vegetation responds to topographically induced moisture variations, especially altitude and aspect. Thirdly, vegetation response could be shown as being in agreement with the wet and dry seasons, with peaks of vegetation response occurring in the autumn and/or winter months. And lastly, evidence was given of the spatial response of vegetation to variations of moisture within a landscape, also heavily influenced by topography. From these results, and in response to the original question, it does

appear to be possible to use synoptic, precipitation and topographic data to understand the vegetation response to available moisture.

8.2 Temporal Changes in the Cycles of Vegetation Response

One of the first things noticed about this particular analysis was the decreasing trend of the mean NDVI signal between 2000 and 2005. Given that results of the PCA analysis point towards three drier than normal winters, this could be of some concern. However, the 5th order polynomial trend line did show evidence of a recovery in 2005, and the absolute decline appeared to be very small, which with irregular rainfall data and a time series of only six years is difficult to draw any concrete conclusions

The PCA of the MODIS NDVI time series was conducted to gain an insight into the sources of variation that appeared in the six year time series, in order to try and understand the natural cycle of events in the region. The results proved difficult to interpret but with the help of a variety of data sources, a number of observations could be made. Images appear to represent three unusually dry winters for years 2000, 2001 and 2003, but the rainfall data on record does not correlate with the winter periods of 2000 and 2001. In the months prior to 2003 though, the rainfall records do show a noticeable absence of rainfall, but at the same time the 2004 year exhibits an even worse shortage of rain, and yet the 2004 winter NDVI signal appears to show a healthy vegetation cover. All of this could very well point to the influence of incoming mists, fog and low level cloud from the cold Benguela current of the West coast (Desmet, 2007). Plants that grow in arid environments are often adapted in ways that minimise moisture loss during the day and yet are able to maximise the gathering of available moisture during nights or early mornings when moisture, in the form of dew or fog, is more accessible to the plant than moisture from an episodic thundershower would be (Jürgens, 2006).

Because rainfall data does not point to dry winter periods, while the respective images do, one could again assume that the images relate to a lack of alternative forms of precipitation, which may very well be the major source of water for this type of vegetation. The assumptions based on alternative precipitation could be proved or disproved by current research occurring in the area as part of a BIOTA South project looking at the harvesting and quantifying fog.

Despite evidence on the relationships between vegetation and precipitation, the imagery does appear to show weak evidence of the two seasons operating in the area, in component 2 of the PCA. This could be due to the dominance of the strong, and predictable, vegetation response in winter months when compared to the more erratic, and some times destructive, summer rainfall patterns. The imagery also shows signs of vegetation change over the years and with differing spatial extents. In some cases these areas of change

appear to be caused by one or two significant events, and yet others appear to be a more consistent trend of vegetation increase or decrease. Looking at the NDVI profiles, these increases and/or decreases do not appear to be significant, however, the true significance of the change is difficult to quantify given the nature of the methods being used, i.e. remote detection of a weak vegetation signal, as well as the characteristics of a region that has a number of sensitive plant species that recover from disturbance very slowly, especially when the seed bank has been disturbed (Jürgens *et al*., 1999; *Jürgens*, 2006).

The seasonality shift analysis was conducted in order to get a better understanding of the natural cycles of the region, and whether or not the seasonality of the region had shifted in time due to the effects of projected climatic threats, such as global warming. The analysis relied heavily on identifying uni- and/or bi-model pixels (i.e. one or two phenological cycles within a year), in order to compare with the six year mean NDVI signal. As can be expected most of these pixels appeared in the highland areas of the region, which would regularly receive winter and/or summer rainfall and therefore exhibit the strongest phenological signals. The results show no significant trends or deviations from the mean NDVI signal, from which it could be concluded that climatic changes have not yet influenced the vegetation phenologies of the region. However, given the usually long term nature of climate change research it is unlikely that conclusions such as this could be made based on only six years of data.

Using this continuous, but course scale, imagery has allowed for the interpretation of vegetation dynamics through time. Despite encouraging results from the attempt to understand vegetation response to available moisture, the results from the temporal analysis appear to show that this relationship is more complex than the methods are able to detect. For example, it is difficult to interpret why there are NDVI maximum peaks during times when total vegetation cover is at a low, or why there isn't more of a seasonality shift during these same apparently unusually dry winter periods. Despite there being no significant shifts in seasonality, the region still appears to have inter-annual (i.e. unusually dry winters for 2000, 2001 and 2003) and intra-annual variations (i.e. component 4 and the temporal profiles of change) that course scale imagery can not fully explain. In response to the second research question, it appears as though the course scale imagery has not been able to fully account for the natural cycles of vegetation response through time, and is not able to conclusively point to any changing climatic conditions in the region. Perhaps more clarity could be achieved with more accurate rainfall/precipitation data and a longer time series of imagery.

8.3 Spatial distribution of vegetation change

Having used course scale MODIS imagery to gain a regional scale understanding of the vegetation dynamics of the study area, the pixel- and object-based approaches were carried out using medium scale Landsat

imagery, in order to determine the presence and spatial distribution of vegetation change on a finer scale. At this scale the results overwhelmingly show the majority of the region's pixels to be stable and without any major vegetation changes, except for those associated with seasonal changes, episodic green-up events and differences due changes in topography. However, the 'negative' change present in the region surrounding Kuboes could be interpreted as showing signs of vegetation change through time. These instances of change do occur on the slopes of upland areas, which would concur with Hendricks (2005, pers.com) who says this is a preferred habitat for the grazing of animals. But, change in the upland areas would also contain uncertainty due to the lack of topographic correction. It is notoriously difficult to validate multi-temporal change detection results, because data on the original state of vegetation is not present (Jensen, 1996) The rest of the change that was detected appears to have been very similar throughout the years. Therefore, not only where the results pointing to a stable region, but also towards a region that exhibits a very similar type and distribution of change between the years. It was somewhat encouraging to see that both methods managed to differentiate the wet 1997 year from the other drier years. With this in mind the results showing differences between 1991 and 2004 are probably a better reflection of the cumulative change that took place during this time. The results show that very little change occurred between 1991 and 2004. There was no advantage in using a segmentation, or object, based approach over the common pixel-based classification approach. Unless the full potential of the object-based classification software has been grasped, it is recommended that pixel-based approaches be used because of the object-based approach of averaging many pixels in order to create one 'object'. There are limitations to both sets of results, due to an inability to meet certain accuracy assessment requirements. Despite the limitations, and in answer to research question three, this data set was able to detect small amounts of vegetation cover change over a 14 year period. However, these changes were predominantly caused by seasonal differences, and once they were removed (i.e. wet season images and 1997 images) the region, at a Landsat scale, appears to be very stable and without significant, detectable, vegetation cover changes. Although the question was entertained, the spatial resolution of the imagery, the environmental factors at play, overlapping boundaries of influence and nomadic lifestyles, it would have been difficult to accurately detect, and justify, any detected grazing impacts around stockposts. However, this question definitely deserves more attention in order to monitor vegetation changes that Hendricks *et al*. (2005a) observed, but it would be best answered using higher spatial resolution imagery. Based on results from contingency accuracy assessments and a reasonable knowledge of the region and imagery, significantly more accurate results would not have been achieved had circumstances been different or limitations avoided.

8.4 Study Limitations and Recommendations

One of the major criticisms of remote sensing is that its potential is often oversold (Currey *et al*. 1987). A successful change detection study must take cognisance of the environmental factors involved in the study

area, and these factors should be balanced against the selection of appropriate remote sensor systems, their cost and processing requirements, as well as the possible change detection methods that can be used (Coppin & Bauer, 1996; Jensen, 1996).

The finances of a change detection study, such as this, play a critical role in the success of the project because they ultimately affect each step of the change detection process chain, from the type of imagery used and how it will be processed, to how many field campaigns for validation are made. Remote sensing projects are expensive. Despite the price of certain types of imagery decreasing or becoming freely available (i.e Landsat and MODIS), in many cases the user would still have to pay for the data to be pre-processed to a certain level that would allow the user to open the data on available software packages, as was the case with this project. Should a user wish to make use of freely available imagery, considerations need to be made in terms of available internet bandwidth and subsequent download times, or alternatively, postage delivery times and costs need to be considered. Common software packages, needed to analyse the data, also constitute a significant capital investment when first starting out, and, in the case of ENVI 4.0 that was purchased for this project, can cost upwards of R25 000. Field campaigns, especially ones that involve travelling very long distances to remote and rugged study areas, also contribute significantly to a projects expense. Despite appropriate planning, a project's field validation trips can be hampered by unfortunate events, and there needs to be sufficient funding in order to buffer against these events. Validation of remote sensing imagery and results should ideally not be limited or influenced by site accessibility and researcher bias, and should strive to achieve adequate sample sizes and distributions in order to satisfy statistical science assumptions (Booth & Tueller, 2003). This project was unable to meet all these requirements as the study area was not only too vast for adequate samples to be taken, but also rugged and difficult to access in parts.

Project funding also influenced the choice of data provider, responsible for partial pre-processing of the images. The pre-processing of imagery in this project appears to have influenced the results of the atmospheric correction programme ATCOR (Richter, pers. comm., 2005). The fact that ATCOR could not be successfully applied to the imagery meant that a) absolute radiometric correction to surface reflectance, as opposed to relative top-of-atmosphere reflectance, could not easily be retrieved, and b) the imagery was not topographically corrected. Images with topographically corrected surface reflectance provide a more accurate reflection of ground targets by eliminating atmospheric noise between the ground and the sensor, as well as correcting for differing sun angles and azimuths that influence the amount of shadow in topographically complex scenes. The topographic correction of imagery also depends on the accuracy and resolution of available digital elevation models (DEMs). In this project none of the three available DEMs could accurately capture the topographic complexity of the Richtersveld region. Surface reflectance values

can pave the way, should the user have the knowledge and experience, to using spectral mixture analysis (SMA) that has shown to be partly successful in arid regions (Ustin *et al*., 1986; Elmore *et al*., 2000). SMA estimates the proportion of each ground pixel's area that belongs to a variety of cover types, by decomposing a combined spectrum into 'spectral endmembers' using linear mixture models and weighting coefficients (Okin & Roberts, 2004). Although SMA has been used with Landsat data (Elmore & Mustard, 2000), hyperspectral data holds more promise as it contains a greater number of useful bands of information than multispectral sensors (Okin & Roberts, 2004). However, Okin *et al*. (2001b), who used hyperspectral data with high signal to noise ratios for vegetation discrimination caution that even SMA does not hold the key to the quantitative detection of sparse vegetation, especially when cover is below 30 %.

Apart from limitations with regard to the pre-processing of the imagery, one of the biggest limitations of the study lies in the spatial resolution of the Landsat imagery used. The spatial resolution of the MODIS imagery was adequate for the regional type assessment that it was used for, but not so for the Landsat analysis. As has been alluded to on numerous occasions, the study area is a hyper-arid region that consists of sparsely distributed vegetation, which is highly adapted to preventing moisture loss and therefore does not have very large leaves, if any at all, and generally grows very close to the ground (Noy-Meir, 1973). The adaptations and spatially disparate nature of this vegetation, together with the dominant signal of underlying geologies, all combine to distort and weaken any vegetation signal that might be present within the $900m^2$ of a Landsat ground pixel. In an environment such as this, and with pixels as big as this, it is very difficult to quantify and make conclusions about changes that may, or may not, be happening within the various mixtures of ground cover that make up a $900m^2$ pixel. Given the relationship between vegetation cover and underlying geologies, remote sensing of vegetation in arid environments would do well to focus on classifying vegetation according to geological boundaries.

Remote sensing change detection requires that the research question, and to a large extent the indicators needed to identify change, be based around the most appropriate and cost effective imagery available. If the research question is detailed and requires specific indicators to be detected, it would then be recommended that high spatial resolution, and potentially, high spectral resolution data be purchased. But high spatial and spectral resolution data are often not available on a continual basis, and are more expensive per square kilometre, therefore they may only be suitable for once off or short term research projects. An illustration of the differences between spatial resolutions can be found in Figure 23, which features a 30m pixel Landsat image and a screen shot of a Quickbird 2.44m pixel image (Google Earth), as well as a crude classification of the Quickbird screenshot. The screenshot and subsequent classification of the Quickbird image seen in Figure 23, shows startling evidence of the differences in available information between sensor systems and also brings to mind a number of possible research questions that could be asked using this type of imagery.

In a region such as the Richtersveld, where results from this study show the region to be predominantly stable on the medium to macro scale, it is this type of imagery that is needed in order to ask more of the finer scale questions, such as the impact of grazing animals on, often sensitive, vegetation communities in the RNP. These kinds of ground-based studies have been done in certain areas (Hendricks *et al.*, 2005a, b), and it would be incredibly informative for the management of the RNP if these studies, and results, could be scaled up to high resolution imagery that is able to capture a greater area of interest with one satellite over-pass.

Another limitation was that the anniversary date Landsat images could have been better selected if all available imagery was checked against rainfall records. Rainfall records related to this project only arrived well after the images were chosen. Checking available imagery against rainfall records allows the user to choose image dates that fall squarely within, or outside of, specific seasons, which would include or exclude phenological characteristics that influence the researchers questions they need answered.

a) Landsat 30m

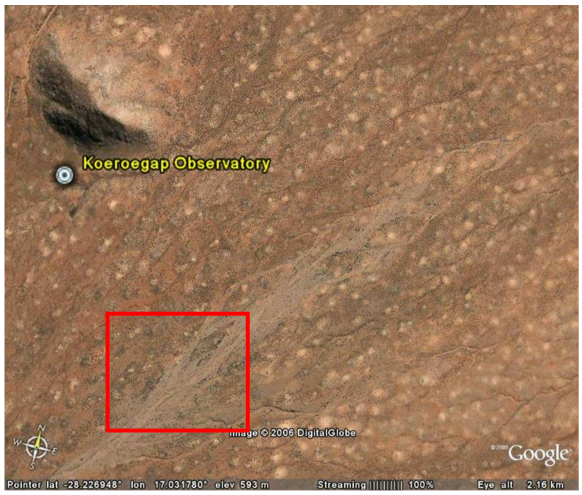

b) Quickbird 2.44m

c) Maximum likelihood classification of the Quickbird screenshot

Figure 23 (a-c): An illustration of different satellite pixel resolutions and the classification results that can be achieved

As has been illustrated in some of the results of this study, vegetation green-up after recent rainfall can mask or distort any real change that might be occurring. When conducting a multi-temporal change analysis within an arid or semi-arid region it is recommended that one takes into account three different timescales at which landscape change can occur. The most rapid of the timescales occurs soon after a precipitation event, where green-up by plant communities is often preceded by a nearly instantaneous green-up of cryptobiotic soil crusts, cyanobacteria, fungi, lichens or mosses, all of which can significantly influence the spectral signal of 'apparent' soil surfaces (Tsoar & Karnieli, 1996). The second time scale occurs at the seasonal scale, which the region as a whole tends to respond to. As has been pointed out in this study area, there are often two rainfall seasons that can complicate the identification of particular phenophases, as well as the

resultant selection of imagery. The third time scale would be vegetation change in response to inter-annual climate variations, or decadal responses to anthropogenic disturbance and/or droughts. These different timescales of landscape change not only influence the dates of imagery to be purchased but also the type of imagery that needs to be purchased in order to avoid superficial vegetation gains. As could be seen in this study, the MODIS imagery, with a continuous 16-day composite temporal resolution over six years, was able to highlight change on two of the above mentioned timescales. On the seasonal scale, three unusually dry winters were detected, while a number of episodic events were also picked up on the smaller time scale. More concrete results may be achieved if the analyses of shifting seasons or decreasing vegetation cover (NDVI) were to be continued using decadal time steps. The Landsat analysis highlighted the problems associated with using periodic satellite systems that are either hampered by cloud cover, or provide a 'snapshot' in time that falls within an undesirable period.

Despite the challenges involved with accurate remote sensing in arid regions, it still holds great potential because of its synoptic and temporal abilities. Synoptic methods that are able to detect and monitor change through time in sensitive regions, such as the Richtersveld, will benefit land managers and decision makers during times of stress. From this studies results, it would be recommended that an emphasis be put on the collection of continuous ground-based climate data in specific areas of interest. Future remote sensing work in the Richtersveld could use course scale imagery to focus specifically on the highland areas, which have the biggest vegetation response, in order to conduct decadal climate change type research. For finer scale research, such as direct and indirect anthropogenic induced vegetation change, it would be recommended that specific representative areas of interest be chosen in order to conduct high spatial and spectral resolution remote sensing research. High spatial resolution space-borne multispectral imagery is available, but is limited by its spectral resolution and resultant ability to differentiate different vegetation classes. It may therefore be a better idea to invest in a detailed field campaign that aims to build spectral libraries of land covers, and then conduct periodic air-borne hyperspectral campaigns. Investment into a detailed digital elevation model would also do well to aid future remote sensing research in the region.

8.4 Summary

Mather (2003) states that there appears to be a good argument against using remote sensing technologies for any quantitative detection of vegetative change, especially in arid or semi-arid regions. There are a variety of factors that combine to distort, or weaken, what is already an inherently poor vegetation signal as a result of plant adaptations, high reflectivity of background geologies, and spatio-temporal variations in vegetation response. Despite these issues it is possible, and should become increasingly possible with advances in satellite technology and methods with which to analyse the data. As remote sensing breaks away from being seen solely for research or military purposes, thanks largely to online programmes such as Google Earth,

satellite data is becoming increasingly more accessible and satellite systems more advanced. With satellite spatial and spectral resolutions decreasing, and temporal resolutions increasing, it will become increasingly possible for researchers to find a balance between satellite limitations, environmental factors, and the necessary detection of specific indicators. Until the day arrives when researchers are able to use daily hyperspectral imagery with 1-3m pixels, it is all a question of finding the right balance between the research question, the costs involved, and the study areas environmental factors. Part of this balance must include adequate, and in some cases detailed, ground sampling procedures because while the value of remote sensing for landscape level change detection is rarely refuted, these methods are often inadequate for detailed inventories or measurements of rangeland condition.

While this study had a number of limitations and fell short on meeting some of the statistically correct requirements, it nevertheless managed to give a reasonable account of the change situation in the Richtersveld, particularly at the medium to large scale. The study was undertaken using a number of methods and datasets that varied in temporal and spatial resolutions. There is little doubt that alternative methods, datasets, or even timescales could have been attempted given more time. The limitations pertaining to these methods and/or datasets have been discussed and can be used to inform and build upon in future remote sensing research in the region. The project could provide a platform from which more detailed research could be launched, should a project with a well planned and thoroughly researched hypothesis, as well as an adequate budget, decide to investigate matters on a smaller scale. Future remote sensing projects in the region would do well to invest in high spatial resolution imagery, which could be used to investigate a number of potential threats to fine scale biodiversity in the region, such as erosion and grazing impacts. Future projects should also put heavy emphasis on detailed ground sampling designs in order to facilitate the scaling up of information or data. Being able to upscale detailed ground-based information to high resolution imagery (e.g. Quickbird), and then from high resolution imagery to medium resolution (e.g. Landsat) imagery, and again to course resolution imagery (eg. MODIS) will be of much greater use to a land manager who often needs to manage available resources at different scales. Given the resolutions that this project was working with, it is unlikely that different results would have been achieved, none the less it would have been interesting to combine results from its two sister projects. One project looked at increasing ground sampling accuracies by using high resolution photography from a mobile raised platform, while the other was to investigate goat movements using GPS telemetry. Unfortunately one of the projects failed to materialise while the others results are still forthcoming. However, it is these types of integrated studies that are needed in order for remote sensing to be truly effective in providing land managers with cost effective information about vast tracks of land. This information can then be used to inform decision making on the allocation of resources, or on intervention strategies to mitigate against biodiversity loss occurring through a combination of threats, such as overgrazing and climate change.

References

Abel, N.O.J. and Blaikie, P. (1989). Land degradation: Stocking rates and conservation policies for the communal rangelands of Botswana and Zimbabwe. *Land Degradation and Rehabilitation*, **1**, 101–123.

Adams, M. (1996). When is ecosystem change land degradation? Comments on land degradation and grazing in the Kalahari by Doughill, A. and Cox, J. (1995) (Pastoral Development Network Paper 38c). *Pastoral Development Network Paper 39e*. London, UK: Overseas Development Institute.

Anyamba, A. and Tucker, C.J. (2005). Analysis of Sahelian vegetation dynamics using NOAA-AVHRR NDVI data from 1981 to 2003, *Journal of Arid Environments*, **63**, 596–614.

Archer, E.R.M. (2004). Beyond the 'climate versus grazing' impasse: using remote sensing to investigate the effects of grazing system choice on vegetation cover in the eastern Karoo. *Journal of Arid Environments*, **57**, 381-408.

Armston, J.D., Danaher, T.J., Goulevitch, B.M. and Byrne, M.I. (2002). Geometric correction of Landsat MSS, TM, and ETM+ imagery for mapping of woody vegetation cover and change detection in Queensland. *Proceedings of the 11th Australasian Remote Sensing and Photogrammetry Conference*, 2-6 September 2002, Brisbane, Australia.

Baatz, M., Benz, U., Dehghani, S., Heynen, M., Höltje, A., Hofmann, P., Lingenfelder, I., Mimler, M., Sohlbach, M., Weber, M. and Willhauk, G. (2004). *eCognition User Guide 4*. Definiens Imaging GmbH, München.

Bannari, A., Morin, D., Bonn, F. and Huete, A.R. (1995). A review of vegetation indices. *Remote Sensing Reviews*, **13**, 95–120.

Baret, F. and Guyot, G. (1991). Potentials and limits of vegetation indices for LAI and APAR assessment. *Remote Sensing of Environment*, **46**, 213–222.

Baret, F., Guyot, G. and Major, D.J. (1989). TSAVI: a vegetation index, which minimizes soil brightness effects on LAI and APAR estimation. *Proceedings of the 12th Canadian Symposium on Remote Sensing*, IGARRSS 1990, Vancouver, British Columbia, Canada, **3**, 1355–1358.

Behnke, R.H. and Scoones, I. (1993). Rethinking rangeland ecology: implications for rangeland management in Africa. In Behnke, R.H., Scoones, I. and Kerven, C. (Eds.) *Range ecology at disequilibrium* (pp. 1-30). London, UK: Overseas Development Institute.

Blench, R.M. and Sommer, F. (1999). *Understanding rangeland biodiversity*. ODI Working Paper No. 121. London, UK: Overseas Development Institute.

Booth, D.T. and Tueller, P.T. (2003). Rangeland monitoring using remote sensing. *Arid Land Research and Management*, **17,** 455–467.

Brandtberg, T. (2002). Individual tree-based species classification in high spatial resolution aerial images of forests using fuzzy sets. Fuzzy Sets and Systems, **132** (3), 371–387.

Brogaard, S. and Ólafsdóttir, R. (1997) Ground-truths or Ground-lies? Environmental Sampling for Remote Sensing Applications Exemplified by Vegetation Cover Data. Available online at: http://www.nateko.lu.se/Elibrary/LeRPG/1/LeRPG1Article.htm.

Bruce, C.M. and Hilbert, D.W. (2004). *Pre-processing methodology for application to Landsat TM / ETM+ imagery of the wet tropics*. Cooperative Research Centre for Tropical Rainforest Ecology and Management. Cairns, Australia: Rainforest CRC.

Campbell, J.B. (1996). *Introduction to Remote Sensing*. 2nd ed. New York: The Guilford Press.

Campbell, J.B. (2002). *Introduction to Remote Sensing*. 3rd ed. New York: The Guilford Press.

Chander, G. and Markham, B.L. (2003). Revised Landsat-5 TM radiometric calibration procedures, and postcalibration dynamic ranges. *IEEE Transactions on Geoscience and Remote Sensing*, **41**, 2674-2677.

Chavez, P.S. Jr. and Mackinnon, D.J. (1994). Automatic detection of vegetation changes in the southwestern United States using remotely sensed images. *Photogrammetric Engineering and Remote Sensing*, **60**, 571–583.

Chavez, P.S. (1996). Image-based atmospheric corrections revisited and improved. *Photogrammetric Engineering and Remote Sensing*, **62**, 1025-1036.

Chen, X., Vierling, L. and Deering, D. (2005). A simple and effective radiometric correction method to improve landscape change detection across sensors and across time. *Remote Sensing of Environment*, **98**, 63-79.

Civico, D.L., Hurd, J.D., Wilson, E.H., Song, M. and Zhang, Z. (2002). A comparison of land use and land cover change detection methods. *ASPRS-ACSM Annual Conference and FIG XXII Congress*, 22-26 April 2002, Washington D.C., USA.

Colby, J.D. (1991). Topographic normalization in rugged terrain. *Photogrammetric Engineering and Remote Sensing*, **57**, 531-537.

Colby, J.D. and Keating, P.L. (1998). Land cover classification using Landsat TM imagery in the tropical highlands: the influence of anisotropic reflectance. *International Journal of Remote Sensing*, **19** (8), 1479-1500.

Colditz, R., Conrad, C., Schmidt, M., Schramm, M., Schmidt, M., and Dech, S. (2006). Mapping regions of high temporal variability in Africa, *ISPRS Commission VII Mid-term Symposium "Remote Sensing: From Pixels to Processes"*, Enschede, the Netherlands, 8-11 May 2006, 172-176.

Colwell, R.N. (1997). History and Place of Photographic Interpretation. In Philipson, W.R (Ed.) *Manual of Photographic Interpretation* 2nd Edition. (pp. 3-47). Bethesda, Maryland: American Society for Photogrammetry and Remote Sensing.

Conese, C., Gilabert, M.A., Maselli, F. and Bottai, L. (1993). Topographic normalisation of TM scenes through the use of an atmospheric correction method and digital terrain models. *Photogrammetric Engineering and Remote Sensing*, **59**, 1745-1753.

Conservation International. (2006). *Biodiversity Hotspots: The Succulent Karoo*. Available online at: http://www.biodiversityhotspots.org/xp/Hotspots/karoo/

Coppin, P. and Bauer, M.E. (1996). Digital change detection in forest ecosystems with remote sensing imagery. *Remote Sensing Review*, **13**, 207-234.

Coppin, P., Jonckheere, I., Nackaerts, K., Muys, B. and Lambin, E. (2004). Digital change detection methods in ecosystem monitoring: a review. *International Journal of Remote Sensing*, **25**, 1565-1596.

Cowling, R.M. and Hilton-Taylor, C. (1999). Plant biogeography, endemism and diversity. In Dean, W.R.J. and Milton, S.J. (Eds.). (pp. 42-56). *The Karoo: ecological patterns and processes*. Cambridge, UK: Cambridge University Press.

Cowling, R.M. and Pierce, S.M. (1999). *Namaqualand: a succulent desert*. Vlaeberg, South Africa: Fernwood Press.

Cowling, R.M., Esler, K.J. and P.W. Rundel. (1999). Namaqualand, South Africa – an overview of a unique winter-rainfall desert ecosystem. *Plant Ecology*, **142**, 3-21.

Currey, B., Fraser, A. S. and Bardsley, K. L. (1987). How useful is Landsat monitoring? *Nature*, **328**, 587-589.

De Haan, C., Steinfeld, H. and Blackburn, H. (1997) *Livestock and the environment: Finding a balance*. A study sponsored by European Commission, FAO, World Bank and others. Suffolk, UK: WRENmedia.

Desmet, P. G. (2007). Namaqualand – A brief overview of the physical and floristic environment. *Journal of Arid Environments*, **70**, 570 – 587.

Desmet, P.G. and Cowling, R.M. (1999). The climate of the Karoo—a functional approach. In Dean, W.R.J. and Milton, S.J. (Eds). *The Karoo: Ecological Patterns and Processes*. Cambridge University Press, pp. 3–16.

Didan, K. (2005). Terrestrial Biophysics and Remote Sensing Lab (TBRS): MODIS compositing algorithm. Available online at: http://tbrs.arizona.edu/project/MODIS/compositing.php

Dorner, B., Lertzman, K. and Fall, J. (2002). Landscape pattern in topographically complex landscapes: Issues and techniques for analysis. *Landscape Ecology*,**17**, 729–43.

Doughill, A. and Cox, J. (1995). Land degradation and grazing in the Kalahari: new analysis and alternative perspectives. *Pastoral Development Network Paper 38c*. London, UK: Overseas Development Institute.

Driver, A., Desmet, P.G., Rouget, M., Cowling, R.M. and Maze, K.E. (2003). *Succulent Karoo Ecosystem Plan Biodiversity Component Technical Report*. Cape Conservation Unit, Botanical Society of South Africa, Cape Town.

Dube, O. and Pickup, G. (2001). Effects of rainfall variability and communal and semi-commercial grazing on land cover in Southern African rangelands. *Climate Research*, **17**, 195–208.

Dudley, N. (2003). No place to hide: the effects of climate change on protected areas, WWF Climate Change Programme. Available at: http://assets.panda.org/downloads/wwfparksbro.pdf

Eastman, J.R. (2006). *IDRISI Andes: Guide to GIS and Image Processing*. Clark University, Worcester, Massachusetts.

Elachi, C. (1987). *Spaceborne Radar Remote Sensing: Applications and Techniques*. New York, USA: IEEE Press.

Ellis, J.E., Coughenour, M.B. and Swift, D.M. (1993). Climate variability, ecosystem stability, and the implications for range and livestock development. In Behnke, R.H., Scoones, I. and Kerven, C. (Eds.). (pp. 31-41). *Range ecology at disequilibrium*. London, UK: Overseas Development Institute.

Elmore A.J., Mustard J.F., Manning S.J., and Lobell D.B. (2000). Quantifying vegetation change in semiarid environments: Precision and accuracy of spectral mixture analysis and the Normalized Difference Vegetation Index. *Remote Sensing of Environment*, **73**, 87-102.

ERDAS Incorporated. (1997). *ERDAS Field Guide* 4th Edition. Atlanta, USA: ERDAS Inc.

Esler, K.J. and Rundel, P.W. (1999). Phenological and growth form divergence in convergent desert ecosystems: a Succulent Karoo and Mojave desert comparison. *Plant Ecology*, **142**, 97–104.

Foden, W., Midgley, G.F., Hughes, G., Bond, W.J., Thuiller, W., Hoffman, M.T., Kaleme, P., Rebelo, A.G. and Hannah, L. (2007). Namib desert tree Aloes feel the heat of climate change. *Diversity and Distributions*, **13**, 645-653.

Foody, G.M. (2001). Monitoring the magnitude of land cover change around the southern limits of the Sahara. *Photogrammetric Engineering and Remote Sensing*, **67**, 841-847.

Franklin, J., Duncan, J. and Turner, D.L. (1993). Reflectance of vegetation and soil in Chihuahuan desert plant communities from ground radiometry using SPOT wavebands. *Remote Sensing of Environment*, **46**, 291-304.

Friedel, M.H., Laycock, W.A. and Bastin, G.N. (2000). Assessing rangeland condition and trend. In Mannetje, L. & Jones, R.M. (Eds.). *Field and Laboratory Methods for Grassland and Animal Production Research*. (pp. 227-262). Wallingford, UK: CAB International.

Fuller, R.M., Groom, G.B. and Jones, A.R. (1994). The land cover map of Great Britain: an automated classification of Landsat Thematic Mapper data. *Photogrammetric Engineering and Remote Sensing*, **60**, 553–562.

Fusco, M., Holachek, J., Tembo, A., Daniel, A. and Cardenas, M. (1995). Grazing influence on watering point vegetation in the Chihuahuan Desert. *Journal of Range Management*, **48,** 32–38.

Goyot, G. and Gu, X. (1994). Effect of radiometric corrections on NDVI-determined from SPOT-HRV and Landsat TM Data. *Remote Sensing of Environment*, **49**, 146-180.

Hanan, N.P., Prince, S.D. and Hiernaux, P.H.Y. (1991). Spectral modelling of multicomponent landscapes in the Sahel. *International Journal of Remote Sensing*, **12,** 1243-1258.

Hendricks, H.H. (2004). *Semi-nomadic pastoralism and the conservation of biodiversity in the Richtersveld National park, South Africa*. PhD dissertation. University of Cape Town, Cape Town, South Africa.

Hendricks, H.H., Midgley, J.J., Bond, W.J. and Novellie, P.A. (2004). Why communal pastoralists do what they do in the Richtersveld National Park. *African Journal of Range and Forage Science*, **21**, 29-36.

Hendricks, H.H., Bond, W.J., Midgley, J.J. and Novellie P.A. (2005a). Plant species richness and composition a long livestock grazing intensity gradients in a Namaqualand (South Africa) protected area. *Plant Ecology*, **176**, 19-33.

Hendricks, H.H., Clark, B., Bond, W.J., Midgley, J.J. and Novellie, P.A. (2005b). Movement response patterns of livestock to rainfall variability in the Richtersveld National Park. *African Journal of Range and Forage Science*, **22**, 117-125.

Hilton-Taylor, C. (1996). Patterns and characteristics of the flora of the Succulent Karoo Biome, southern Africa. In van der Maesen, L.J.E., van der Burgt, X.M. and van Medenbach de Rooy, J.M. (Eds.). *The Biodiversity of African Plants*. Dordrecht, The Netherlands: Kluwer Academic Publishers, pp. 58-72.

Hoffman, M. T. and Cowling, R. M. (1987). Plant physiognomy, phenology and demography. In: Cowling, R. M. and Roux, P. W. (Eds.). The Karoo biome: a preliminary synthesis. Part 2, vegetation and history. South African National Scientific Programme Report 142, pp. 1-34.

Hoffman, M.T., Cousins, B., Meyer, T., Petersen, A. and Hendricks, H. (1999). Historical and contemporary land use and the desertification of the karoo. In Dean, W.R.J and Milton, S.J. (Eds). *The Karoo: Ecological patterns and processes*. Cambridge University Press, Cambridge, pp 257-273.

Huang, C., Wylie, B., Yang, L., Homer, C. and Zylstra, G. (2002). Derivation of a tasselled cap transformation based on Landsat 7 at-satellite reflectance. *International Journal of Remote Sensing*, **23**, 1741-1748.

Hudak, A.T. and Brockett, B.H. (2004). Mapping fire scars in a southern African savanna using Landsat imagery. *International Journal of Remote Sensing*, **25**, 3231 – 3243.

Huete, A.R., Jackson, R.D. and Post, D.F. (1985). Spectral response of a plant canopy with different soil backgrounds. *Remote Sensing of Environment*, **17**, 37-53.

Huete, A.R. and Jackson, R.D. (1987). Suitability of spectral indices for evaluating vegetation characteristics on arid rangelands. *Remote Sensing of Environment*, **23**, 213-232.

Huete, A.R. (1988). A soil-adjusted vegetation index (SAVI). *Remote Sensing of Environment*, **25**, 50-70.

IPCC, (2007a). Summary for Policymakers. In Solomon, S., Qin, D., Manning, M., Chen, Z., Marquis, M., Averyt, K.B., Tignor, M. and Miller, H.L. (Eds.). *Climate Change 2007: The Physical Science Basis. Contribution of Working Group I to the Fourth Assessment Report of the Intergovernmental Panel on Climate Change*. Cambridge University Press, Cambridge, pp 1-18

IPCC, (2007b). Summary for Policymakers. In Parry, M.L., Canziani, O.F., Palutikof, J.P., van der Linden, P.J. and Hanson, C.E. (Eds.). *Climate Change 2007: Impacts, Adaptation and Vulnerability. Contribution of Working Group II to the Fourth Assessment Report of the Intergovernmental Panel on Climate change*, Cambridge University Press, Cambridge, pp 7-22.

Jensen, J.R. (1996). *Introductory Digital Image Processing: A Remote Sensing Perspective*, 2nd Edition. New Jersey, USA: Prentice Hall.

Jensen, J.R. (2000). *Remote Sensing of the Environment: An Earth Resource Perspective*. New Jersey, USA: Prentice Hall.

Jürgens, N. (1991). A new approach to the Namib Region. I: Phytogeographic subdivision. *Vegetatio*, **97**, 21–38.

Jürgens, N., Gotzmann, I.H. & Cowling, R.M. (1999). Remarkable medium-term dynamics of leaf succulent Mesembryanthemaceae shrubs in the winter-rainfall desert of northwestern Namaqualand, South Africa. *Plant Ecology*, **142**, 87–96

Jürgens, N. (2006). Desert Biome. In Mucina, L. and Rutherford, M.C. (Eds). *The vegetation of South Africa, Lesotho and Swaziland*. Strelitzia, volume19, 220-299. South African National Biodiversity Institute, Pretoria, South Africa.

Kauth, R.J. and Thomas, G.S. (1976). The tasseled cap: A graphic description of the spectral temporal development of agricultural crops as seen by Landsat. *Proceedings of the Symposium on Machine Processing of Remotely Sensed Data*, June 29-July 1 1976, Purdue University of West Lafayette, Indiana, pp. 41-51.

Kwarteng, A. Y. and Chavez, P. S. Jr. (1998). Change detection study of Kuwait city and environs using multitemporal Landsat Thematic Mapper data. *International Journal of Remote Sensing*, **19**, 1651–1661.

Laliberte, A.S., Rango, A., Havstad, K.M., Paris, J.F., Beck, R.F., McNeely, R. and Gonzalez, A.L. (2004). Object-oriented image analysis for mapping shrub encroachment from 1937 to 2003 in southern New Mexico. *Remote Sensing of Environment*, **93** (1-2), 198-210.

Leroux, A. (2004). Alex's Remote Sensing Imagery Summary Table. Available at: http://homepage.mac.com/alexandreleroux/arsist/arsist.pdf

Lillisand, T.M. and Kiefer R.W. (1979). *Remote Sensing and Image Interpretation*. New York, USA: John Wiley.

Lillisand, M.T. and Kiefer, W.R. (1994). *Remote Sensing and Image Interpretation*. Third edn. New York, USA: John Wiley & Sons, Inc.

Lu, D., Mausel, P., Brondizio, E. and Moran, E. (2003). Change detection techniques. *International Journal of Remote Sensing*, **25**, 2365-2407.

Lyon, J.G., Yuan, D., Lunetta, R.S., and Elvidge, C.D. (1998). A change detection experiment using vegetation indices. *Photogrammetric Engineering and Remote Sensing*, **64**, 143– 150.

Maccherone, B. (date unknown). National Aeronautics and Space Administration, MODIS Website, Available online at: http://modis.gsfc.nasa.gov/data/

Mather, P.M. (2003). *Computer Processing of Remotely Sensed Images: An Introduction*, 2nd. Edition. Chichester, England: John Wiley & Sons Ltd.

McGwire K., Minor T., and Fenstermaker L. (2000). Hyperspectral mixture modeling for quantifying sparse vegetation cover in arid environments. *Remote Sensing of Environment,* **72**, 360-374.

Meadows, M.E. and Hoffman, M.T. (2002). The nature, extent and causes of land degradation in South Africa: legacy of the past, lessons for the future? *Area*, **34**, 428-437.

Meyer, P., Itten, K.I., Kellenberger, T., Sandmeier, S. and Sandmeier, R. (1993). Radiometric Corrections of Topographically Induced Effects on Landsat TM Data in an Alpine Environment. *ISPRS Journal of Photogrammetry and Remote Sensing*, **48**, 17-28.

Midgley, G.F. and O'Callaghan, M. (1993). Review of likely impacts of climate change on southern African flora and vegetation. In Markham, A., Dudley, N. and Stolen, S. (Eds.). *Some like it hot: Climate change, biodiversity and survival of species*. Gland, Switzerland: World Wildlife Fund for Nature.

Midgley, G.F., Chapman, R.A., Hewitson, B., Johnston, P., De Wit, M., Ziervogel, G., Mukheibir, P., van Niekerk, L., Tadross, M., van Wilgen, B.W., Kgope, B., Morant, P., Theron, A., Scholes, R.J. and Forsyth, G.G. (2005*). A Status Quo, Vulnerability and Adaptation Assessment of the Physical and Socio-Economic Effects of Climate Change in the Western Cape*. Report to the Western Cape Government, Cape Town, South Africa. Report No. ENV-S-C 2005-073. Stellenbosch, CSIR.

Midgley, G.F. and Thuiller, W. (2007). Potential vulnerability of Namaqualand plant diversity to anthropogenic climate change. *Journal of Arid Environments*, **70**, 615–628.

Miller, J.R. and Hobbs, R.J. (2002). Conservation where people live and work. *Conservation Biology*, **16**, 330-337.

Milton, S.J. (2001). Rethinking ecological rehabilitation in arid and winter rainfall regions of southern Africa. *South African Journal of Science,* **97**, 47-48.

Milton, S. and Hoffman, M.T. (1994). The application of state and-transition models to rangeland research and management in arid succulent and semi-arid grassy Karoo, South Africa. *African Journal of Range and Forage Science*, **11**, 18–26.

Milton, O.S., Ustin, S.L., Adams, J.B. and Gillespie, A.R. (1990). Vegetation in deserts: A regional measure of abundance from multispectral images. *Remote Sensing of Environment*, **31**, 1–26.

Mucina, L. and Rutherford, M.C. (Eds). (2006). *The vegetation of South Africa, Lesotho and Swaziland*. Strelitzia, volume19, 220-299. South African National Biodiversity Institute, Pretoria, South Africa.

Mucina, L., Jurgens, N., le Roux, A., Rutherford, M.C., Schmiedel, U., Elser, K.J., Powrie, L.W., Desmet, P.G. and Milton, S.J. (2006). Succulent Karoo Biome. In Mucina, L. and Rutherford, M.C. (Eds). *The vegetation of South Africa, Lesotho and Swaziland*. Strelitzia, volume19, 220-299. South African National Biodiversity Institute, Pretoria, South Africa.

Mukheibir, P. and Sparks, D. (2005). *Climate variability, climate change and water resource strategies for small municipalities*. Report WRC K5/1500, September 2005. Pretoria, South Africa: Water Research Commission.

Naveh, Z. and Whittaker, R.H. (1979). Structural and floristic diversity of shrublands and woodlands in Northern Israel and other mediterranean areas. *Vegetation*, **41**, 171–190.

Nicholson, S. (2005). On the question of the "recovery" of the rains in the West African Sahel. *Journal of Arid Environments*, **63**, 615–641.

Nicholson, S.E., Davenport, M.L. and Malo, A.R. (1990). A comparison of the vegetation response to rainfall in the Sahel and East Africa, using normalized difference vegetation Index from NOAA AVHRR. *Climatic Change*, **17**, 209–241.

Nordberg, M. and Evertson, J. (2003). Monitoring change in mountainous dry-heath vegetation at a regional scale using multitemporal Landsat TM data. *Ambio*, **32**, 502-509.

Noy-Meir, I. (1973) Desert Ecosystems: Environment and Producers, *Annual Review of Ecology and Systematics*, **4**, 25-51.

Noy-Meir, I., Gutman, M. and Kaplan, Y. (1989). Responses of Mediterranean grassland plants to grazing and protection. *Journal of Ecology*, **77**, 290–310.

O'Neill, A.L., Head, L.M. and Marthick, J.K. (1993). Integrating remote sensing and spatial analysis techniques to compare Aboriginal and pastoral fire patterns in the East Kimberley, Australia. *Applied Geography*, **13**, 67-85.

Okin, G.S. and Roberts, D.A. (2004). Remote sensing in arid regions: challenges and Opportunities. In Ustin, S. (Ed.). *The Manual of Remote Sensing*, 3rd Edition, (pp. 30). Volume 4. place. John Wiley & Sons, Ltd.

Okin, G.S., Murray, B. and Schlesinger, W.H. (2001a). Degradation of sandy arid shrubland environments: observation, process modelling, and management implications. *Journal of Arid Environments*, **47**, 123-144.

Okin G. S., Okin W. J., Murray B. and Roberts D. A. (2001b). Practical limits on hyperspectral vegetation discrimination in arid and semiarid environments. *Remote Sensing of Environment*, **77**, 212-225.

Olsvig-Whittaker, L.S., Hosten, P.E., Marcus, I. and Shochat, E. (1993). Influence of grazing on sand field vegetation in the Negev Desert. *Journal of Arid Environments*, **24**, 81–93.

Palmer, A.R. and van Rooyen, A.F. (1998). Detecting vegetation change in the southern Kalahari using Landsat TM data. *Journal of Arid Environments*, **39,** 143–153.

Pech, R.P., Graetz, R.D. and Davis, A.W. (1986). Reflectance modelling and the derivation of vegetation indices for an Australian semi-arid shrubland. *International Journal of Remote Sensing*, **7**, 389–403.

Peters, A.J. and Eve, M.D. (1995). Satellite monitoring of desert plant community response to moisture availability. *Environmental Monitoring and Assessment*, **37**, 273-287.

Pickup, G. (1995). A simple model for predicting herbage production from rainfall in rangelands and its calibration using remotely-sensed data. *Journal of Arid Environments*, **30**, 227–245.

Pickup, G., Chewings, V.H. and Nelson, D.J. (1993). Estimating changes in vegetation cover over time in arid rangelands using Landsat MSS data. *Remote Sensing of Environment*, **43**, 243–263.

Pickup, G., Bastin, G.N. and Chewings, V.H. (1994). Remote sensing-based condition assessment for non-equilibrium rangelands under large-scale commercial grazing. *Ecological Applications*, **4**, 497–517.

Pilon, P.G., Howarth, P.J., Bullock, R.A. and Adeniyi, P.O. (1988). An enhanced classification approach to change detection in semi-arid environments. *Photogrammetric Engineering and Remote Sensing*, **54**, 1709–1716.

Pons, X. and Sole-Sugranes, L. (1994). A simple radiometric correction model to improve automatic mapping of vegetation from multispectral satellite data. *Remote Sensing of Environment*, **48**, 191-204.

Qi, J., Chehbouni, A., Huete, A., Kerr, Y. H. and Sorooshian, S. (1994). A modified soil adjusted vegetation index. *Remote Sensing of Environment*, **48**, 119-126.

Ram, B. and Kolarkar, A. S. (1993). Remote sensing application in monitoring land use changes in arid Rajasthan. *International Journal of Remote Sensing*, **14**, 3191–3200.

Ray, T.W. (1995). *Remote Monitoring of Land Degradation in Arid/Semiarid Regions*. PhD. Thesis, California Institute of Technology.

Reid, H., Fig, D., Magome, H. and Leader-Williams, N. (2004). Co-management of Contractual National Parks in South Africa: Lessons from Australia. *Conservation and Society*, **2**, 377-409.

Riaño, D., Chuvieco, E., Salas, J. and Aquado, I. (2003). Assessment of different topgraphic corrections in Landsat TM data for mapping vegetation types. *IEEE Transactions on Geoscience and Remote Sensing*, **41**, 1056-1061.

Richardson, A.J. and Wiegand, C.L. (1977). Distinguishing vegetation from soil background information. *Photogrammetric Engineering and Remote Sensing*, **43**, 1541–1552.

Richter, R. (2001). *Atmospheric and Topographic Correction Model: ATCOR 3*. Unpublished Users Handbook.

Richter, R. (2003). *Atmospheric/topographic correction for satellite imagery: ATCOR-2/3 user guide*, version 5.5, January 2003, ReSe Applications Schläpfer, Wessling

Riginos, C. and Hoffman, M. T. (2003). Changes in population biology of two succulent shrubs along a grazing gradient. *Journal of Applied Ecology*, **40**, 615–625.

Ringrose, S., van der Post, C. and Matheson, W. (1997). Use of image processing and GIS techniques to determine the extent and possible causes of land management/fenceline induced degradation problems in the Okavango area, northern Botswana. *International Journal of Remote Sensing*, **18** (11), 2337-2364.

Roberts, D.A., Adams, J.B. and Smith, M.O. (1990). Predicted distribution of visible and near-infrared radiant-flux above and below a transmittant leaf. *Remote Sensing of Environment*, **34**, 1-17.

Rouse, J.W., Haas, R.H., Schell, J.A., Deering, D.W. and Harlan, J.C. (1974). *Monitoring the Vernal Advancements and Retrogradation (Greenwave Effect) of Natural Vegetation*. NASA/GSFC Final Report, NASA, Greenbelt, MD, USA.

Rutherford, M.C., Midgley, G.F., Bond, W.J., Powrie, L.W., Musil, C.F., Roberts, R. and Allsopp, J. (1999a). *South African Country Study on Climate Change: Terrestrial Plant Diversity Section, Vulnerability and Adaptation*. Pretoria, South Africa: Department of Environmental Affairs and Tourism.

Rutherford, M.C., Powrie L.W. and Schultz, R.E. (1999b). Climate change in conservation areas of South Africa and its potential impact on floristic composition: a first assessment. *Diversity and Distributions*, **5**, 253-262.

Schmidt, H. and Karnieli, A. (2000). Remote sensing of the seasonal variability of vegetation in a semi-arid environment. *Journal of Arid Environments*, **45**, 43-59.

Scoones, I. (1995). New directions in pastoral development in Africa. In Scoones, (Ed.). *Living with Uncertainty: New directions in pastoral development in Africa*. (pp. 1-36). London, UK: Intermediate Technology Publications Ltd., London.

Seely, M.K. (1978). The Namib Dune Desert: an unusual ecosystem. *Journal of Arid Environments*, **1**, 117-128.

Singh, A. (1988). Review Article: Digital change detection techniques using remotely-sensed data. *International Journal of Remote Sensing*, **10**, 989 – 1003.

Smith, R.B. (2005). Computing radiances, reflectance and albedo from DN's. Available online at: http://www.yale.edu/ceo/Documentation/ComputingReflectanceFromDN.pdf Yale, USA: Yale University.

Smith, J.A., Tzue, L.L. and Ranson, K.J. (1980). The lambertian assumption and Landsat data. *Photogrammetric Engineering and Remote Sensing*, **46**, 1183-1189.

Smith, M.O., Ustin, S.L., Adams, J.B. and Gillespie, A.R. (1990). Vegetation in deserts: a regional measure of abundance from multispectral images. *Remote Sensing of Environment*, **31**, 1-26.

Song, C., Woodcock, C.E., Seto, K.C., Lenney, M.P. and Macomber, S.A. (2001). Classification and change detection using Landsat TM data: When and how to correct atmospheric effects? *Remote Sensing of Environment*, **75**, 230-244.

South African National Parks (SANParks TM) Official website. (2005) Ai-Ais Richtersveld Transfrontier National Park. Available at: http://www.sanparks.org/parks/richtersveld/

Stow, D.A. (1999). Reducing the effects of misregistration on pixel-level change detection. *International Journal of Remote Sensing*, **20**, 2477-2483.

Succulent Karoo Ecosystem Programme (SKEP). (2006). Greater Richtersveld. Available at: http://www.skep.org/greater_richtersveld.html

Terhorst, A. (2004). *Mission support by CSIR SAC exceeds expectations during 2004*, SAC News, 26, pg 14, CSIR Satellite Applications Centre (SAC), Pretoria, South Africa.

Thiam, A. K. (1998). *Geographic Information Systems and Remote Sensing Methods for Assessing and Monitoring Land Degradation in the Sahel Region: The Case of Southern Mauritania*. Unpublished Ph.D. Dissertation, Graduate School of Geography, Clark University

Thompson, M.W. (1996). A standard land-cover classification scheme for remote sensing applications in southern Africa. *South African Journal of Science*, **92**, 34-42.

Thrash, I. (1998) Impact of water provision on herbaceous vegetation in the Kruger National Park, South Africa. J. Arid Environ. 38, 437– 450.

Todd, S. and Hoffman, M.T. (1999). A fence-line contrast reveals effects of heavy grazing on plant diversity and community composition in Namaqualand, South Africa. *Plant Ecology*, **142**, 169–178.

Townshend, J.R.G., Justice, C.O. and Gurney, C. (1992). The impact of misregistration on change detection. *I.E.E.E. Transactions on Geoscience and Remote Sensing*, **30**, 1054-1060.

Trodd, N.M. and Dougill, A.J. (1998). Monitoring vegetation dynamics in semi-arid African rangelands. *Applied Geography*, **18**, 315-330.

Tsoar, H. and Karnieli, A. (1996), What determines the spectral reflectance of the Negev-Sinai sand dunes? *International Journal of Remote Sensing.* **17**, 513-525.

Tucker, C. J. and Sellers, P. J. (1986) Satellite remote sensing of primary production. *International Journal of Remote Sensing*, **7**, 1395 - 1416.

Tucker, C. J., Justice, C. O. and Prince, S. D. (1986) Monitoring the grasslands of the Sahel 1984–1985. *International Journal of Remote Sensing*, **7**, 1571–1581.

Tucker, C. J., Dregne, H. E. and Newcomb, W. W. (1991). Expansion and contraction of the Sahara desert from 1980 to 1990. *Science*, **253**, 299–301.

Tucker, C.J., Newcomb, W.W. and Dregne, H.E. (1994). Improved data sets for determination of desert spatial extent. *International Journal of Remote Sensing*, 15, 3519-3545.

Turner, W., Spector, S., Gardiner, N., Fladeland, M., Sterling, E. and Steininger, M. (2003). Remote Sensing for Biodiversity Science and Conservation. *Trends in Ecology and Evolution*, **18**, 306-314.

United States Geological Survey (USGS): Earth Resources Observation and Science. (2006). Landsat Thematic Mapper Data (TM). Available at: http://eros.usgs.gov/guides/landsat_tm.html

Ustin, S.L., Adams, J.B., Elvidge, C.D., Rejmanek, M., Rock, B.N., Smith, M.O., Thomas, R.W., and Woodward, R.A. (1986). Thematic Mapper studies of semiarid shrub communities. *BioScience,* **36**, 446-452.

van Leeuwen, W. J. D., Huete, A. R. and Laing, T.W. (1999). MODIS vegetation index compositing approach: a prototype with AVHRR data. *Remote Sensing of Environment*, **69**, 264–280.

Vermote, E.F., El Saleous, N.Z. and Justice, C.O. (2002). Atmospheric correction of MODIS data in the visible to middle infrared: first results. *Remote Sensing of Environment*, **83**, 97-111.

Verstraete, M. (1994). The contribution of remote sensing to monitor vegetation and to evaluate its dynamic aspects. In Veroustraete, R. and Ceulemans, R. (Eds.). *Vegetation, Modeling and Climate Change Effects*. (pp 207-212). The Hague, Netherlands, SPB Academic Publishing.

Vogelmann, J.E., Helder, D., Morfitt, R., Choate, M.J., Merchant, J.W. and Bulley, H. (2001). Effects of Landsat 7 Enhanced Thematic Mapper Plus radiometric and geometric calibrations and corrections on landscape characterization. *Remote Sensing of Environment*, **78**, 55-70.

von Willert, D.J., Eller, B.M., Werger, M.J.A. and Brinckmann, E. (1990). Desert succulents and their life strategies. *Vegetatio*, **90**, 133–143.

Waser, N.M. and Price, M.V. (1981). Effects of grazing on diversity of annual plants in the Sonoran Desert. *Oecologia*, **50**, 407–411.

West, N.E. (1993). Biodiversity of rangelands. *Journal of Range Management*, **46**, 2-13.

Westoby, M., Walker, B. and Noy-Meir, I. (1989). Opportunistic management for rangelands not at equilibrium. *Journal of Range Management*, **42**, 266-274.

Wikipedia contributors. 2006. Remote sensing. Wikipedia, The Free Encyclopedia. 2006 Nov 3, 17-22 UTC [cited 2006 Nov 8].Available from: http://en.wikipedia.org/w/index.php?title=Remote_sensing&oldid=85502782.

Wikipedia contributors. 2007. Interface description language. Wikipedia, The Free Encyclopedia. 2007 Nov 11, 18:55 UTC [cited 2007 Nov 17]. Available from: http://en.wikipedia.org/w/index.php?title=Interface_description_language&oldid=170795965.

Willhauck, G. (2000). Comparison of object oriented classification techniques and standard image analysis for the use of change detection between SPOT multispectral satellite images and aerial photos. ISPRS, vol. 33, Amsterdam, Netherlands.

Zhou, Q., Robson, M. and Horn, G. (1998). Comparisons between the results from different ground vegetation cover estimation methods in a rangeland environment. *Proceedings of the 9th Australasian Remote Sensing and Photogrammetry Conference*, 1998, Sydney, vol. **1** (71).